Quantitative polymer-additive analysis using Pyrolysis-GC/MS

Dissertation

zur Erlangung des Grades

"Doktor der Naturwissenschaften"

im Promotionsfach Chemie

am Fachbereich Chemie, Pharmazie und Geowissenschaften der Johannes Gutenberg-Universität in Mainz

Ralph Nicholas Sebastian Harms
geb. in Limburg an der Lahn

Mainz, 2018

1. Berichterstatter:
2. Berichterstatter:
Namen für Online-Publikation aus Datenschutzgründen entfernt

Tag der mündlichen Prüfung: 08. Juni 2018

Declaration of Authorship

This dissertation is the result of work carried out in the central laboratory for organic materials at the International Technical Development Center of the Opel Automobile GmbH in Rüsselsheim am Main between April 2015 and March 2018.

Part of this work, mainly sample production and reference measurements, was conducted in collaboration with the Fraunhofer Institute ICT Pfinztal, Lyondell Basell, BASF and BASF Schweiz AG.

The preparation of this thesis was supervised by ... of the University of Mainz and ... of the University of Applied Sciences Darmstadt as well as my supervisors at the Opel laboratory ... and ...

Except where specific reference is made to the work of others, this thesis is entirely my own work and has not been previously published.

Due to the EU General Data Protection Regulation, all names had to be removed prior to online publication.

"Knowledge is power. Information is liberating. Education is the premise of progress in every society, in every family."

Kofi Annan

Johannes Gutenberg Universität Mainz

Abstract

Quantitative polymer-additive analysis using Pyrolysis-GC/MS

by Sebastian Harms

In the automotive industry, as in most branches of modern life, polymers have belonged to the most relevant material classes for several decades and continuously grow more important every year. One of their most important properties for use in everyday applications is their capability to resist oxidation. For most polymers, especially the extremely widespread class of polyolefines, this property is mostly dependent on stabilization by antioxidant additives. The analysis of this class of additives as well as their antioxidative effect and influential factors thereof are the focus of this study.

The main objective was the development of a quantitative analysis method employing gas chromatography/mass spectrometry augmented with a pyrolysis module. After optimizing pyrolysis time and temperature, a mass spectral library was created for the additives used in the reference samples, made from polyamide-6 and polypropylene. With this, single ion monitoring methods were developed, allowing reproducible direct quantification of most additives within their polymer matrix. The method's efficacy could be proven while monitoring additive concentrations during oven-aging experiments.

$150\,°C$ oven-aging experiments with subsequent mechanical tests on standard polypropylene test specimens, which represent the state of the art in lifetime prediction based on accelerated aging, were accompanied by oxidation induction time measurements in a DSC instrument. A comparison served to evaluate the possibility of performing lifetime predictions solely with information gathered from the DSC/OIT measurements. It was shown that this is not possible due to different effective stabilization temperatures of certain common antioxidant classes, leading to varying orders of oxidation resistance at $200\,°C$ compared to the $150\,°C$ of the oven test.

Finally, the influence of carbon black on the oxidation resistance of polypropylene was examined using the same methods on test specimens with and without the colorant. A reduced stability was observed for the compound containing carbon black, which displayed an approximately $20\,\%$ shorter induction period before degrading. The focus of these projects lay solely on thermo-oxidation processes.

Acknowledgements

Even a journey of a thousand miles begins with a single step. And often, it ends with a reflection upon the people who accompanied and aided this journey. The way that has lead me to this point feels like at least a thousand miles. Also, I could use a thousand adjectives to describe it. However, this page is about you.
Unfortunately, the EU General Data Protection Regulation requires the removal of all names from this online publication. However, this does not affect my gratitude towards all who were involved in this work. Thank you all.
Also, I am always willing to repeat the washing-machine story to those who are interested.

Contents

List of Figures

List of Tables

List of Abbreviations

DSC	Dynamic scanning calorimetry
amu	Atomic mass unit
APCI	Atmospheric pressure chemical ionization
APPI	Atmospheric pressure photo ionization
APPy	Atmospheric pressure pyrolysis
ASAP	Atmospheric solid analysis probe
ASE	Accelerated solvent extraction
ASTM	American Society for Testing and Materials
BHT	Butyl hydroxyltoluene
CAS	Chemical Abstracts Service
CIS4	Cold injection system 4
CPS	Cycles per second
C$_x$	Alkyl chain with x carbon atoms
DCM	Dichloromethane
DIN	Deutsche Industrie Norm
DLO	Diffusion limited oxidation
DTG	Differential thermogravimetry
EI	Electron ionization
ELSD	Evaporative light scattering detector
EN	European standard (European norm)
EPDM	Ethylene propylene diene monomer rubber
ESI	Electron spray ionization
FID	Flame ionization detector
GPC	Gel permeation chromatography
HALS	Hindered amine light stabilizer
HAS	Hindered amine stabilizer
HPLC	High-performance liquid chromatography
ICT	Institute for Chemical Technology
If	Irgafos
iPP	Isotactic polypropylene
ISO	International Organization for Standardization
Ix	Irganox
LDPE	Low density polyethylene
LDR	Linear dynamic range
LoD	Limit of detection
LoQ	Limit of quantification
LTTS	Long term thermal stabilizer
m*/*z	Mass-to-charge ratio
MAE	Microwave assisted extraction
MALDI	Matrix-assisted laser desorption/ionization
MB	Masterbatch
MPS	Multi purpose sampler
MS	Mass spectrometry

MSD	Mass spectrometric detector
NIST	National Institute of Standards and Technology
OIT	Oxidation induction time
PA	Polyamide
PDMS	Polydimethylsiloxane
PE	Polyethylene
pH	Potential of hydrogen
PP	Polypropylene
PS	Polystyrene
PTV	Programmable temperature vaporization
Py-GC/MS	Pyrolysis gas chromatography mass spectrometry
RSD	Relative standard deviation
SD	Standard deviation
SEC	Size-exclusion chromatography
SFE	Supercritical fluid extraction
SIM	Single ion monitoring
STSA	Statistical thickness surface area
$\mathbf{T}_c$	Crystallization temperature
TDU	Thermal desorption unit
$\mathbf{T}_g$	Glass temperature
TG	Thermogravimetry
TGA	Thermogravimetric analysis
TIC	Total ion current
Tin	Tinuvin
$\mathbf{T}_m$	Melting temperature
ToF	Time of flight
TPA	Total peak area
T-Ramp	Temperature ramp
TWIM	Travelling wave ion mobility
UL94	Underwriters Laboratory flame rating standard 94
USD	United States Dollar
UV	Ultraviolet
Vis	Visual

For my soulmate, whom I love dearly

Chapter 1

Introduction

In 2016, the German automotive industrie reached an annual turnover of 407 billion euro [1]. The industry was made up of 1.327 businesses employing a total of 828.000 people. Apart from steel, polymers are arguably the second most important class of raw materials used in the production of modern automobiles. Tires, sealants, fuel tanks, hoses, casings and virtually the complete interior trim only begin the listing of parts that wholly depend on this resource. The performance of most of these parts is critical either to safety or customer satisfaction. Both factors have massive impact on a companies success and thereby on the lives of countless consumers and employees.

A good example is interior trim. Large parts of an automobile's interior paneling is comprised of polypropylene and blends thereof. Modern day customers expect high quality in respect to all sensory impressions such as touch, smell and appearance. While this has always been true for premium segments, the demand trickled down to mid and entry-level, where the use of leather and wood is not feasible. Apart from feeling, looking and smelling good on the date of purchase, it is also inherently important that this impression lasts throughout the vehicle's lifetime and under all reasonably to be expected conditions. The conditions include but are not limited to prolonged exposure to strong solar radiation and the accompanying build up of heat, especially under large glass surfaces, such as the windshield. A 2009 study on maximum vehicle cabin temperatures [2] carried out in Athens, Georgia (USA) during the summer months found a maximum temperature inside the test vehicle of $76\,^{\circ}\mathrm{C}$. The temperature sensor used was situated $150\,\mathrm{mm}$ under the vehicles ceiling and never exposed to direct sunlight. It is therefore reasonable to expect higher temperatures on the instrument panel and other more exposed areas.

For polypropylene, a polymer which is very susceptible to oxidation due to the tertiary carbon in it's chain, these conditions pose a major challenge. To meet them and ensure both the costumer's satisfaction as well as the engineer's success, several important aspects have to be considered. One must know as much as possible about internal factors on the polymer's oxidation resistance, such as the influence of colorants, mold release agents and other aspects of the formulation. It is also imperative to have reliable test methods for the compounds oxidation stability, for use both during part development and for quality control purposes. Lastly, it is important to

use adequate stabilization packages tailored both to the part production process and the expected lifetime conditions of the product.

All these aspects were considered in this thesis. The starting point was the desire to analyze the additive content of an unknown polymer sample. While the reference method for this is liquid extraction followed by quantitative HPLC, it was the goal of this work to find an alternative which does not require prior extraction of the additives from the polymer. The ability to use the NIST EI MS library for identifying additives and their degradation products was also part of the motivation. It was therefore decided to develop a quantitative method for additive analysis using a commercially available Agilent/Gerstel Pyrolysis-GC/MS system and to establish a corresponding additive library containing both retention times and mass spectral data. Due to their wide application range in modern automobiles, polypropylene and polyamide-6 were chosen as the model systems for this development. As mentioned before, polypropylene is one of the most prevalent polymers used in automotive interior applications such as paneling. However, it also finds it's use in exterior parts, such as bumpers. Polyamide-6 is the material of choice when toughness or resistance to high temperatures is wanted. With glass or carbon fibre reinforcement, it is a common material for seat structures and is even used for pedals, when weight reduction is a key priority. Another common application is the *under the hood* range of parts. Polyamides are often found in connectors, hoses, beauty covers or air intake manifolds, as well as many other structural components.

Another aspect of this thesis is lifetime prediction from oxidation stability tests. State of the art is the standardized oven-aging procedure. Test specimen and parts are aged in air circulated ovens at $150\,^{\circ}\mathrm{C}$ while monitoring their optical and mechanical properties. The elevated temperature causes faster depletion of the antioxidants used in the stabilization package. This is roughly based on Van't Hoff's rule, which states that the velocity of a reaction multiplies by a factor of 2 to 4 when the temperature is increased by $10\,\mathrm{K}$ (Q_{10} factor) and represents the *best practice* within the industry. However, even testing under accelerated aging conditions still requires several weeks of oven time depending on the respective specifications, as well as accompanying mechanical tests, which are a time and cost factor in itself. It is therefore desirable to gain a faster method, which generally means testing at even higher temperatures. Of course, for polypropylene, there is a definitive temperature limit when mechanical testing is desired. The material's melting point lies between $160\,\mathrm{d}$ to $180\,\mathrm{d}$epending on crystallinity and potential blend components. This problem can be circumvented by using a differential scanning calorimeter (DSC) instrument. At $200\,^{\circ}\mathrm{C}$ and higher, the polymer is subjected to a pure Oxygen atmosphere and the time until the exothermic oxidation peak appears is taken. This oxidation induction time correlates with the level of antioxidants in the polymer. Whether this method can be employed as a faster alternative to oven aging was examined by aging samples with varying stabilizer composition and comparing the results to the corresponding DSC/OITs.

In addition, the previously developed quantitative Py-GC/MS method was used to monitor the actual additive levels during aging. This offered the chance to prove the efficacy and precision of the method and offers insights into the relationship of additive concentration, DSC/OIT and oxidation stability.

The final project was aimed at gaining more information on the influence of colorants on a polymers oxidation stability. Due to it's high prevalence in automotive applications, carbon black was chosen. Polypropylene was used as base polymer, both because of it's widespread use and it's susceptibility to oxidation. Two sample formulations varying only in their carbon black content were compared using the same methods already employed in the DSC - oven comparison.

Taken together, it is the aim of this thesis to further advance our understanding of polymer additive interaction and our methods of studying these. In future, this will help with developing new compounds for lighter and more fuel efficient vehicles, correctly and efficiently predicting the lifetime of polymer components as well as faster root cause and failure analysis.

1.1 Literature Review

Additive analysis The aim of this section is to give an overview of current literature on the topics of this thesis. It starts with additive analysis using liquid chromatography, highlights some alternatives such as MALDI-ToF before summarizing the state of the art in pyrolysis methods. Following this, the topics of additive degradation during aging and polymer lifetime prediction are elucidated.

As was mentioned in the introduction, the established method for quantitative additive analysis in polymers is HPLC combined with varying prior extraction steps such as standard liquid-solid extraction, soxhlet extraction, microwave assisted extraction or accelerated solvent extraction. The standard method of detection is via UV, but MS detectors using atmospheric pressure photo-ionization (APPI) or chemical ionization (APCI) as well as electron spray ionization (ESI) are also in use.

Carrero et al. [3] studied the influence of mineral fillers on the additive content of polyolefines. For their analysis, they used accelerated solvent extraction (ASE) under high pressure combined HPLC-UV. They found, that talcum has a significant effect on the recovery rates of the additives in use compared to calcium carbonate. However, they concluded that this was due to heightened antioxidant consumption during processing rather than the hindering of the extraction process.

Beißmann et al. [4] studied the effects of aging on several antioxidants, both in their respective polymer matrix and isolated in polymer-mimicking squalene. They identified several colored and non colored oxidation products and degradation pathways. HPLC-MS/MS was used for qualitative analysis and HPLC-UV for quantification. Extraction was performed in toluene at $150\,^{\circ}\mathrm{C}$ with subsequent precipitation. This publication is a must-read for everyone concerned with the effect of aging on additives and their analysis.

Reingruber et al. [5] addressed the underestimation of stabilizer content often observed in round robin tests. They also studied the influence of talcum on stabilizer degradation at elevated temperatures in solvent, coming to the same conclusion as was later reached bei Beißmann et al. APPI, APCI, ESI and UV detection were used for the analysis following separation via HPLC. Since all experiments were performed from prepared stock solutions, no extraction steps were necessary.

Himmelsbach et al. [6] compared APPI, APCI and ESI for additive analysis following separation via HPLC, touching on the advantages and downsides of each method. No extraction step was used, since the additives were prepared as stock solutions in acetonitrile.

Marcato and Vianello [7] compared one-step and two-step microwave assisted extraction (MAE), using HPLC for separation and both UV detection and evaporative light scattering detection (ELSD) for analysis. Their focus was to show which method of extraction is suited for a wide range of common additives in polyolefines.

An early approach was published by Richard Nielson in 1993 [8], focussing on

extraction under ultrasonic bath conditions and subsequent analysis via liquid chromatography. Problems such as additive degradation during extraction and separation in protic solvents as well as co-elution of additives are discussed.

A very comprehensive view on extraction methods for additives in polymers was published by Vandenburg et al. [9] comparing dissolution/precipitation in solvent, soxhlet extraction, super critical fluid extraction (SFE), microwave assisted extraction (MAE) and accelerated solvent extraction (ASE). Their conclusion is, that the dissolution/precipitation is a good and cheap method, which however can pose problems with re-precipitation of the additive. Soxhlet, while very thorough has issues with discrimination of volatile additives during the lengthy extraction at high temperatures. Of the instrumental techniques, the ASE was deemed superior if enough effort was invested in finding the ideal solvent for extracting the additives without dissolving the polymer. A study published later goes into more detail on this method [10].

Another approach to additive analysis found in literature is the direct application of MS techniques without prior separation. Paine et al. [11] published an extensive review on this topic in 2014, focusing on atmospheric pressure techniques which allow fast analysis time due to the omitted separation step. A further comprehensive review on this matter, which also features a comparison of mass spectrometry with and without prior separation was published by Christian Klampfl [12].

A more exotic method was used by Barrère et al. [13], combining the atmospheric ionization technique ASAP (atmospheric solid analysis probe) which is similiar in effect to pyrolysis, with travelling wave ion mobility tandem mass spectrometry (TWIM-MS/MS), adding the collision cross section (Ω) of the generated ions to the mass spectrometers analytical spectrum. This allowed the parallel qualitative analysis of both the polymer and the additives in use.

A quantitative approach using MALDI-ToF MS with tetraphenylporphyrine as internal standard was published by Schwarzinger et al. [14]. Heterogenous distribution of the sample and the matrix in the spot was prevented by using a solvent free sample preparation. While not reaching the accuracy possible with HPLC separation after extraction, the technique is both easy to handle and fast according to Schwarzinger.

One paper often referenced when discussing direct additive analysis methods is a publication from Trimpin et al. [15] comparing solvent-free MALDI with ASAP and atmospheric pressure pyrolysis (APPy). Additive analysis was successful with the non quantitative ASAP approach.

Having reviewed several non pyrolysis methods, the following paragraphs will concern themselves first with pyrolysis after prior separation of polymer matrix and additives and finally direct pyrolysis and separation by gas chromatography. The newest contribution comes from Brandner and Wold [16] who quantified high molecular light stabilizers in polycarbonate using size exclusion chromatography (SEC) of the polymer sample dissolved in dichloromethane as the extraction step.

The seperated fractions were then transfered to the pyrolysis-GC/MS system where they were characterized and quantified. Advancement over the 2007 publication bei Kaal et al. [17] being the use of SEC columns optimized for resolution of lower molecular weights and the use of cryo-focusing after pyrolysis of the fractions.

When summarizing pyrolysis techniques one cannot omit the early works of Wampler and Levi [18–20] in which they studied fundamental aspects of the technique such as the effect of the heating rate during pyrolysis, cryogenic focusing and the general reproducibility. Early works on additive analysis were contributed by Frank Wang in 2000 [21–24] concerning the characterization of different additive classes via Py-GC/MS after an initial extraction step.

In 2003, Herrera, Matuschek and Kettrup [25] published a novel pyrolysis approach, using a so called double shot technique, exploiting the higher volatility of most additives compared to their respective polymer matrices. Pyrolysis was performed in two steps, first at a lower temperature to volatize the additives, and at a higher temperature in the second step to analyze the polymer. Additionally, single ion monitoring (SIM) was used to heighten the mass detectors sensitivity towards the masses of interest.

Coulier et al. [26] combined the analytical power of Py-GC/MS with the quantification capabilities of HPLC-UV and HPLC-ELSD to identify the polymeric hindered amine light stabilizers (HALS) used in polypropylene samples and then quantify them after successful extraction via the dissolution/precipitation method mentioned earlier.

Jansson, Zawodny and Wampler [27] successfully used pyrolysis combined with SIM and extracted ion mass spectrometry to qualitatively analyze several polymer sample's additive content. Additives analyzed include important representatives such as Irgafos 168 and Irganox 1010. This publication contains very useful data on the pyrolytic fragmentation of these common additives.

Lifetime prediction In the early phases of this thesis, Reil et al. [28] published a comprehensive study on the parameters influencing the outcome of oxidation induction time measurements performed on a differential scanning calorimetry instrument (DSC/OIT). They also describe the application of DSC/OIT for the early predictions of the service life of polyolefines, assuming a correlation between the DSC/OIT recorded at high temperatures above the sample's melting point and it's oxidation stability. However, they warn of extrapolating results toward common use temperatures due to the high number of variables, such as stress and environmental factors. A comparison of the DSC/OIT results with results from oven aging at $150\,^{\circ}\mathrm{C}$ with different stabilizer packages was not provided, motivating a secondary project of this thesis.

A comprehensive review on the topic of polymer aging and lifetime prediction was published by Mathew Celina in 2013 [29]. He goes into detail on topics such

as the importance of diffusion limited oxidation (DLO), degradation kinetics, prediction models and common analysis methods. Together with an earlier review published on non-Arrhenius behavior of polymer degradation studies in 2005 [30], Celina provides a broad knowledge base for polymer degradation and stability.

A study published in 2009 by Müller et al. [31] examined the correlation of actual antioxidant levels in polypropylene samples, determined by liquid extraction-HPLC, with DSC/OIT values taken throughout a long term aging process at $80\,^{\circ}\mathrm{C}$ and $90\,^{\circ}\mathrm{C}$ both in air and water. The correlations found varied, depending on the stabilizer package used. Some HALS containing samples showed good long term stability at low temperatures while showing very low DSC/OIT values.

Schmid and Affolter [32] compared the results of interlaboratory DSC/OIT tests in respect to the oxidation induction time and the oxidation induction temperature. They highlight critical factors in OIT and it's use for stability measurements and provide insights on how these measurements can be improved. This study is well augmented by a publication on the potential interfering parameters in the determination of the OIT by Rosa et al. [33].

1.2 Scope of this Thesis

Development of a quantitative Py-GC/MS method for polymer additive analysis The primary goal of this thesis, which is also reflected in it's title, is the development of a quantitative Py-GC/MS method for the direct analysis of additives in polymers. The primary focus are common antioxidants compounded into two widely used polymers in the automotive industry, polyamide-6 and polypropylene.

The motivation for this project is having a reliable method for quantification, without the need for prior extraction. Also, the combination with the analytical capability of the GC's mass spectrometer is a significant benefit in failure analysis of unknown samples. Especially when comparing it's ease of use with available HPLC/MS solutions.

Comparison of DSC/OIT and oven-aging for the prediction of service life A secondary goal of this work is to assess the correlation between the established oven aging procedure for lifetime prediction with the faster and less resource intensive DSC/OIT measurement. It shall be clarified whether DSC/OIT represents an alternative for quality control and material development. This will be done by comparing several samples with varying stabilizer packages aimed at either producing a good OIT or delivering a long lifetime at lower temperature conditions. The expected outcome of this study is, that no simple extrapolation of results from common DSC/OIT temperatures ($T > 200\,^{\circ}C$) to the results from oven-aging is possible. The main motivation for this is to prevent false conclusions if this is not the case.

Additionally, additive quantification will be performed on the aged samples, both to validate the newly developed method and to further understand the correlation of antioxidant levels with the DSC/OIT.

The influence of carbon black on the oxidation stability of polypropylene Finally, the influence of a commonly used colorant (carbon black) on the oxidation stability of polypropylene will be examined. In an oven aging experiment, a sample containing carbon black and an identical sample with only the carbon black missing will be compared. With the help of the results, future stabilization packages can be better adjusted to the needs of the specimen.

Chapter 2

Fundamentals

2.1 Methods

In this work, several methods of material analysis were used. These include Pyrolysis-GC/MS and HPLC for chemical analysis, DSC and TGA for thermal analysis and the three-point flexural test for mechanical analysis. The following sections will give an overview of these techniques.

2.1.1 Pyrolysis-GC/MS

Pyrolysis-GC/MS combines the ease of use and analytical power of modern GC/MS systems with the extended range of suitable samples obtained by pyrolysis, unlocking the field of polymer analytics to gas chromatography. This is realized by equipping the programmed temperature vaporizing (PTV) injector with a pyrolysis unit. The samples are prepared in quartz-vials and introduced into the pyrolyzer by means of an autosampler. For cases in which it is required, the injector includes a cryo-focusing mechanism employing liquid nitrogen. It cools the injector to a minimum temperature of $-196\,^{\circ}\mathrm{C}$, preventing any pyrolysis products from moving to the column. After the pyrolysis process is complete, the injector heats up and all analytes enter the column simultaneously, potentially leading to sharper peaks and therefore a higher resolution. After separation, the analytes are detected by the quadrupole MS, allowing subsequent identification and quantification using the appropriate GC/MS analysis software (Figure 2.1).

Pyrolysis

The main constraint of gas chromatography, as we will see in the following subsection, is the requirement of volatility which has to be met by all analytes. They must be readily desorbed or evaporated without decomposition in order to separate them chromatographically and obtain reproducible results [34]. The consequence for most commonly used technical polymers is, that conventional GC injection methods only allow analysis of their volatile components. The polmer itself or any non-volatile components (under GC conditions) cannot be analyzed [35].

To solve this problem, a pyrolyzer-unit is connected to the injector to quickly heat a small sample to temperatures of up to $1400\,^{\circ}\mathrm{C}$, breaking the large molecules into

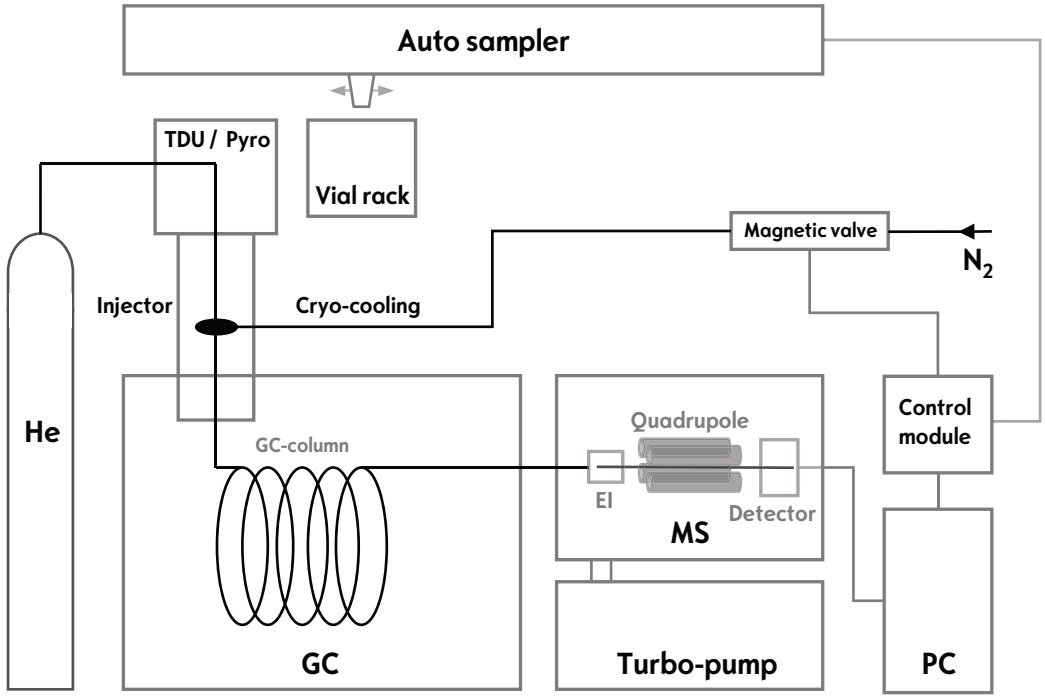

FIGURE 2.1: Schematic of a Pyrolysis-GC/MS device

smaller, volatile ones [36]. The repeatability of this pyrolysis process is so reliable, that the resulting fragment can readily be used to characterize the original polymer [20, 34]. The main criteria for this reliability are the heating rate, which should be as fast as possible, the sample mass, which should be as small as possible to ensure good heat transfer and a precise and stable equilibrium temperature, for a well-defined amount of thermal energy delivered to the sample.

The three main types of pyrolyzers in use today are the curie-point pyrolyzer, the resistively heated or foil pyrolyzer and the isothermal furnace. The first utilizes a high frequency magnetic field applied to a sample holder made of a ferromagnetic material. The field will rapidly heat the sample holder to its curie-point, which is the temperature at which the ferromagnetic materials becomes paramagnetic and is no longer heated by the field. Resistively heated pyrolyzers contain a platinum filament with a very low thermal mass, allowing an electric current to produce pyrolysis temperatures at extremely high rates of under $10\,\mathrm{ms}$ from room temperature to $1400\,^{\circ}\mathrm{C}$ [34], also leading to the term *pulse pyrolysis*. Lastly, the isothermal furnace is a small oven which is kept at the pyrolysis temperature while the sample is dropped inside, eliminating the need for high heating-rates.

The degradation reactions that take place during pyrolysis follow common organic mechanisms. In case of polymers, it depends on the monomer, whether statistical chain fission or depolymerization takes place. In case of stabile monomers such as styrene (PS) or ε-Caprolactame (PA-6), the main reaction is depolymerization to the original monomer. For many olefinic polymers such as polypropylene or

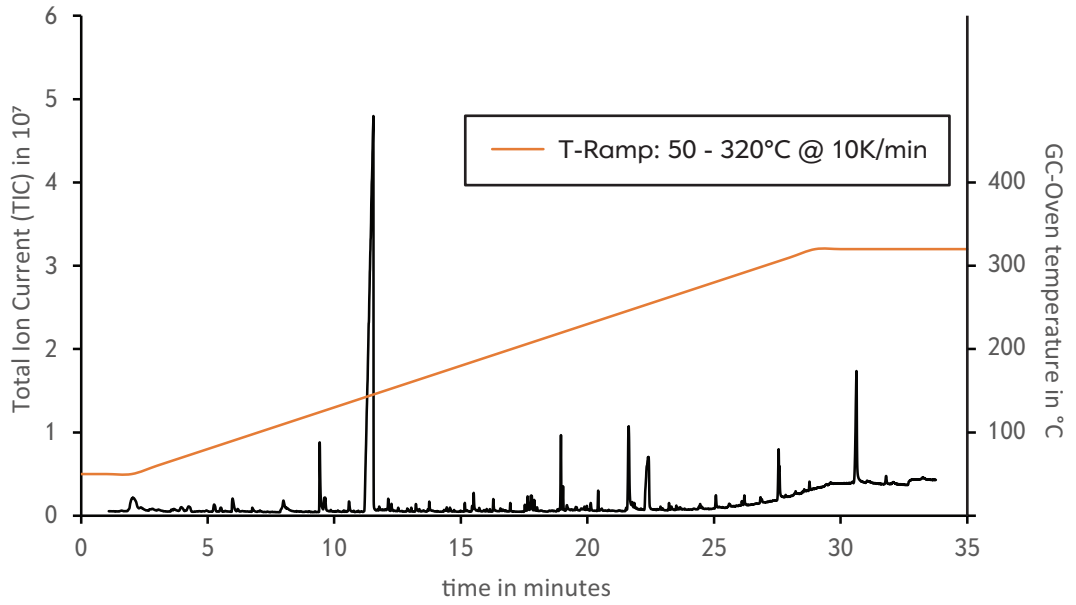

FIGURE 2.2: Chromatogram with GC-oven temperature-ramp

polyethylene, statistical chain fission dominates. Next to hemolytic cleavage, common reactions are β-elimination and hydrolysis [37]. At higher temperatures decarboxylation and aromatization become the dominant reactions . For this reason, the information content of pyrograms is greatly diminished at temperatures in excess of $800\,^{\circ}\mathrm{C}$ for most polymers and other organic compounds. Consequently, the ideal pyrolysis temperature is as high as required to pyrolyze the sample, but as low as possible.

Gas Chromatography

Since M.S. Tswett first published the principle of chromatography in 1910 and the first GCs were made commercially available in 1955, followed by the first GC/MS system in 1968, gas chromatography has become one, if not the, major workhorse of modern analytical, organic chemistry. Its purpose is to separate mixtures of organic compounds. To achieve this, the analytes are evaporated in the injector-unit of the GC and then carried through the column by the carrier gas, which represents the mobile phase. In most modern GCs, helium or in some cases nitrogen are used. The actual separation of the analytes then relies on their varying interaction strength with the stationary phase. This phase is usually made up of a sub-micrometer film of polydimethylsiloxane (PDMS) coated onto the inner wall of a glass capillary. The film and the capillary form the chromatography column, which commonly has an inner diameter of $0.25\,\mathrm{mm}$ to $0.5\,\mathrm{mm}$ and a length of $20\,\mathrm{m}$ to $100\,\mathrm{m}$. To tweak the stationary phase's polarity, the PDMS can be chemically modified with different organic groups such as phenols. In rare cases, a stationary phase of polyethylene glycol can be used to achieve very high polarity. This is used when separating very polar analytes and derivatization is not an option.

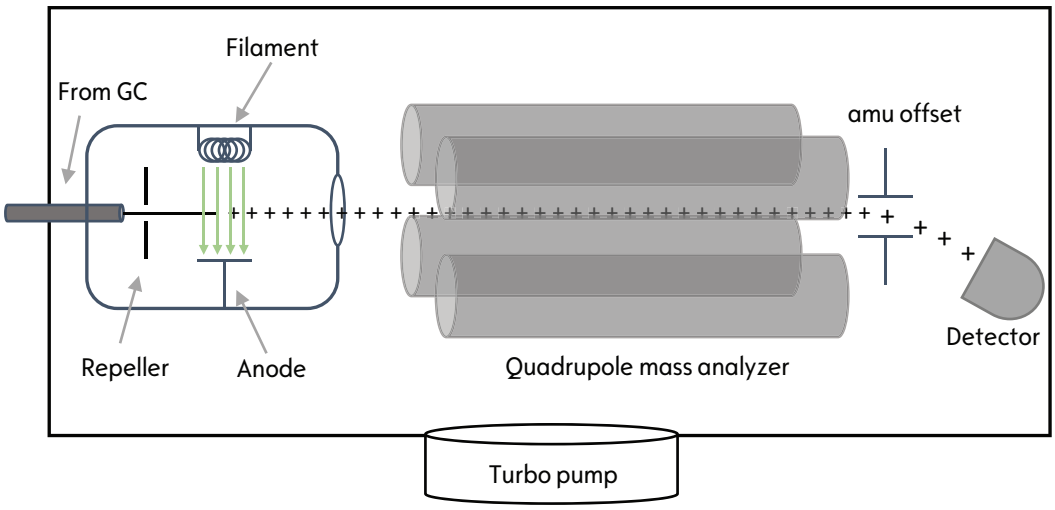

FIGURE 2.3: Schematic of quadrupol MS-instrument

In addition to separation by polarity, GC methods generally also use a temperature program to separate the analytes by their boiling points. A typical temperature ramp would start at $50\,^{\circ}\mathrm{C}$ and slowly ramp up to e.g. $300\,^{\circ}\mathrm{C}$. The column is then held at this temperature until the end of the run, allowing all analytes to elute (Figure 2.2). Depending on the analytes and the temperature resistance of the stationary phase, temperatures of up to $450\,^{\circ}\mathrm{C}$ can be achieved.

The use of a temperature program and it's very significant effect on retention times, makes gas chromatography an incredibly flexible and easy to use method of analysis. In most cases, instead of having to change the column or experiment with different solvents, it is sufficient to tweak the temperature ramp and carrier gas flow rates to achieve the chromatographic separation needed for the problem.

Another vast advantage of gas chromatography is the easy coupling to a mass spectrometer. Because the only solvent consists of inert gas and the amount of analyte is microscopic, GCs can be directly coupled to an MS system using electron or chemical ionization. This not only simplifies the systems use, it also makes component identification via the NIST MS libraries very convenient. Within the limitations of gas chromatography, the simplicity of the coupling together with the analytical power of mass spectrometry, gives GC/MS a huge advantage over HPLC systems.

Mass Spectrometry

In gas chromatography, there is a wide range of detectors available for detecting the eluting analytes. Next to mass spectrometry, the flame ionization detector (FID) is probably the most common. However, while the FID is a superior detector in terms of response factor or dynamic range, it is lacking in the mass spectrometers specialty: compound identification. A modern electron impact quadrupole mass spectrometer not only provides very high scan-rates, a good dynamic range and reproducible peak areas for quantitative analysis, it also delivers valuable information about the compound itself. The controlled fragmentation of the analyte, following known and

predictable chemical mechanisms, allows both the identification via databank comparison and reasonably elaborate deductions of unknown compounds.

The basic principle of mass spectrometry is to ionize the analyte and then separate and detect the resulting ions by their mass to charge ratios (m/z) in a magnetic and/or electric field or by measuring varying, mass-dependent, speeds in a time-of-flight (ToF) tube.

A schematic of a tabletop MS system, the electron impact – quadrupole mass spectrometer, is shown in Figure 2.3. A heated transfer line connects the GC with the MS, where the analyte enters the electron impact ionizer. The analyte molecules are ionized in an electron beam formed between a cathodic filament and an opposing anode. The most common accelerating voltage used in EI sources is $70\,\mathrm{V}$. Using a standardized voltage allows for reproducible fragmentation of the analyte molecules. In turn, this allows the build-up of MS libraries for spectrum comparison, significantly simplifying the identification of the analyte. Once the ions have formed, they are accelerated into the mass analyzer by the repeller and focused by a number of electromagnetic lenses. The quadrupole rods in the mass analyzer are exposed to a potential comprised of a direct and a high frequency alternating voltage.

$$u(t) = U + V cos(\omega t) \tag{2.1}$$

In concordance with the Mathieu function [38], there is a stable path for every m/z, which can be controlled by varying the voltages. So, for a given voltage, only one m/z can pass through the analyzer to the detector. By changing the voltages, one can scan through a range of m/z and obtain a mass spectrum of the current analyte. The amu offset deflects the ion beam onto the detector, which is set up at an angle in order to prevent gamma rays formed in the EI source to falsify the detector signal. The turbo pump is important to achieve a sufficient mean free path for the ions to reach the detector without collision. Typical pressures inside the mass analyzer lie in the range of $10^{-5}\,\mathrm{hPa}$ to $10^{-8}\,\mathrm{hPa}$.

Quantitative Analysis

Next to a qualitative analysis of the sample with the goal of identifying the base polymer and the additives used, it is often desired to quantify the components in a mixture. To achieve this, a correlation between the peak area (i.e. the integrated signal intensity) and the quantity of the component in the original sample has to be found.

First however, there are several problems which should be considered. One is the scan-rate used by the mass spectrometer. As opposed to a Flame Ionization Detector (FID), the MS does not measure continuously. Conventional scan-rates usually lie between $0.5\,\mathrm{s}$ to $1.0\,\mathrm{s}$. Due to the high performance of modern GC instruments, this must be considered slow [34]. In his Handbook of GC/MS Hübschmann recommends using an early eluting component to determine the necessary scan-rate,

indicating, that 10 datapoints should suffice to describe a symmetrical peak and that 6 to 8 datapoints are usually sufficient from a statistical point of view [34]. This can lead to problems, when base widths lie well beneath $10\,\mathrm{s}$. Unfortunately, setting a higher scan-rate can lead to severe sensitivity problems due to shorter ion dwell times. A possible solution is using the instrument in SIM mode. With a drastically reduced amount of m/z ratios per scan, it is possible to reduce scan-times without risking insufficient sensitivity. Another solution would be to use the MS solely for peak identification and quantify in a second run, using the FID, which is very common as an alternative detector on many GC/MS systems. This detector measures continuously, is highly sensitive and offers a broad linear dynamic range, eliminating any uncertainty concerning peak areas.

The next problem arises from a combination of the limit of detection (LoD), the limit of quantitation (LoQ) and the linear dynamic range (LDR) of the MS instrument. Since typical concentrations for additives in polymers often lie well below $1\,\mathrm{wt}\%$. As a consequence, one has to balance the need for more sample-mass in order to surpass the LoD and LoQ against overloading the detector by going beyond the LDR. As with the scan-rate problem, using the instrument in SIM mode can help with overcoming this problem, as long as the desired additive shows characteristic ions not inherent to the base polymer. With these issues resolved, it is time to engage the calibration function. To do this, measurements with known concentrations are made and the substance amount plotted against the return signal. Ideally, the range in which the correlation is proportional is as large as possible, enabling the operator to use a linear regression and obtain a linear function with a_0 as the blank value and a as the instruments sensitivity.

$$f(x) = a_0 + ax \tag{2.2}$$

It is imperative, that the calibration function only be used in the range of experimental data. How the correlation behaves outside this range cannot be derived from either the data or the fit. Self-evidently, all experimental data-points should lie within the linear dynamic range of the Instrument. Above this range, where the instrument is entering saturation, the signal becomes asymptotic.

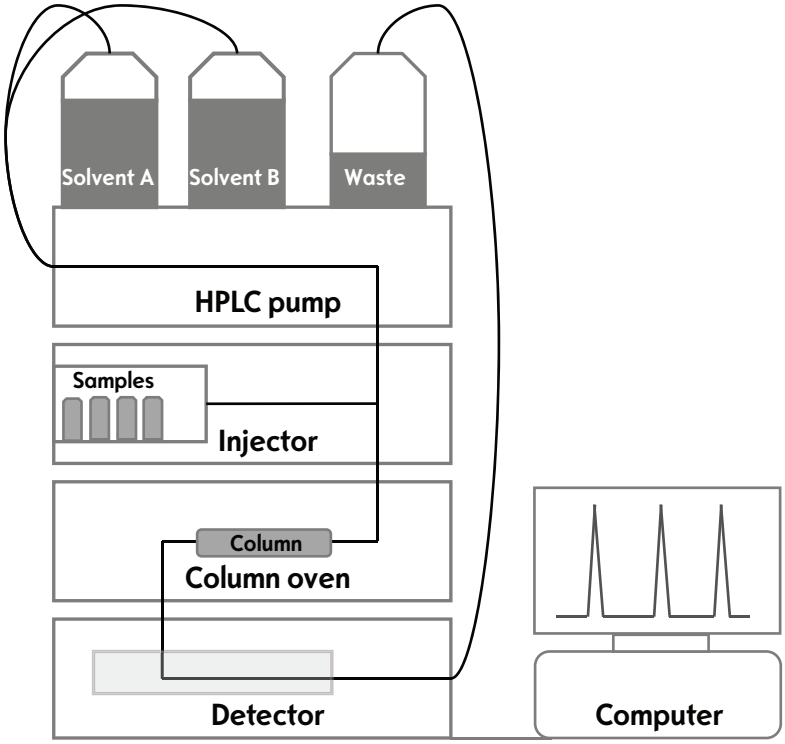

FIGURE 2.4: Schematic of an HPLC instrument

2.1.2 HPLC-UV

Beginning with the development of the first high pressure variations of liquid chromatography techniques such as the amino acid analyzer and the gel-permeation chromatograph (GPC) in the 1950s, followed by normal-phase HPLC in the 1960s, reversed-phase high performance liquid chromatography nowadays represents the dominant form of general-usage liquid column chromatography [39]. While the amino acid analyzer separates amino acids via their isoelectric point by varying the pH value and GPC relies solely on the hydrodynamic radius of the analytes for separation, both limiting the respective methods to the separation of amino acids or determining the molecular weight distribution of polymers, HPLC exploits the analytes polarity to achieve separation through a suitable combination of stationary- and mobile phase polarity. This allows an extremely broad range of analytes, since the only real requirement is the analyte's solubility in the employed solvent.

While the first HPLC columns were packed simply with silica, which is a polar stationary phase (normal phase) due to the hydroxyl groups, later columns were made using silica particles functionalized with octadecylsilane or octylsilane chains (C_{18} or C_8) and other non-polar molecules (reversed phase). The columns themselves are made from metal so they can endure the high pressures used in HPLC. The size of the particles used for packing commonly lies in the range of $1.5\,\mu\mathrm{m}$ to $5\,\mu\mathrm{m}$ in diameter. The ability to reliably manufacture silica particles of this size with an adequately small size distribution and controlled porosity was one of the major milestones in the development of this technique. The importance of particle size and

porosity can easily be explained using the Van-Deemter equation, where particle-size (d_P) and size distribution (λ) are the major contributors to the A-term. The smaller the particles get, the smaller A becomes, which in turn reduces the height of the theoretical plates and thus increases the columns resolving power. Particle-porosity (ω) impacts the mass-transfer term C, since movement of the analyte inside the particles pores is governed mainly by diffusion (D_m).

$$HETP = A + \frac{B}{\nu} + (C_s + C_m) \cdot \nu = 2 \cdot \lambda \cdot d_P + \frac{2\lambda D_m}{\nu} + \frac{\omega d_P^2}{D_m} \cdot \nu \tag{2.3}$$

The instrument itself is comprised of several modules, as seen in Figure 2.4. Two or more reservoirs for solvents and one for waste ensure the availability of eluent. The solvent is mixed according to the method used and pressurized in the pump. The sample is added in the injector, separation takes place inside the column oven, typically at isothermal conditions. Finally, a host of detectors are available for HPLC. The most common of which is the UV/Vis detector, which works for most organic compounds and can be supplemented by derivatization of the sample prior to injection. The collected data is then analyzed using an appropriate chromatographic software.

As an analogy to the GCs temperature-program, the HPLC can be used either in isocratic mode, which corresponds to isothermal mode in a GC program, or in gradient mode, which corresponds to a ramped temperature-program. However, instead of temperature, the solvent composition is used to achieve better separation. The most commonly used eluents are mixtures of water with either acetonitrile or methanol. Isopropanol and tetrahydrofuran also come to use, albeit less common. To insure a smooth analysis it is important that the solvents be nonviscous, stable and transparent at short wavelengths if UV detection is desired. Temperatures are often slightly above room temperature ($30\,^{\circ}\mathrm{C}$ to $35\,^{\circ}\mathrm{C}$).

While MS detectors for HPLC are becoming ever more common with the development of new ionization sources which can handle both the solvent amounts and the ambient pressures necessarily present in the HPLC-MS interface, UV/Vis detectors are still the most prevalent in most analytical labs. Due to their broad range of use, their ease of use and their low maintenance cost when compared with an HPLC compatible MS system, they are very attractive, even without the identification capabilities of mass spectrometry. UV detectors generally measure the absorbance A of a sample by comparing light in the UV range transmitted through the sample with its source, according to Beer's law.

$$A = log\frac{I_0}{I} = \varepsilon \cdot c \cdot d \tag{2.4}$$

Here, I_0 and I are the initial and the transmitted intensity, ε is the samples extinction, c the concentration and d the length of transmitted sample.

The wavelength dependence of a substances absorbance gives the user several different options when using a UV/Vis detector. When a certain substance with

known absorbance maximum is looked for, one can operate the detector at this specific wavelength, which can offer considerable advantages, especially when confronted with problematic sample matrices. For a more universal detection, wavelengths below $260\,\mathrm{nm}$ are used. A lower wavelength limit can be posed by the solvent. While water/acetonitrile can be used down to $200\,\mathrm{nm}$ without a problem, methanol shows absorbance below $210\,\mathrm{nm}$, which poses a problem when aliphatic compounds are meant to be detected.

Several instrumentation variants are/were available for UV/Vis detection. In the past, fixed wavelength detectors were common, which often used a low-pressure mercury lamp to create UV-light at $254\,\mathrm{nm}$. Today, variable-wavelength detectors are the standard. Depending on the necessary speed and resolution of the measurement, one can use a scanning type which creates a spectrum from white-light with a diffraction grating prior to sample-transmittance and scanning the sample one wavelength at a time using a slit-aperture, or a diode-array detector which transmits white-light through the sample and uses a diffraction grating after the sample to project the resulting spectrum onto a diode-array. The first variant generally offers a better resolution, since it is not limited by the amount of diodes in the array (usually 512 or 1024). The latter offers superior speed, since the whole available spectrum can be monitored continuously.

2.1.3 Dynamic Scanning Calorimetry - DSC

Differential scanning calorimetry is one of the most widespread thermo-analytical techniques in materials testing laboratories today. Developed in 1962 by M. J. O'Neill and E. S. Watson of the Perkin Elmer Corporation [40], it is based on the amount of energy needed to increase a samples temperature relative to a reference sample. The technique provides information on 1st and 2nd order thermal transitions such as melting-/freezing points or glass transition temperatures. Also, it can be used to explore a polymers thermal history, monitor polymer degradation through the descending melting point (T_m), estimate the percentage of crystallinity or studying the polymers resistance to thermo-oxidative degradation by measuring the oxidative induction time (OIT).

For all thermal transitions, DSC makes use of their energetic properties. All transitions either consume or release energy in form of heat. They are endo- or exothermal. The device registers this energy release or consumption by registering a higher or lower power usage in relation to the reference sample while running a linear temperature program. Essentially, the device is measuring the samples heat capacity at constant pressure C_p, which allows the examination of the sample's thermal properties and calculating the enthalpy of it's thermal transitions as can be seen in the following thermodynamic relations.

$$dH = \delta Q + V dP \tag{2.5}$$

$$C_p = \left(\frac{\delta Q}{\delta T}\right)_p = \left(\frac{\delta H}{\delta T}\right)_p \tag{2.6}$$

When plotting the heat flow or the heat capacity against the temperature, one obtains a graph with minima and maxima corresponding to the energetic properties of it's thermal transitions. These transitions can appear as broader temperature-ranges instead of sharply defined temperatures. This is due to the partial crystallinity of many polymers, as well as their molecular weight distribution. In this example, the t_1 to t_2 interval shows an endothermal melt peak, while exothermal decomposition starts at t_4.

During processing, many polymers develop areas which are subject to an increased mechanical stress due to in-homogeneous pressure and cooling during e.g. injection molding. These are part of the polymers thermal history at a given point in time. In a DSC experiment it is possible to observe this history due to energy uptake/release during the relaxation of e.g. stressed areas. As a consequence, it is possible to quantify the amount of stress a polymer sample was under by comparing the first and second cycle of a DSC experiment. The first cycle shows the polymers thermal history in addition to its inherent thermal properties such as T_C, T_G and T_M, while the second cycle only shows the latter, since prior stress has been released.

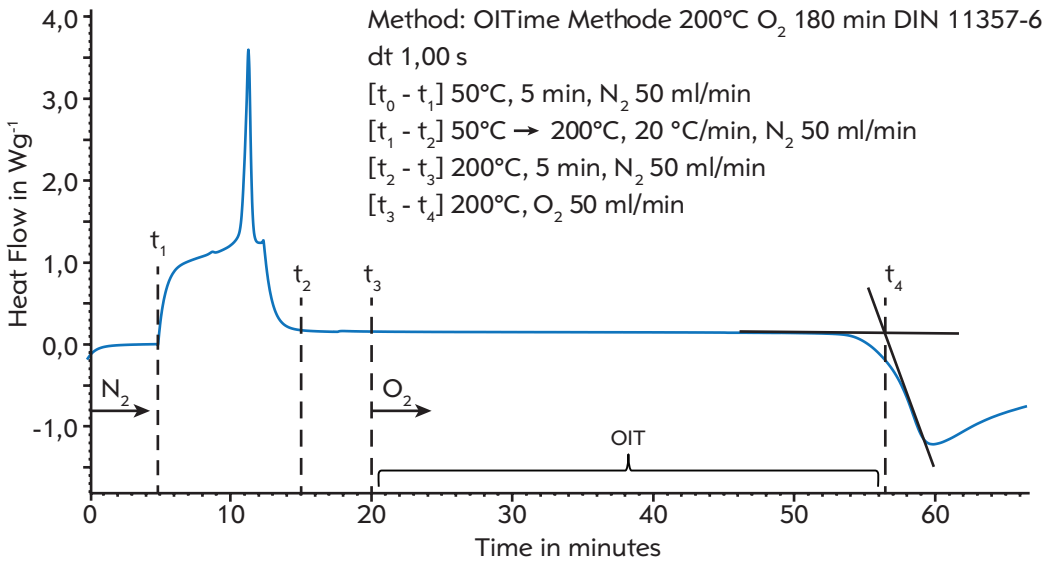

FIGURE 2.5: Example for a DSC/OIT experiment using polypropylene

In order to obtain valid results, it is of course important to choose the cool-down parameters in a way that does not introduce new stress into the polymer.

The main use of DSC in this work is to monitor the polymers oxidative induction time or OIT. At a given temperature, this is the time from changing to an oxidizing gas (i.e. O_2) until the onset of degradation, observed in form of an irreversible exothermic reaction (t_3 to t_4 in Figure 2.5). To obtain this information, the sample is heated to a defined temperature (usually above its melting point; resulting in an OIT of more than 10 minutes but less than 60 minutes [41]) in an inert atmosphere (i.e. N_2). The gas mix is then changed to an oxidizing one, usually with either synthetic air ($21\,\%\,O_2$) or pure oxygen. For a while there will be no measureable reaction of the polymer due to its stabilizing additives. Once these have been depleted, an exothermic degradation can be observed. The depletion process itself can usually not be observed in the DSC since antioxidants are commonly employed in the permille range. The period of time in which the polymer remains stable in the oxidizing atmosphere is called the OIT. It can be used to directly compare the oxidation resistance of two or more samples at a given temperature or monitor a samples ageing in a prolonged weathering or oven test. Whether or not this is a suitable technique for the service-life prediction of a polymer sample has been the subject of some debate. While some cautiosly endorse this approach [28], Mathew Celina concluded, that mechanistic changes at the heightened temperatures used in OIT experiments as well as diffusion limited oxidation and liquid-state vs. solid-state kinetics can have a major impact on the prediction results in his review of polymer oxidation and its relationship with materials performance and lifetime prediction [29].

The corresponding standard [41] provides two methods of analysis for the onset of degradation. The preferred method is the standard tangent method shown in Figure 2.5, resulting in an onset-time t_4. However, if degradation in the sample

occurs slowly, the exothermal oxidation peak can display a shoulder, resulting in a falsely lengthened OIT. This is often observed in samples containing hindered amine light stabilizers (HALS). In order to obtain valid in spite of this, the standard offers an alternative offset method. Here, the baseline is offset by -$0.05\,\mathrm{W\,g^{-1}}$ and thus making it possible to avoid the oxidation peak's shoulder.

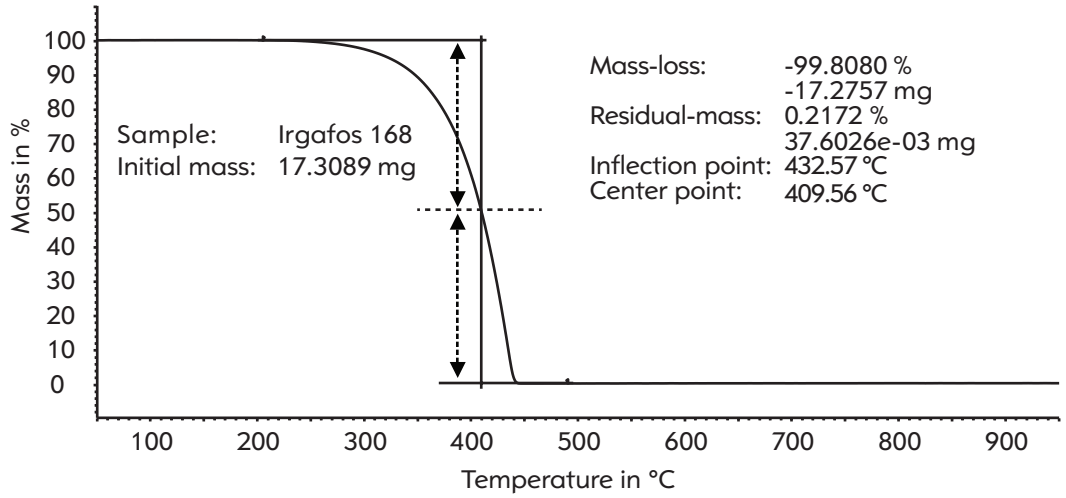

FIGURE 2.6: Example for a TGA experiment based on Irgafos 168

2.1.4 Thermogravimetric Analysis - TGA

Next to DSC, thermogravimetric analysis is the second widespread thermoanalytical method common to materials testing labs. While DSC measures the heat flow necessary to heat a sample at a specified rate, TGA measures a samples mass while heating. It essentially is a microbalance within a furnace. It gives us information about the physical and chemical behavior of a substance throughout a certain temperature range. Usually, it ranges from ambient temperature to $1000\,°\mathrm{C}$ at a constant rate in most polymer applications. The conditions used for this thesis correspond to DIN EN ISO 11358-1 [42].

TGA allows the investigation of a polymer samples thermal degradation behavior, it's degradation mechanisms and kinetics and the amount of volatile additives and inorganic filler used. The general approach is weighing in a small amount of sample (i.e. $10\,\mathrm{mg}$ to $100\,\mathrm{mg}$ [42]) and heating the sample at a constant rate from ambient to high temperatures in a choice of inert (N_2), oxidizing (air or O_2) or reducing atmosphere ($8\,\%$ to $10\,\%$ H_2 in N_2), depending on the issue. The obtained data is usually plotted either as thermogravimetric TG curve (mass-loss vs. temperature or time as seen in Figure 2.6) or as differential thermogravimetric DTG curve (rate of mass-loss vs. temperature or time).

The analysis of TG curves is done using the baseline-tangent procedure shown in Figure 2.6. The center point is determined by the intersection point of the midway line between the two baselines with the TG curve.

2.1.5 Three-point flexural test

Flexural stress is common in the service life of plastic components and structures. From doorhandles to bumpers and even brake pedals in the case of Lanxess' award winning Tepex pedal. For this reason, among others, the three-point flexural test is a standard method in modern plastics testing.

As seen in Figure 2.7, the basic setup is a simple one. A standardized specimen (DIN EN ISO 178 [43]) of 80 x 10 x $4\,\mathrm{mm}^3$ is mounted on two variable radii which are fastened on two counterforts mounted on a positioning slide. From above, a bending fin is pressed onto the specimens center with a defined flexural force F, bending it until it breaks or the resulting strain remains constant. The distance L between the radial contact points is important, as it will determine whether the test delivers results predominantly from flexural stress, or mixed with shear stress. It's ideal value is dependent on the specimens size:

$$L = (16 \pm 1)h \tag{2.7}$$

In the case of a three-point flexural test according to DIN EN ISO 178, this leads to a distance of $64 \pm 1\,\mathrm{mm}$.

The test provides three values. The modulus of elasticity in bending or bending modulus E_f, flexural stress σ_f and flexural strain ε_f.

The bending modulus, also called flexural modulus, is defined as the stress to strain ration in the first $0.05\,\%$ to $0.25\,\%$ i.e. the elastic portion of flexural deformation. It is usually calculated as secant modulus, in analogy to the young modulus, with f as the middle deflection and w and h as the specimens width and height (equation 2.8).

$$E_f = \frac{FL^3}{4fwh^3} = \frac{\sigma_2 - \sigma_1}{\varepsilon_2 - \varepsilon_1} \tag{2.8}$$

The flexural stress σ_f is determined by measuring the restoring force exerted by the specimen. When referring to the flexural stress measured during a three-point flexural test, the maximum registered stress σ_{fM} is usually meant, which is the definition of the materials flexural strength. In the case of brittle samples (Figure 2.8a, σ_{fM} can equal the flexural stress at yield point σ_{fB}. It can be calculated using the maximum flexural force exerted during the experiment (equation 2.9).

$$\sigma_{fM} = \frac{3F_{max}L}{2wh^2} \tag{2.9}$$

Finally, the flexural strain ε_f is calculated from the specimens size and the middle deflection at either σ_{fB}, σ_{fM} or σ_{fC}, depending on the specimens elasticity. For the experiments performed in this thesis, ε_{fM} was used, since all samples were in the medium elasticity range.

$$\varepsilon_{fM} = \frac{6f_M h}{L^2} \tag{2.10}$$

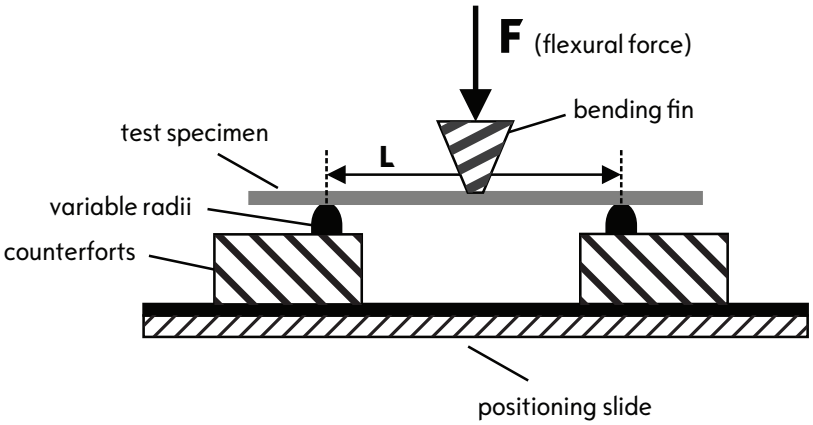

FIGURE 2.7: Schematic of a three-point flexural test

Three-point flexural test vs. Tensile Test

Another standard test for plastic components is tensile testing. Here, samples are clamped into the tensile setup on the universal testing machine also used for flexural testing. However, instead of bending the sample, it is pulled along it's main axis until it breaks. The machine records the exerted force and the resulting elongation. From this, the Young-modulus, yield strength and several other properties can be calculated.

When comparing the tensile test to the three-point flexural test in regard to aging-induced mechanical deterioration, one has to take into account, that aging effects begin to show in the samples outer layers. Therefore, it is logical, that the testing method used to monitor the samples degradation should be sensitive to changes it the samples surface. For the flexural test this is more true than for the tensile test, since the latter exerts strain along the samples main axis and is therefore more dependent on the samples core, while the flexural test's perpendicular strain is more dependent on the samples surface.

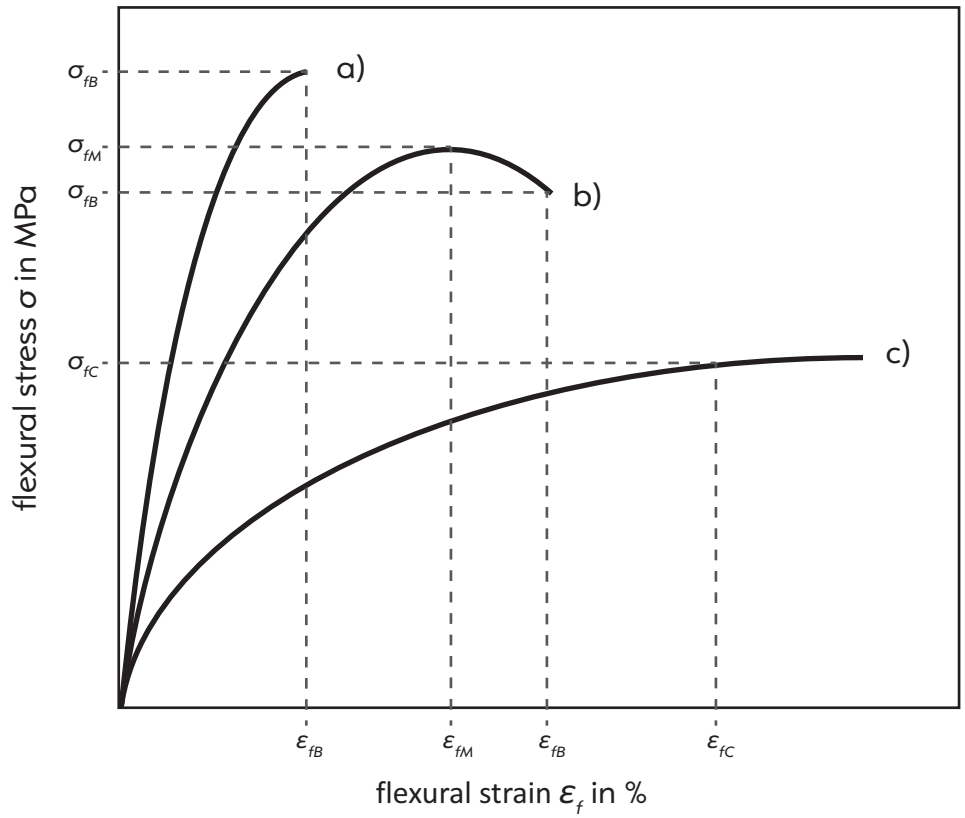

FIGURE 2.8: Three-point flexural test of samples ranging from brittle (a) to flexible (c)

2.2 Materials Chemistry

2.2.1 Polymers

In this work, two polymers were used for sample manufacturing. Polyamide-6 and polypropylene. The following section will give an overview of these polymers and discuss their degradation mechanisms, both thermo-oxidative as well as pyrolytically in an oxygen free environment.

Also, polymer additives in general and specifically those used in this work will be discussed concerning their general properties and stabilizing mechanisms.

Polyamide-6

The first artificial polyamide was invented by Wallace H. Carothers in 1935 for the American chemical company DuPont. He successfully harnessed the polycondensation of adipic acid and hexamethylenediamine, creating polyamide 66, also known as Nylon. A few years later in 1938, after carefully studying the patent documents, Paul Schlack, working for the German IG Farben group in Berlin, found a way to polymerize ε-caprolactam in the presence of water via a ring-opening mechanism, yielding polyamide-6 or Perlon. Next to cheap pantyhose, these polymers facilitated

the production of parachutes for the air force without being dependent on Japanese silk during the war.

In the automotive industry today, polyamides are widely used where structural integrity is a key factor (usually glass or carbon fiber reinforced) and in thermally demanding environments as found in all "under the hood" applications.

While PA-6 and PA-66 share the same molecular formula $(C_6H_{11}ON)_n$, there is a subtle structural difference leading to different properties. While in PA-66 every carbonamide group can form H-bonds to one another, this is only true for every second carbonamide group in PA-6. This leads to a lower melting point ($220\,^{\circ}C$ for PA-6 vs. $255\,^{\circ}C$ for PA-66) and a higher uptake of water due to the lower structural integrity [44].

When producing asymmetric polyamides such as PA6, one can generally choose between two routes. The ring-opening mechanism using a lactame as the monomer, or a polycondensation starting from the ω-aminoacid. Which route is industrially relevant mostly depends on the availability of the monomer. In the case of PA6, ε-caprolactam is more available then aminocaproic acid.

The ring-opening polymerization can be catalyzed hydrolytically, anionically or cationically [45]. Industrially manufactured PA6 is generally produced hydrolytically (Figure 2.9 b-d) with the exception of anionic catalysis in the case of in-cast polymerization applications. The first step of the reaction is the hydrolysis of the ring molecule at high temperatures, leading to Aminocaproic acid. Subsequently, both condensation reactions of the amino acids as well as polyaddition reactions of the amino acid to ε-caprolactam take place. The latter again leads to an opening of the ring and is thought to be the main reaction in the formation of the final polymer chain [46]. In addition to chain growth, transamidation reactions lead to the typical distribution in molecular weight.

As seen in Figure 2.9 a, the monomer ε-caprolactam is mainly synthesized from cyclohexanone with hydroxylamine forming an oxime. In a second step this oxime reacts via Beckmann-rearrangement forming the lactame. Approximately $90\,\%$ of the world supply is manufactured this way. About $10\,\%$ is obtained from cyclohexane and nitrosyl chloride, also forming an oxime which is subsequently subjected to Beckmann-rearangement. The reason for this alternative is cyclohexane being the cheaper raw material.

Polypropylene

The first successful polymerization of propylene was published in 1951 by the American chemists John Paul Hogan and Robert Banks, both working for Phillips Petroleum. Three years later, in 1954, Giulio Natta developed stereospecific mixed catalysts based on Karl Ziegler's work at the Max Planck institute in Muehlheim. They enabled him to synthesize isotactic polypropylene (iPP), a highly ordered polymer. Independantly, Karl Rehn reached the same goal. However, Giulio Natta and the

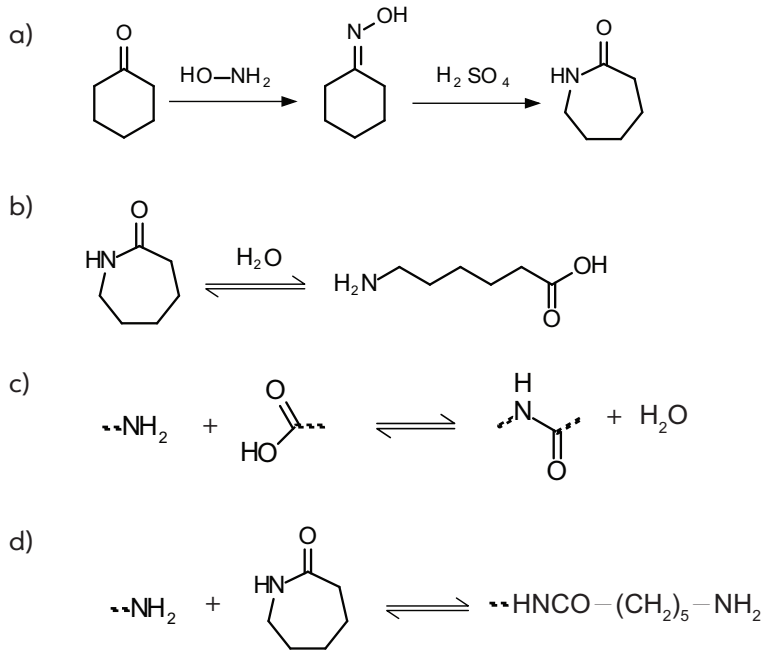

FIGURE 2.9: Synthesis of ε-caprolactam (a) and PA6 (b-d)

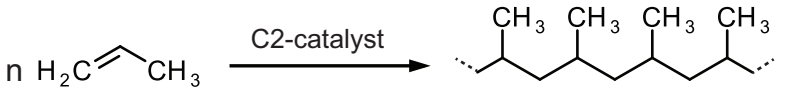

FIGURE 2.10: Synthesis of isotactic polypropylene

Montecatini Chemical Company were first to patent the process. Today, polypropylene is surpassed only by LDPE in tons per year production reaching 45.1 million tons in 2007, grossing approximately 65 billion USD in revenue. With a growth rate of roughly $6\,\%$ p.a., polypropylene is expected to reach 145 billion USD in 2019 according to a study by Ceresana [47]. For the automotive industry, polypropylene and blends thereof are the most important plastics for interior applications.

Modern catalysts for the production of polypropylene are mainly based on metallocenes [44]. Depending on their stereo chemistry it is possible to synthesize all types of PP. For example, the isotactic polypropylene used in this work can be synthesized with a C2-symmetric Kaminsky catalyst [48], while C1 or C3 symmetry would lead to atactic or syndiotactic products, respectively. The polymer's molecular weight and polydispersity can also be modulated by the choice of catalyst. If desired, it is possible to achieve tightly distributed high molecular weights, leading to high crystallinity and stiffness. The resulting brittleness can be countered by blending with EPDM or PE allowing the production of high quality components, usually via injection molding.

Compared to polyamide-6, iPP has a considerably lower melting point of $160\,^{\circ}\mathrm{C}$ to $165\,^{\circ}\mathrm{C}$. This is due to the weaker intramolecular interactions of the polymer chains. As seen in Figure 2.10, polypropylene contains no polar groups capable of

forming hydrogen bonds, and therefore relies solely on Van-der-Waals interaction.

Polypropylene is also very susceptible to oxidation due to the tertiary carbon found in every repeating unit. They readily sacrifice their sole hydrogen when exposed to attack by radicals such as oxygen. For this reason, stabilization is a very important aspect in the production, processing and use of polypropylene. A base stabilization containing low amounts of phenolic and phosphitic antioxidants is usually added directly after polymerization.

Degradation Mechanisms

For any kind of polymer application it is inherently important, that the polymer's properties remain unaltered for the duration of use. Important in this respect are optical appearance, odor and mechanical properties such as impact resistance or elasticity. To protect the polymer's characteristics from deterioration, one has to understand the various forms of degradation. The most important ones being thermo-oxidative, UV-induced, thermal and hydrolytic degradation. Based on the scope of this work, the following paragraphs will cover both thermo-oxidative and thermal degradation.

Thermo-Oxidative Degradation The oxidation of polymers at elevated temperatures is the most important degradation pathway for most polymer applications, especially when disregarding extreme situations such as constant direct sunlight or strongly hydrolytic environments such as engine cooling circuits in regard to polar polymers (i.e. polyamides). It has been shown, that virtually no degradation is observed below processing temperatures in oxygen-free environments [49, 50], while introducing oxygen to the gas stream in a TGA or DSC experiment significantly lowers the temperature at which the polymer begins to decompose . Also, in oxygenic environments, a correlation between oxygen consumption and polymer degradation has been observed [51].

This leads to the necessity of using process stabilizers during processing, such as extrusion or injection molding. The polymers are heated to high temperatures and subjected to oxygen, according to Epacher et al. [52]. They claim, that small amounts of oxygen adsorb to the polymers surface and consequently lead to degradation during processing despite degassing measures.

For many polymers, polyolefins in particular, the decomposition mechanism is radical in nature (Figure 2.11). The initiation step is the thermally induced formation of an alkyl radical from the polymer chain. It is followed by the propagation reaction, which consists of the oxidation of the alkyl radical to form a peroxide radical (k_1), which in a second step abstracts a hydrogen atom from a polymer chain (k_2). The second step is much faster than the first [53], making the rate-determining step of the propagation reaction directly dependent on the C-H bond strength of the polymer chain. This explains why polypropylene is oxidized at a faster rate than

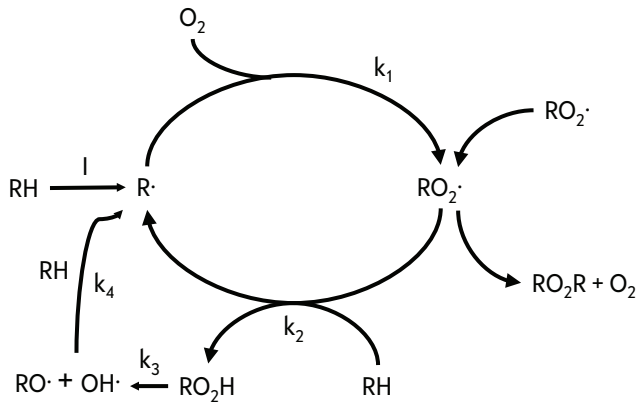

FIGURE 2.11: Thermo-oxidative degradation mechanism according to D.R. Kohler [58]

polyethylene, since hydrogen abstraction leads to the formation of more stable tertiary radicals. The hydro-peroxides form in the second step of the propagation reaction play an important role, as their decomposition is thought to be the incitement of the auto-oxidation process [54]. This reaction can be further catalyzed by transition metal ions such as copper, iron or titanium, further fueling the polymers degradation as was shown by Fritz Haber and Joseph Weiss [55]. The termination reaction of the mechanism strongly depends on the formed radicals. In case of polypropylene, the tertiary peroxide radicals can only react to dialkyl peroxides and oxygen. However, isotope studies have shown, that this reaction is of minor importance [56]. For polyethylene, Russell et al. proposed a termination reaction leading to an alcohol and a ketone [57] as well as the formation of double bonds and cross-linkage from alkyl radicals.

Pyrolytic Degradation For the oxygen free thermal degradation taking place in the pyrolyzer-unit of a typical pyrolysis-GC/MS, there are three main degradation mechanisms to consider. Which one plays the dominant role is dependent on the type of polymer and the bonds it is comprised of. For polyolefines, all bonds are more or less equivalent. Therefore, its degradation follows a random scission mechanism leading to oligomers of varying length. In a total ion chromatogram (TIC) of a pyrolyzed polyolefin such as polyethylene, one finds a spectrum of triplet signals representing those alkane oligomers with their respective alkenes and dienes. For a polymer such as polyamide-6, the weakest link is the bond between two monomers in the polymer backbone. For this reason, the dominant degradation mechanism is an unzipping or depolymerization, with the original monomer being the main degradation product. Finally, some polymers exhibit their weakest link between the backbone chain and the side-group. For polyvinyl chloride, it is the C-Cl bond which breaks first, leading to a β-elimination of HCl and a highly saturated polymer chain. This is then fragmented and degrades to a range of aromatics such as benzene, toluene etc. While this describes the main reactions taking place in an inert atmosphere, there is a plethora of other thermally driven chemistry taking place,

dependent on the conditions and the polymers components such as additives, water or impurities.

2.2.2 Additives

In polymer processing and application, additives are essential. Their purpose ranges from protecting the polymer during processing and during it's lifetime to achieving the desired optical and haptic properties, preventing combustion and making it's surface anti-bacterial. After giving a general overview, the additives used for this work will be viewed in more detail.

While there are several different extensive monographs on polymer additives, the *Handbuch Kunststoff-Additive* by Maier and Schiller [59] as well as Murphy's *Additives for plastics handbook* [60] were predominantly used in this work.

Commonly, additives are grouped according to their purpose. Important representatives are antioxidants, light stabilizers, proton scavengers, colorants, flame retardants and surfactants such as anti-scratch additives. Within individual categories it is also customary to characterize subgroups by their substance class. Prominent examples are phenolic and phosphitic antioxidants or hindered amine light stabilizers (HALS). As can be seen in the following paragraphs, a further classification according to their functioning principle is also possible. In this work e.g. we differentiate between primary and secondary antioxidants.

The amount of additives used in polymers varies based on the type of polymer and additive. However, most additives are used in the one-tenth of a percent range. Exceptions can most notably be found among flame retardants, where mass fractions of $10\,\%$ to $20\,\%$ are not uncommon, especially when a UL94 compliant V-0 rating is required.

Antioxidants

In section 2.2.1*Thermo-Oxidative Degradation* it was mentioned, that oxidation is the most important degradation pathway in most polymer applications. A direct consequence of this is the importance of antioxidants among other additives. Without them, most polymers would not be suitable for any long-term application or even processing of any sort. The importance of antioxidants also becomes clear when taking a look at global consumption. In 2007, more than 300 kilotons of antioxidants were used globally, grossing approximately 2 billion USD in sales revenue [59]. About $80\,\%$ of these antioxidants being phenolic and phosphitic ($50\,\%$ each).

As mentioned above, antioxidants can be classified by more than their chemical structure. They also differ in their functioning principle, allowing them to be divided into primary and secondary antioxidants.

Primary Antioxidants Radical scavengers have a very important role in preventing polymer oxidation. Figure 2.11 shows the cycle of oxidation and autoxidation.

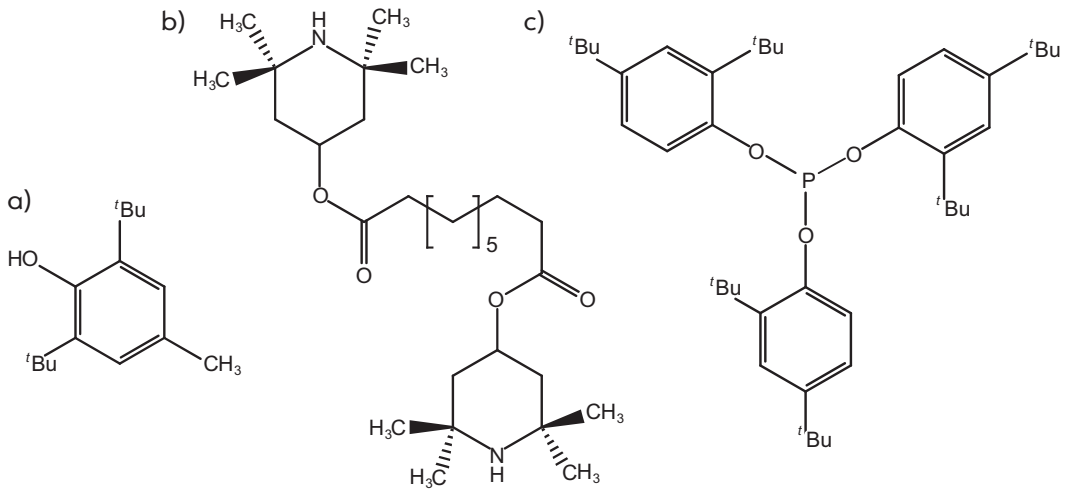

FIGURE 2.12: Antioxidants: a) BHT, b) Tinuvin 770, c) Irgafos 168

As can be seen, radicals are a major contributor to this cycle. Simply put, alkyl radicals develop during aging and react with oxygen to form peroxyradicals. This cycle can be interrupted by scavenging the alkyl radicals, converting them to stable radicals. The long-term stabilization effect of HALS (Figure 2.12 b) is based on this (therefore, some sources refer to them as HAS - hindered amine stabilizers instead of HALS - hindered amine light stabilizers). Another option is deactivating peroxyradicals through proton donation as is the case for phenolic stabilizers(Figure 2.12 a). The phenolic radical formed in this process is generally stabilized by tertiary butyl groups to either side of the hydroxy group.

In summary, antioxidants functioning as radical scavengers, whether by actually reacting with an alkyl radical or by donating a proton to a peroxyradical, are referred to as *primary antioxidants*.

Secondary Antioxidants The role of secondary antioxidants is to prevent the decay of the hydroperoxides formed by phenolic antioxidants into other highly reactive radicals such as hydroxyl radicals ($HO^{\bullet}$) or alkoxyl radicals ($RO^{\bullet}$). This is achieved by oxygen scavengers such as the phosphite ester (2,4-di-tert-butylphenyl)phosphite (Irgafos 168, Figure 2.12 c). The driving force behind this mechanism being the formation of a PO double bond.

The hydroperoxide formation of the phenolic antioxidant followed by the oxygen scavenging by the phosphitic antioxidant is often described as a synergistic process. This is a very important reason why they are often used in combination, ideally also combined with an alkyl scavenger such as the prominent HALS Tinuvin 770.

Chapter 3

Experimental

3.1 Sample manufacturing

The experiments performed within the scope of this thesis required three sets of standard samples. For the Py-GC/MS method development a simple polyamide-6 formulation was chosen. For the color-dependent oxidation studies, two differently colored, application-related polypropylene formulation, which varied only in the amount of carbon black were used. The uncolored (natural) variant was also used in the Py-GC/MS method development. Finally, for the DSC/OIT vs. Oven/OIT project, three differently stabilized, application related and uncolored polypropylene samples were produced.

The polyamide-6 samples were extruded at $240\,^{\circ}\mathrm{C}$ to $260\,^{\circ}\mathrm{C}$ with a rotational speed of $250\,\mathrm{rpm}$. Degassing was performed at $180\,\mathrm{mbar}$.

The polypropylene samples were extruded at $180\,^{\circ}\mathrm{C}$ to $205\,^{\circ}\mathrm{C}$ with a rotational speed of $400\,\mathrm{rpm}$. Degassing vacuum was applied but no details were provided.

Injection molding was done after drying for $8\,\mathrm{h}$ at $60\,^{\circ}\mathrm{C}$. Temperatures ranged from $200\,^{\circ}\mathrm{C}$ to $230\,^{\circ}\mathrm{C}$. The polymer mass was injected with $200\,\mathrm{bar}$ injection pressure and the injection molding tool operated at $600\,\mathrm{kN}$ clamping force.

TABLE 3.1: Formulation: PA6 standard sample

Material:	
Polyamide-6 / Pellets	97%
PA-6 / Mixing-powder	2%
Irganox 1098	0.4%
Irgafos 168	0.4%
Tinuvin 770	0.2%

The polyamide-6 sample (Table 3.1) is comprised of the base polymer Ultramid B 27E, an unreinforced polyamide-6 type produced and supplied by BASF SE Ludwigshafen. In pellet and powder form respectively, it was used as the basis and mixing powder for the polyamide-6 formulation. The additives used for this sample are Irganox 1098, Irgafos 168 and Tinuvin 770. Irganox 1098 (Figure 3.1 e) is primary phenolic antioxidant containing two phenolic groups and equipped with two amide groups to optimize it for use in polyamides. It is used as a long term

temperature stabilizer (LTTS). Irgafos 168 (Figure 3.1 a) is one of the most widely used phosphitic secondary antioxidants. It's main use is as a process stabilizer at high temperatures. Tinuvin 770 (Figure 3.1 b) is a also widely used hindered amine light stabilizer containing two tetra-methyl piperidine groups. It's light stabilizing functionality is based on the radical scavenging capability of the piperidine, which also enables it's use as a LTTS. All additives were supplied by BASF Schweiz AG Basel. Compounding of the sample was performed in the BASF pilot plant in Ludwigshafen.

TABLE 3.2: Formulation: PP standard colored samples

Material:	**Natural**	**Black**
Moplen EP 300N	82%	80%
Steamic T1CA	15%	15%
Black-MB 40%	-	2%
Acrawax C	0.2%	0.2%
Moplen HF501N	2.1%	2.1%
Irganox 1076	0.3%	0.3%
Irgafos 168	0.23%	0.23%
Tinuvin 770	0.20%	0.20%
Irganox 1010	0.05%	0.05%

The colored polypropylene samples (Table 3.2) are based on Moplen EP300N, a pelletized, heterophasic impact-modified PP/PE copolymer stabilized with $0.05\,\%$ Irganox 1010 and $0.1\,\%$ Irgafos 168 (included in the table), produced and supplied by Lyondell Basell. Moplen HF501N, a unstabilized, non pelletized PP homopolymer powder was used as mixing powder. The base package also contains Steamic T1CA (finely ground talcum), a $40\,\%$ carbon black masterbatch with PP substrate containing the *Raven PFEB* pigment by Birla Carbon (supplied by Polyplast Müller) and Acrawax C (lubricant). The carbon black pigment was produced via the furnace process, has a low oxygen and sulfur content on it's surface and a neutral pH. The external surface area (STSA - statistical thickness surface area), determined using the method described in ASTM D6556 [61], is $(91 \pm 7)\,\mathrm{m^2\,g^{-1}}$

In addition to the base stabilization, the additive package contains Irganox 1076, Irgafos 168 and Tinuvin 770. Irganox 1076 (Figure 3.1 c) is a primary phenolic antioxidant containing one phenol group for stabilization and a C_{18}-chain for improved solubility in non-polar polymers such as polypropylene. Irganox 1010 (Figure 3.1 d) is also a primary phenolic antioxidant containing four phenolic groups. Like Irganox 1076 and 1098 it is based on the classic antioxidant butylhydroxytoluene (BHT), but increased in size to reduce mobility within the polymer. All additives were supplied by BASF Schweiz AG Basel. The base package was supplied by Lyondell-Basell in Bayreuth. Sample compounding and injection molding of the type 1A test specimens according to DIN EN ISO 527-2 [62] were carried out by the Fraunhofer Institute für Chemische Technologie (ICT) in Pfinztal. The test specimens were modified

according to DIN EN ISO 178 [43] using a Mutronic DIADISC 4200 R cut-off saw.

TABLE 3.3: Formulation: PP standard OIT samples

Material:	V-1	V-2	V-3
Moplen EP 300N	80%	80%	80%
Steamic T1CA	15%	15%	15%
Acrawax C	0.2%	0.2%	0.2%
Moplen HF501N	4.4%	4.4%	4.3%
Irganox 1010	**0.35%**	0.15%	0.15%
Irgafos 168	0.2%	**0.4%**	0.2%
Irganox PS 802	0.0%	0.0%	**0.3%**

The polypropylene samples with varying stabilization (Table 3.3) for the OIT experiments are made up of the same base package as the colored samples. However, no carbon black masterbatch was used. The samples contain varying amounts of Irganox 1010, Irgafos 168 and Irganox PS 802. Irganox PS 802 (Figure 3.1 f) is a sulfide based secondary antioxidant. All additives as well as the base package were provided by Lyondell Basell. Sample compounding and injection molding of the type 1A test specimens according to DIN EN ISO 527-2 [62] as well as modification according to DIN EN ISO 178 [43] were performed in the Lyondell Basell pilot plant in Bayreuth.

TABLE 3.4: All additives used

Additive	Molar mass in g/mol	Category	CAS-#
Irganox 1098	637	Phenolic AO (prim.)	23128-74-7
Irganox 1010	1178	Phenolic AO (prim.)	6683-19-8
Irgafos 168	647	Phosphitic AO (sec.)	31570-04-4
Tinuvin 770	481	HALS (prim.)	52829-07-9
Irganox 1076	531	Phenolic AO (prim.)	2082-79-3
Irganox PS 802	683	Sulfidic AO (sec.)	693-36-7

Figure 3.1 shows all additives used for the manufacturing of the standard samples mentioned in section 3.1. Table 3.4 provides their molar mass, melting point and CAS number.

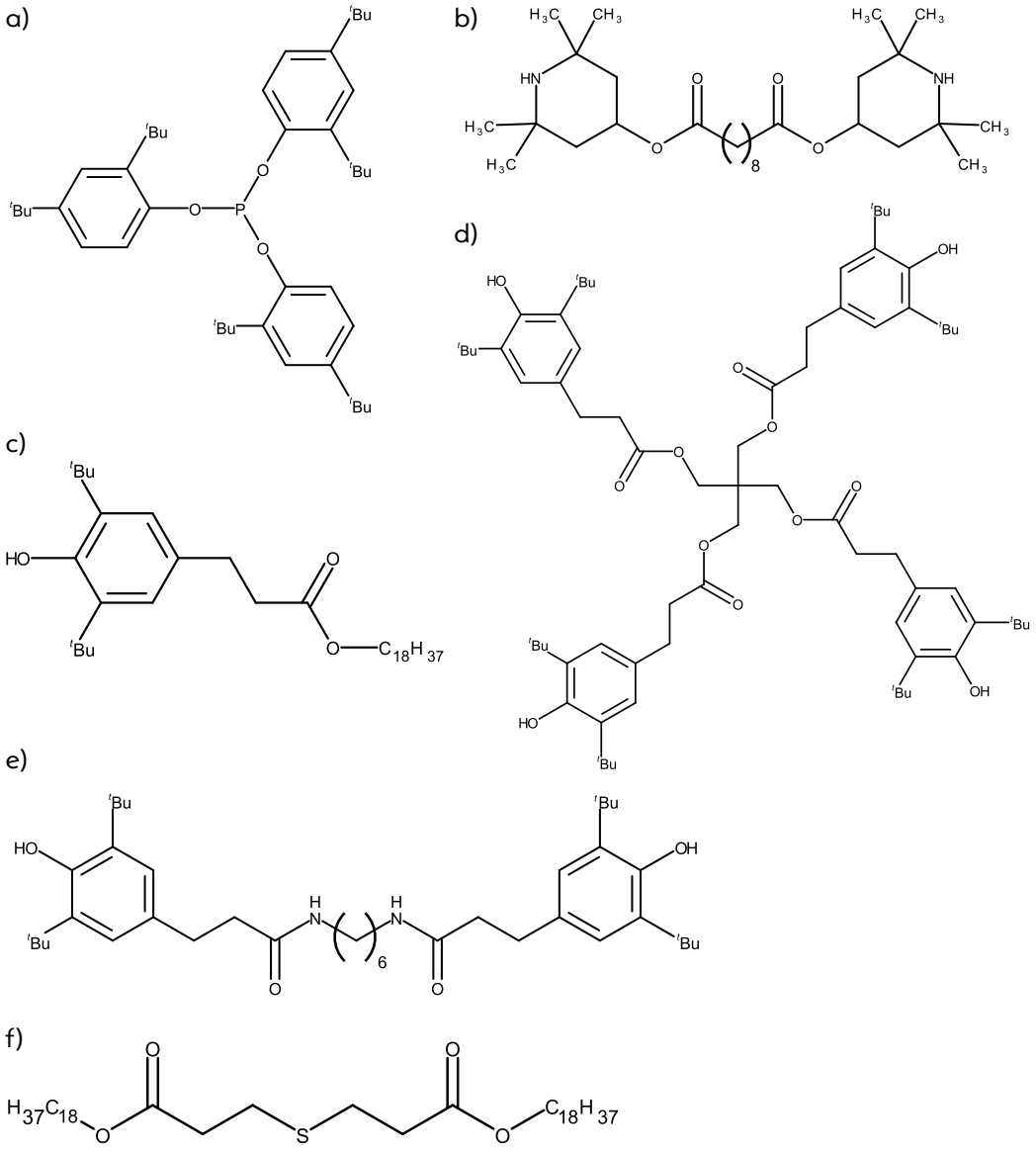

FIGURE 3.1: Structures of a) Irgafos 168, b) Tinuvin 770, c) Irganox 1076, d) Irganox 1010, e) Irganox 1098, f) Irganox PS 802

3.2 Pyrolysis-GC/MS

All pyrolysis measurements were performed on a mixed Agilent/Gerstel setup consisting of an Agilent 7890A GC system with a 5975C mass spectrometer. The GC was equipped with an Agilent J&W DB-5ms Ultra Inert $30\,\mathrm{m}$ x $0.25\,\mathrm{mm}$ x $0.25\,\mu\mathrm{m}$ ($5\,\%$ diphenyl, $95\,\%$ dimethyl) capillary column. The pyrolysis setup consisted of a Gerstel MPS autosampler, pyrolysis module, TDU thermal desorption unit and CIS4 cold injection system. The carrier gas used was helium ($99.999\,\%$). Data acquisition and instrument control was done using the Agilent *MSD Chemstation E.02.02.1431* software enhanced with the Gerstel *Maestro version 3.5* control module.

The pyrolysis temperature varied between $450\,^{\circ}\mathrm{C}$ to $600\,^{\circ}\mathrm{C}$ depending on the experiment and the pyrolysis time was $40\,\mathrm{s}$ consistently. During the pyrolysis / desorption process, the TDU was kept at a constant $300\,^{\circ}\mathrm{C}$ for two minutes. Then it was cooled to $40\,^{\circ}\mathrm{C}$ once the GC run had started to prevent further desorption. The CIS unit and TDU transfer line were both constantly heated to $320\,^{\circ}\mathrm{C}$. A split ratio of 1:50 was used for all experiments. An inlet pressure of $48.7\,\mathrm{kPa}$ was applied, resulting in a column flow of $1\,\mathrm{mL\,min^{-1}}$ at an average velocity of $36\,\mathrm{cm\,s^{-1}}$ and a hold-up time of $1.38\,\mathrm{min}$.

The GC oven's initial temperature was $40\,^{\circ}\mathrm{C}$, which was held for $2\,\mathrm{min}$. It was then raised to a maximum temperature of $320\,^{\circ}\mathrm{C}$ at a rate of $10\,^{\circ}\mathrm{C\,min^{-1}}$. Subsequent hold time was $29\,\mathrm{min}$ allowing all high-boiling pyrolysis products to elute.

The GC-MSD transfer line was heated to $330\,^{\circ}\mathrm{C}$. The MS source was kept at $230\,^{\circ}\mathrm{C}$ and the quadrupoles at $150\,^{\circ}\mathrm{C}$. The pressure inside the MSD was approximately $5 \times 10^{-4}\,\mathrm{Pa}$.

In scan mode the m/z range was 10 to 550 with a threshold of 50 and a solvent delay of $1\,\mathrm{min}$. The scan rate was $2.71\,\mathrm{scans/s}$.

IN SIM mode two to three ions were chosen for each peak. The default dwell time of $100\,\mathrm{ms}$ per ion resulted in a good compromise between sensitivity and number of data points per second, the latter being important for accurate quantification. Depending on the number of ions monitored, this gave $3.1\,\mathrm{cycles/s}$ to $4.5\,\mathrm{cycles/s}$. The exact SIM parameters for the methods used in this work can be found in Table 3.5 ($450\,^{\circ}\mathrm{C}$), 3.6 ($600\,^{\circ}\mathrm{C}$ - PA6), 3.7 ($600\,^{\circ}\mathrm{C}$ - PP) and 3.8 ($600\,^{\circ}\mathrm{C}$ - PP aged).

TABLE 3.5: SIM parameters: 450_SIM.M

Start time	**Group**	**Cycles $\mathbf{s^{-1}}$**	**Ion 1**	**Ion 2**	**Ion 3**
0.0 min	Tin 770	4.5	124.1	98.1	
10.0 min	If 168	4.5	206.1	191.1	
22.0 min	Tin 770	4.5	140.1	124.1	
30.0 min	If 168	4.6	441.3	147.1	
31.9 min	Ix 1076	3.1	530.5	515.5	219.1

TABLE 3.6: SIM parameters: 600_SIM_PA6.M

Start time	Group	Cycles s^{-1}	Ion 1	Ion 2	Ion 3
0.0 min	Tin 770	4.5	124.1	107.1	
10.0 min	Ix 1098	3.1	176.1	161.1	133.1
14.8 min	If 168	4.5	206.1	191.1	
16.0 min	Ix 1098	4.5	232.1	217.1	
19.0 min	Ix 1098	4.5	259.1	244.1	
22.0 min	Tin 770	4.5	140.1	124.1	
27.0 min	Tin 770	3.1	342.1	140.1	124.1
30.0 min	If 168	4.6	441.3	191.1	

TABLE 3.7: SIM parameters: 600_SIM_PP.M

Start time	Group	Cycles s^{-1}	Ion 1	Ion 2	Ion 3
0.0 min	Tin 770	4.5	124.1	107.1	
14.4 min	Ix 1010 & 1076	3.1	176.1	161.1	133.1
14.8 min	If 168	4.5	206.1	191.1	
16.0 min	Ix 1010 & 1076	4.5	232.1	217.1	
17.5 min	Ix 1076	3.1	252.1	111.1	97.1
19.0 min	Ix 1010	4.5	292.1	277.1	
23.0 min	Tin 770	4.5	140.1	124.1	
28.0 min	Tin 770	3.1	342.1	140.1	124.1
30.0 min	If 168	4.6	441.3	191.1	
31.0 min	Ix 1076	4.5	530.5	515.5	

TABLE 3.8: SIM parameters: SIM_Aging.M

Start time	Group	Cycles s^{-1}	Ion 1	Ion 2	Ion 3
10.0 min	Ix 1010	3.1	176.1	161.1	133.0
14.7 min	If 168	4.5	206.1	191.1	-
16.0 min	Ix 1010	4.5	217.1	232.1	-
19.0 min	Ix 1010	4.5	292.1	277.1	-
30.0 min	If 168	3.1	441.3	147.1	191.1
31.7 min	If 168	4.6	316.2	191.1	-

Additives The pyrolysis temperature series on additives, the additive library build up and all calibration measurements were performed with the pure additives solved in GC grade dichloromethane (MS Suprasolv, purchased from Sigma Aldrich). $1\,\%$ stock solutions were prepared and diluted to $0.04\,\%$ for the $450\,°C$ quantification and $0.02\,\%$ for all other measurements. The stock solutions were prepared using a Mettler Toledo XP205 DeltaRange analytical scale with a measurement accuracy of $0.01\,\mathrm{mg}$ and standard $10\,\mathrm{mL}$ volumetric flasks.

The samples were analyzed in Gerstel slitted quartz vials for liquid and solid samples filled with some quartz wool. Pipetting of the samples was done with the Gilson positive displacement pipette Microman M10 ($1\,\mu L$ to $10\,\mu L$) using the CP10 $10\,\mu L$ pipette tips.

For every measurement point, five samples were prepared. In the case of the additive library build up, eight samples were used per measurement point.

Polymer samples All solid polymer samples were ground to powder form using the cryo mill. For the analysis, $200\,\mu g$ to $300\,\mu g$ of the polymer powder was weighed into Gerstel slitted quartz vials for liquid and solid samples using the Mettler Toledo XP205 DeltaRange analytical scale and a Gerstel powder dosage unit. Some quartz wool was then inserted into the vials to insure no polymer powder was still clinging to the vial walls. As with the additive measurements, five samples were prepared for every measurement point.

3.3 DSC/OIT

The DSC/OIT measurements were performed on a Mettler Toledo DSC 3+ STAR^e System instrument according to DIN EN ISO 11357-6 [41]. The samples were cut from the standard test specimens produced using a Reichert-Jung Polycut E microtome and weighed on a Mettler Toledo M3 microbalance. Care was taken to always cut the sample from the same location on the specimens midpoint and with a narrow weight distribution to prevent systematic differences between measurements.

Dynamic OIT tests yielded $210\,^{\circ}\mathrm{C}$ as the optimum temperature for the unaged standard samples. However, since the DSC/OIT was supposed to be monitored through the course of the aging experiments and prior test revealed the exponential decay of these values with aging duration, a lower temperature ($200\,^{\circ}\mathrm{C}$) was chosen in order to expand the range of possible experiments. Although the lower temperature yielded OITs for the unaged samples which lay distinctly above the range recommended in the norm, this was deemed to be the best solution.

The resulting method can be seen in Figure 2.5 (fundamentals). To begin, the sample chamber which contained the approximately $10\,\mathrm{mg}$ samples was purged with $50\,\mathrm{mL\,min^{-1}}$ N_2 at $50\,^{\circ}\mathrm{C}$ for five minutes. The sample was then heated to $200\,^{\circ}\mathrm{C}$ with a rate of $20\,^{\circ}\mathrm{C\,min^{-1}}$. At $200\,^{\circ}\mathrm{C}$ the sample was allowed to equilibrate for another five minutes, still in $50\,\mathrm{mL\,min^{-1}}$ N_2. The atmosphere was then changed to $50\,\mathrm{mL\,min^{-1}}$ pure O_2. This switch signifies the begin of the OIT. The measurement is ended $2\,\mathrm{min}$ after the maximum of the exothermal oxidation peak has passed. The data was analyzed using the offset-method described in 2.1.3. This method proved to be better suited for the measurements performed in this work.

Five measurements each were performed on the unaged samples in order to determine the accuracy of the experiment (Figure 4.32). For the aged samples two measurements were performed. When the deviation of the two measurements was greater than expected, the measurements were repeated.

The software *STAR^e Version 15.00* was used for instrument control, data acquisition and analysis.

3.4 Oven-aging

Oven aging was carried out according to DIN EN ISO 4577 [63] with standard test specimen manufactured according to DIN EN ISO 178 [43]. The test specimen were prepared by a hole with a $1.5\,\mathrm{mm}$ diameter on one end, using a Bosch CSB 450-2E hammer drill. The samples were then hung inside Binder FD 56 air circulating ovens as shown in Figure 3.2 using stainless steel hooks. Stainless steel was used due to it's relatively low thermal conductivity of $15\,\mathrm{W\,mK^{-1}}$. The spatial uniformity of the temperature within the oven was tested and confirmed prior to the experiment. The temperature deviation within the sample level was less then $2\,^{\circ}\mathrm{C}$. Aging took place at $150\,^{\circ}\mathrm{C}$ with the air-circulation turned on. The extraction intervals for the samples were determined in a prior test run.

FIGURE 3.2: Test specimens inside Binder FD 56 oven

3.5 Mechanical testing

The mechanical three-point flexural tests were performed on a Zwick/Roell 1445 universal testing machine according to DIN EN ISO 178 [43]. The radii of the bending fin and the supporting contact points were $5\,\mathrm{mm}$ each as specified for specimen with a thickness greater $3\,\mathrm{mm}$. The ideal distance between contact points was calculated as $64\,\mathrm{mm}$. The test was performed with a test speed of $5\,\mathrm{mm\,s^{-1}}$. The machine was equipped with force transducer with a nominal force of $100\,\mathrm{N}$. In accordance with the standard, five specimen were used for each data point.

For machine control and data acquisition, the software *testXpert II* was used. The software recorded data in a calculated stress-strain diagram as seen in Figure 2.8. The values recorded for the experiments in this work are the flexural strain ε_f, the flexural strength σ_f and the flexural modulus E_f.

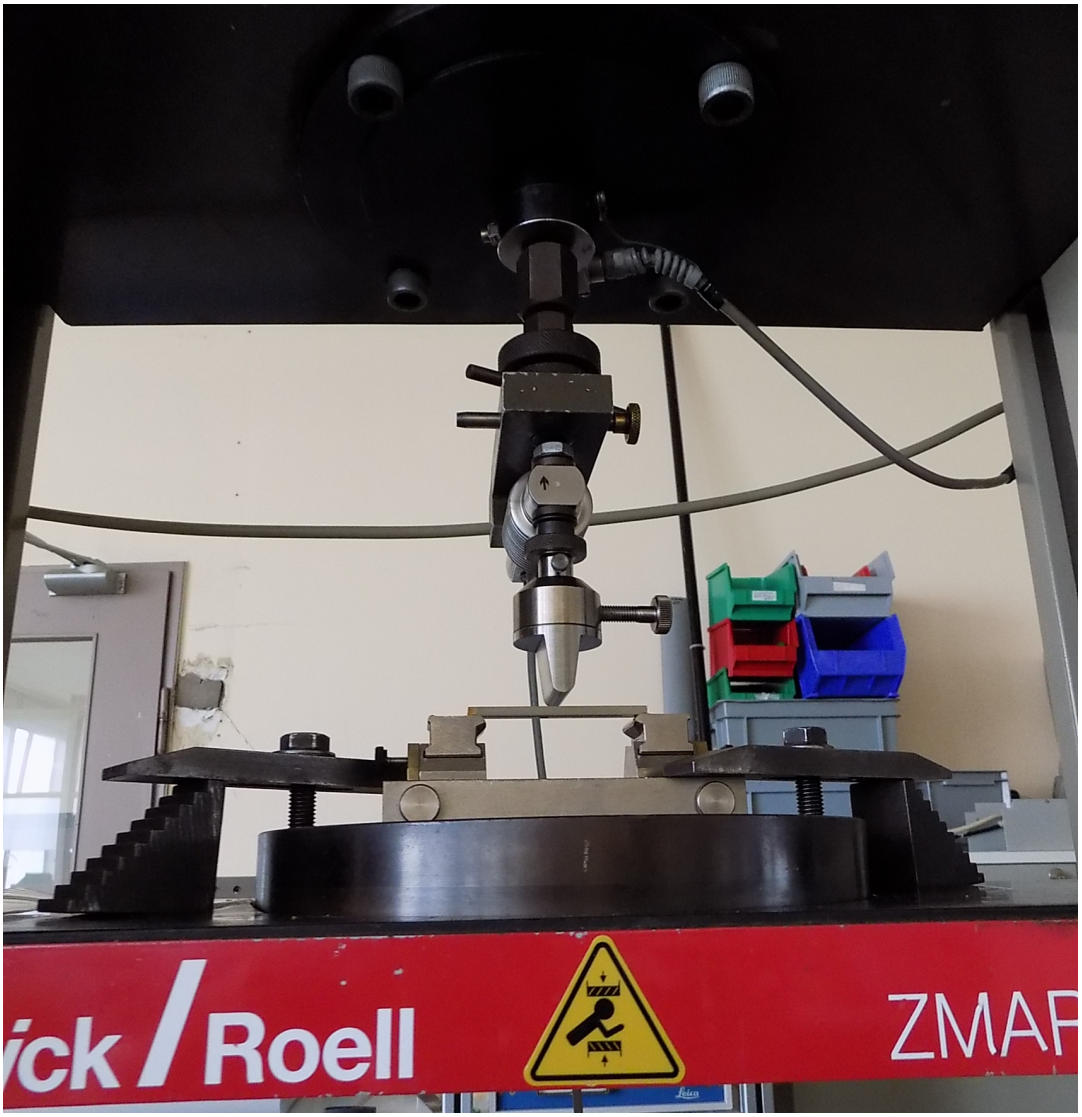

FIGURE 3.3: Test specimen in three-point flexural test

3.6 Thermogravimetric analysis

The TGA instrument used was the Mettler Toledo TGA/DSC 3+ STAR^e System with the *STAR^e Version 15.00* software. The samples ($14\,\mathrm{mg}$ to $20\,\mathrm{mg}$) were placed in $70\,\mu\mathrm{L}$ alumina crucibles. The measurement chamber was flushed with $60\,\mathrm{mL\,min^{-1}}$ Nitrogen and heated from $50\,^\circ\mathrm{C}$ to $800\,^\circ\mathrm{C}$ with a heating rate of $40\,\mathrm{K\,min^{-1}}$. Then, the atmosphere was switched to pure oxygen and heating was continued to $950\,^\circ\mathrm{C}$ at the same rate. These conditions correspond to the standard DIN EN ISO 11358-1 [42]. Analysis of the data was performed using the tangent center point method described in section 2.1.4.

3.7 Cryo-mill

All solid samples were cryo ground using the SPEX Sample Prep 6775 Freezer/Mill. The milling chamber in use was the $5\,\mathrm{g}$ polycarbonate model with stainless steel end caps and impactor. The grinding chamber was submerged in liquid nitrogen and precooled for $10\,\mathrm{min}$ before grinding. The grinding process was performed with an impact rate of $15\,\mathrm{collisions/s}$ (CPS) for $2\,\mathrm{min}$ followed by another $2\,\mathrm{min}$ cooling phase. This cycle was repeated four times, totaling $26\,\mathrm{min}$ method duration. About $1\,\mathrm{g}$ to $2\,\mathrm{g}$ of polymer sample were ground per run.

Chapter 4

Results and Discussion

4.1 Pyrolysis-GC/MS method development

The main goal of this thesis was the development of a quantitative polymer additive analysis method for Pyrolysis-GC/MS. The first step of this project was a complete thermal characterization of both the polymer samples as well as the individual additives by TGA and Py-GC/MS. In the course of this step, an additive pyrogram peak library and information concerning the reproducibility of pyrolysis were obtained. From these experiments, two methods of quantification were derived and tested. The results were compared to the original formulation of the samples and to a reference analysis provided by the BASF Schweiz AG via HPLC.

4.1.1 TGA of polymers and additives

The polyamide-6 (Table 3.1) and the natural polypropylene (Table 3.2) samples as well as the additives Irganox 1010, Irganox 1098, Irganox 1076, Irgafos 168 and Tinuvin 770 were subjected to thermo gravimetric analysis. The results of the main decomposition stage are displayed in Table 4.1. The corresponding TGA plots can be found in Figure 4.1 to Figure 4.7).

TABLE 4.1: TGA results of polymer samples and additives

Sample	Stage	Residue	Center point (°C)
Polyamide-6	-98.1%	0.7%	462
Polypropylene	-85.8%	14.0%	485
Irganox 1010	-95.9%	4.1%	449
Irganox 1098	-96.4%	3.6%	441
Irganox 1076	-99.2%	0.8%	403
Irgafos 168	-99.8%	0.2%	410
Tinuvin 770	-99.6%	0.4%	366

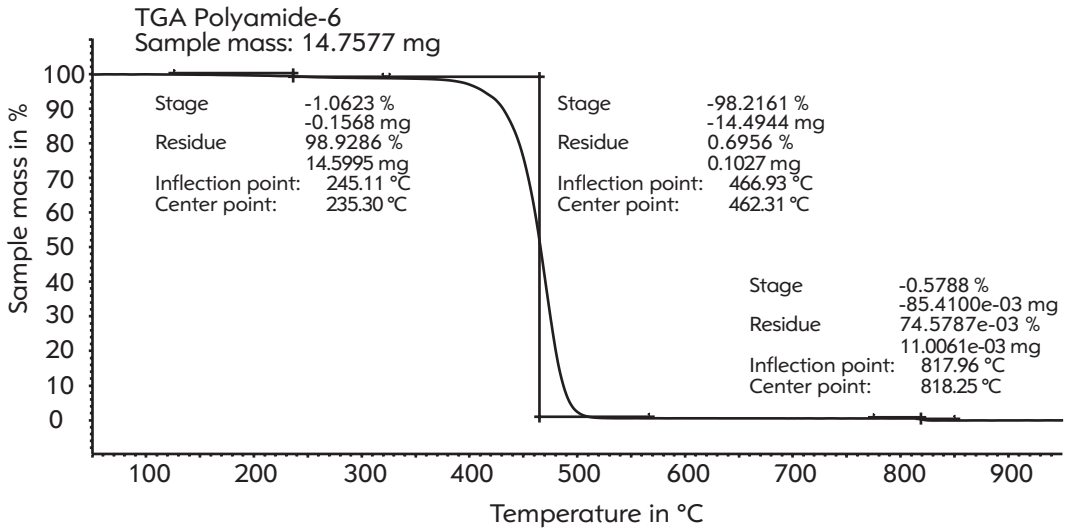

FIGURE 4.1: TGA: Polyamide-6

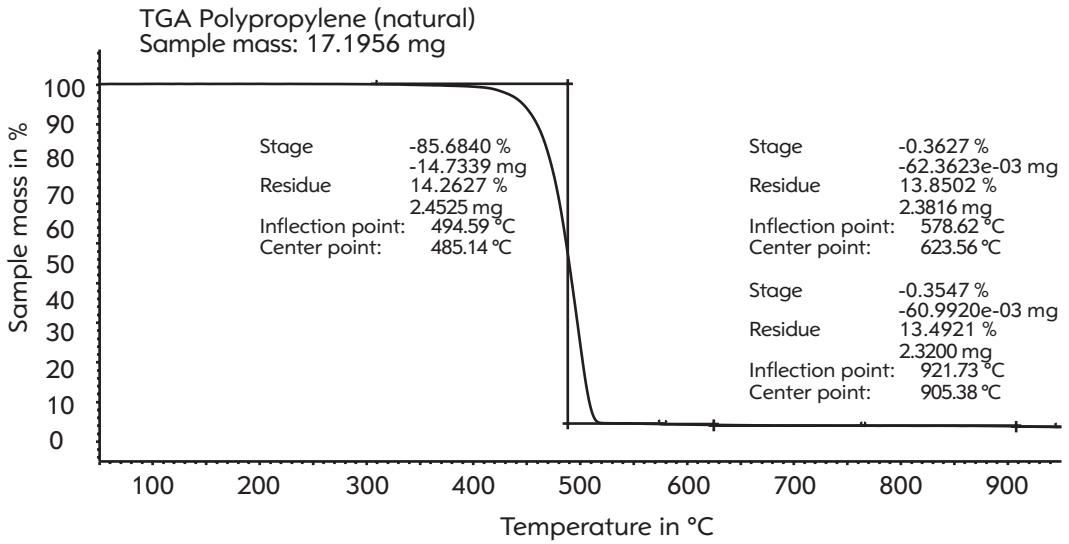

FIGURE 4.2: TGA: Polypropylene (natural)

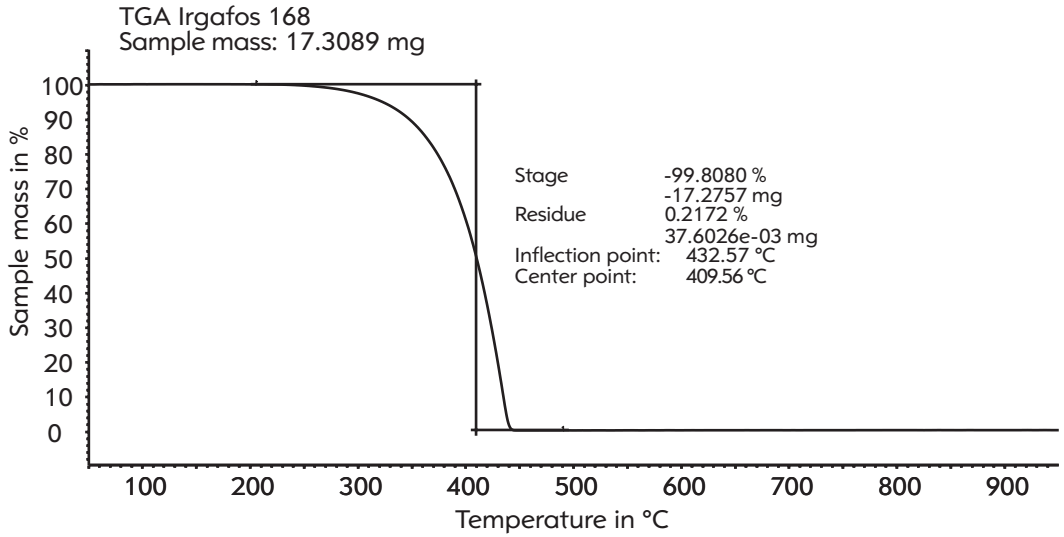

FIGURE 4.3: TGA: Irgafos 168

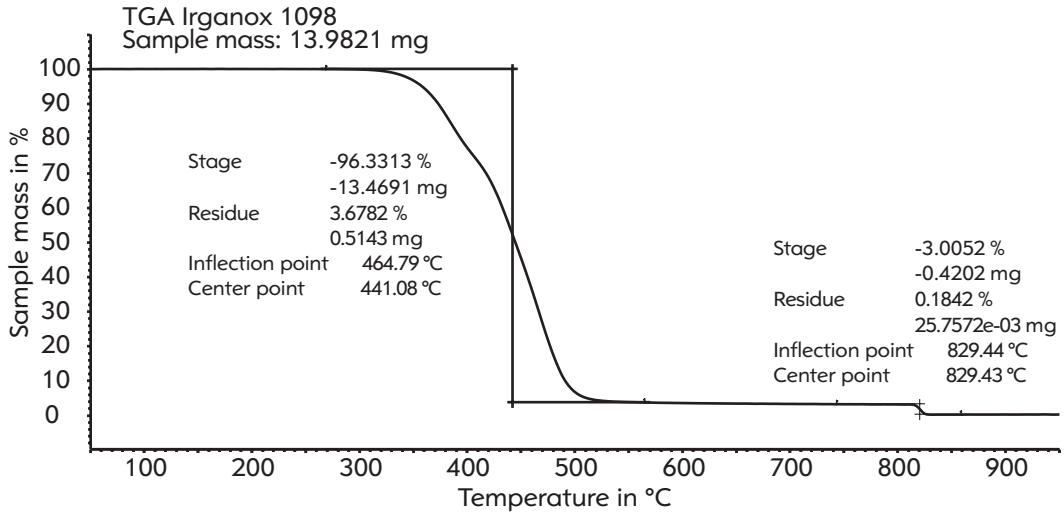

FIGURE 4.4: TGA: Irganox 1098

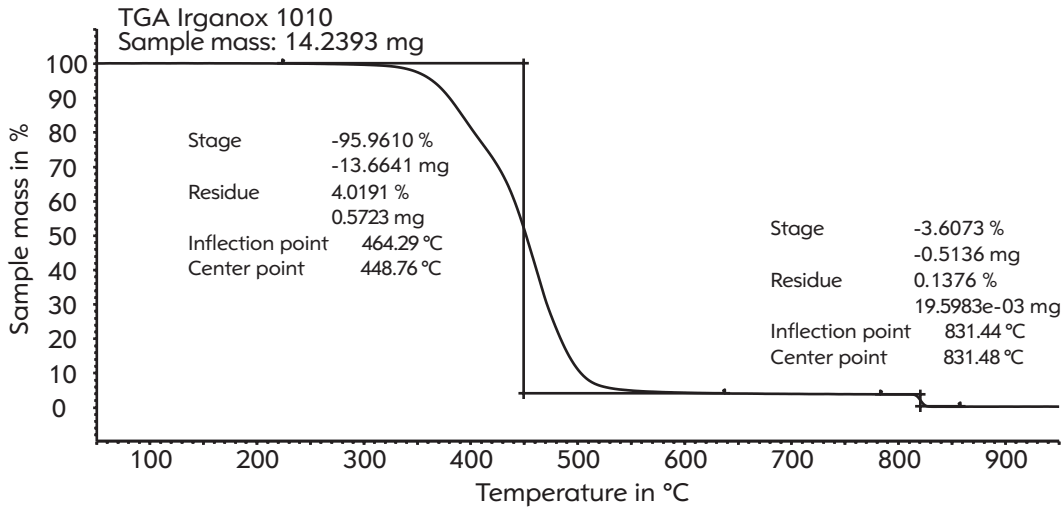

FIGURE 4.5: TGA: Irganox 1010

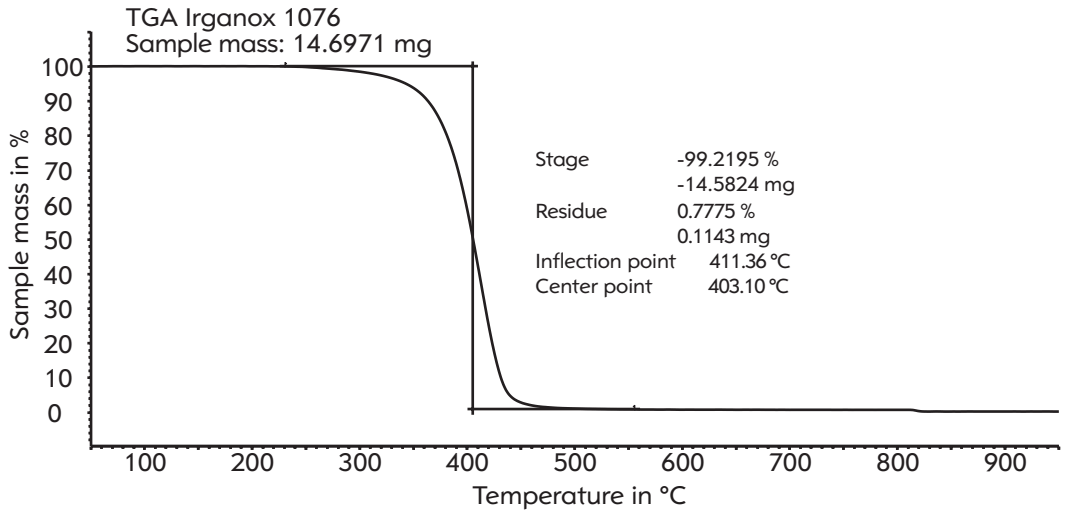

FIGURE 4.6: TGA: Irganox 1076

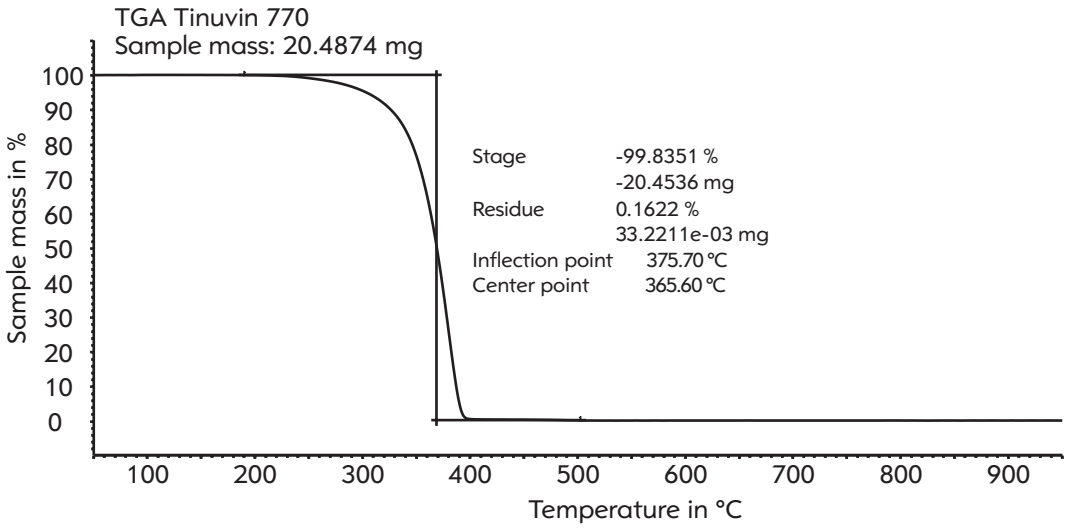

FIGURE 4.7: TGA: Tinuvin 770

Except for the polypropylene sample, which contains $15\,\%$ talcum, all samples show a main decomposition stage distinctly above $90\,\%$. For Irganox 1076, Irgafos 168 and Tinuvin 770, the center point of this stage lies at least $52\,°C$ below that of the polyamide-6 and $75\,°C$ below that of polypropylene. Irganox 1010 and Irganox 1098 show higher decomposition temperatures, lying approximately at the same temperature as polyamide-6 and only approximately $35\,°C$ below polypropylene. Also, Irganox 1010 and Irganox 1098 show a higher residue ($4.1\,\%$ and $3.6\,\%$) after the main decomposition stage than the other additives, which all lie below $1\,\%$.

4.1.2 Pyrolysis temperature series - additives

In order to determine the best pyrolysis temperature for additive analysis, a temperature series consisting of measurements from $450\,°C$ to $600\,°C$ in $50\,°C$ steps of all

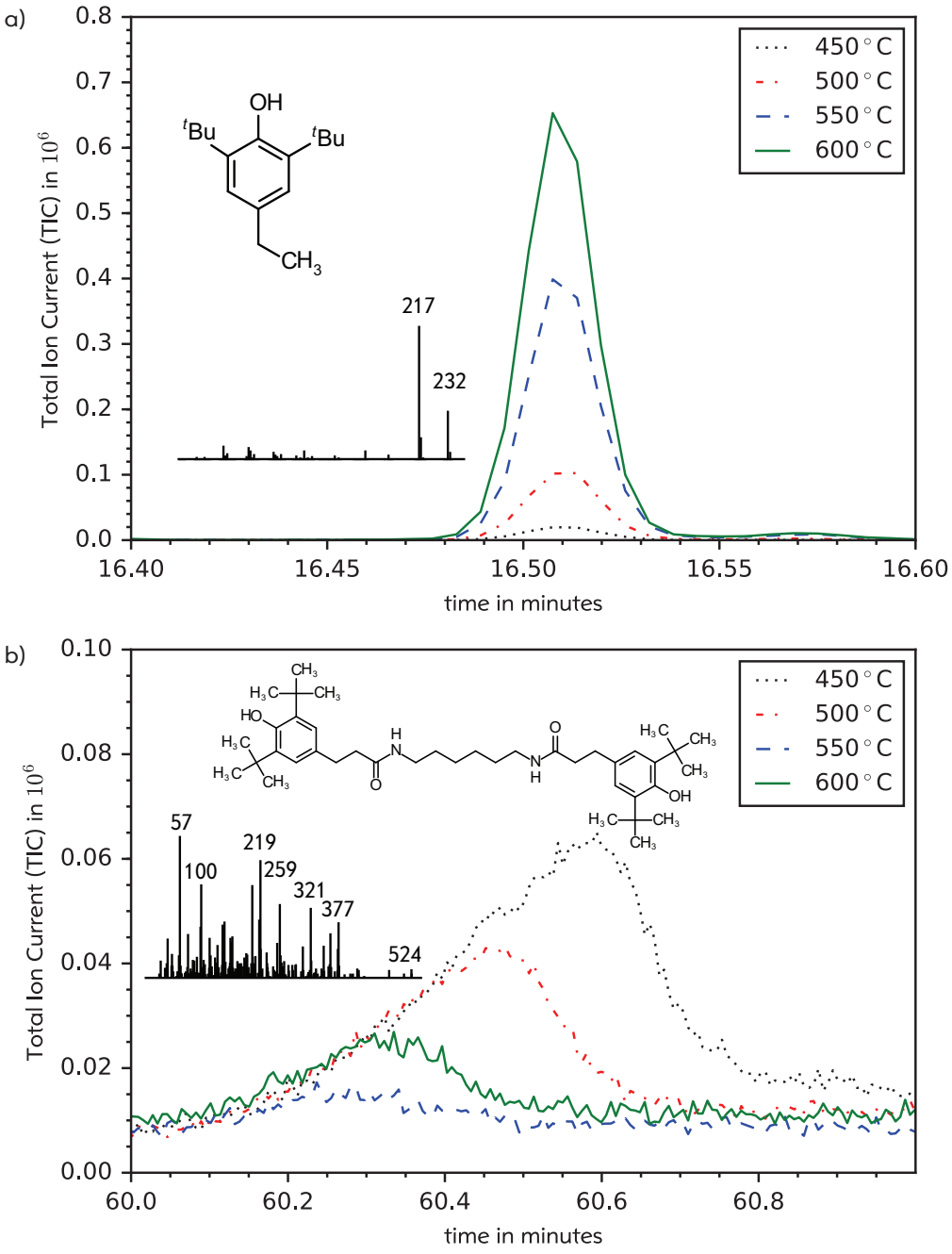

FIGURE 4.8: T-Pyro series of Irganox 1098 @ 450 °C to 600 °C

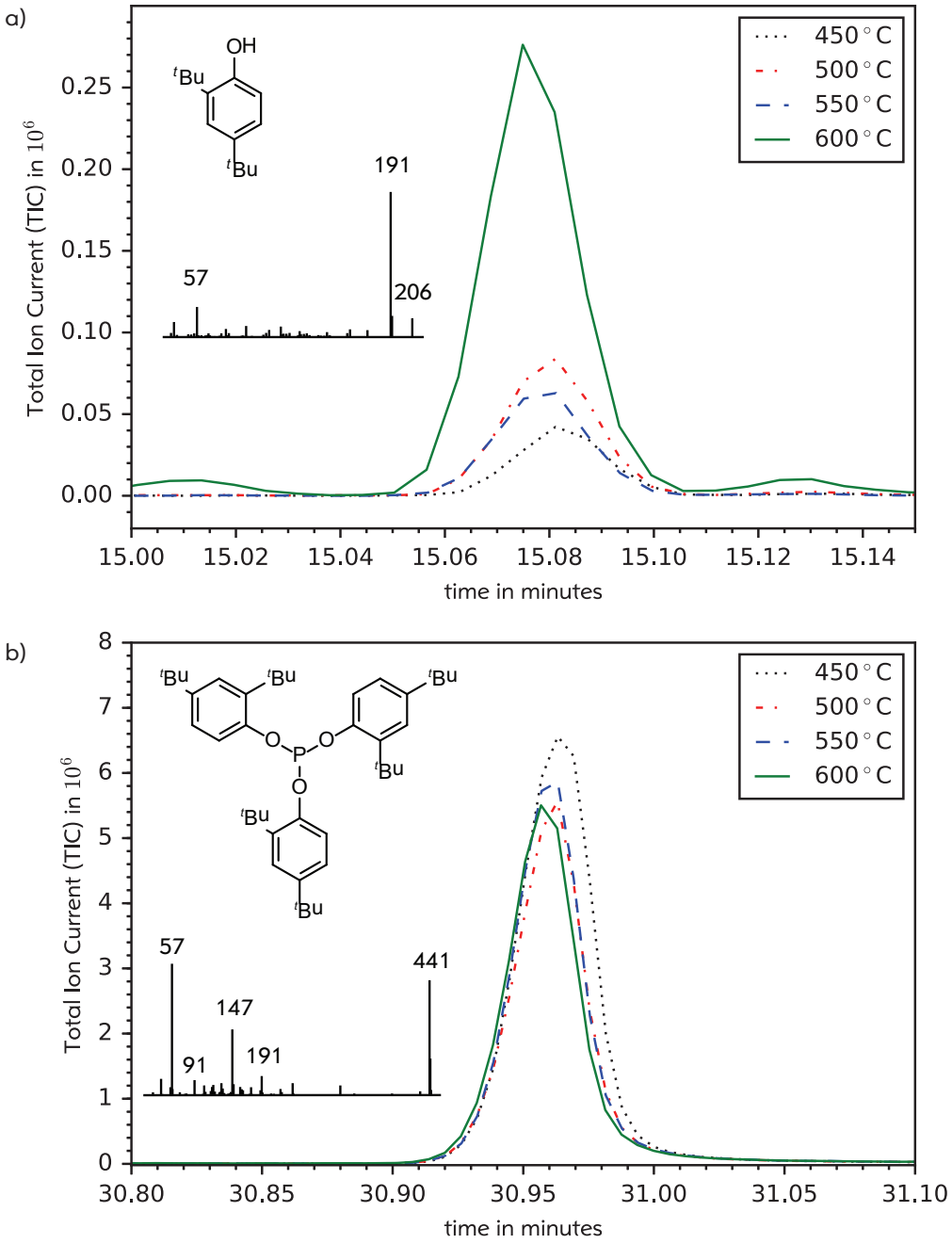

FIGURE 4.9: T-Pyro series of Irgafos 168 @ 450 °C to 600 °C

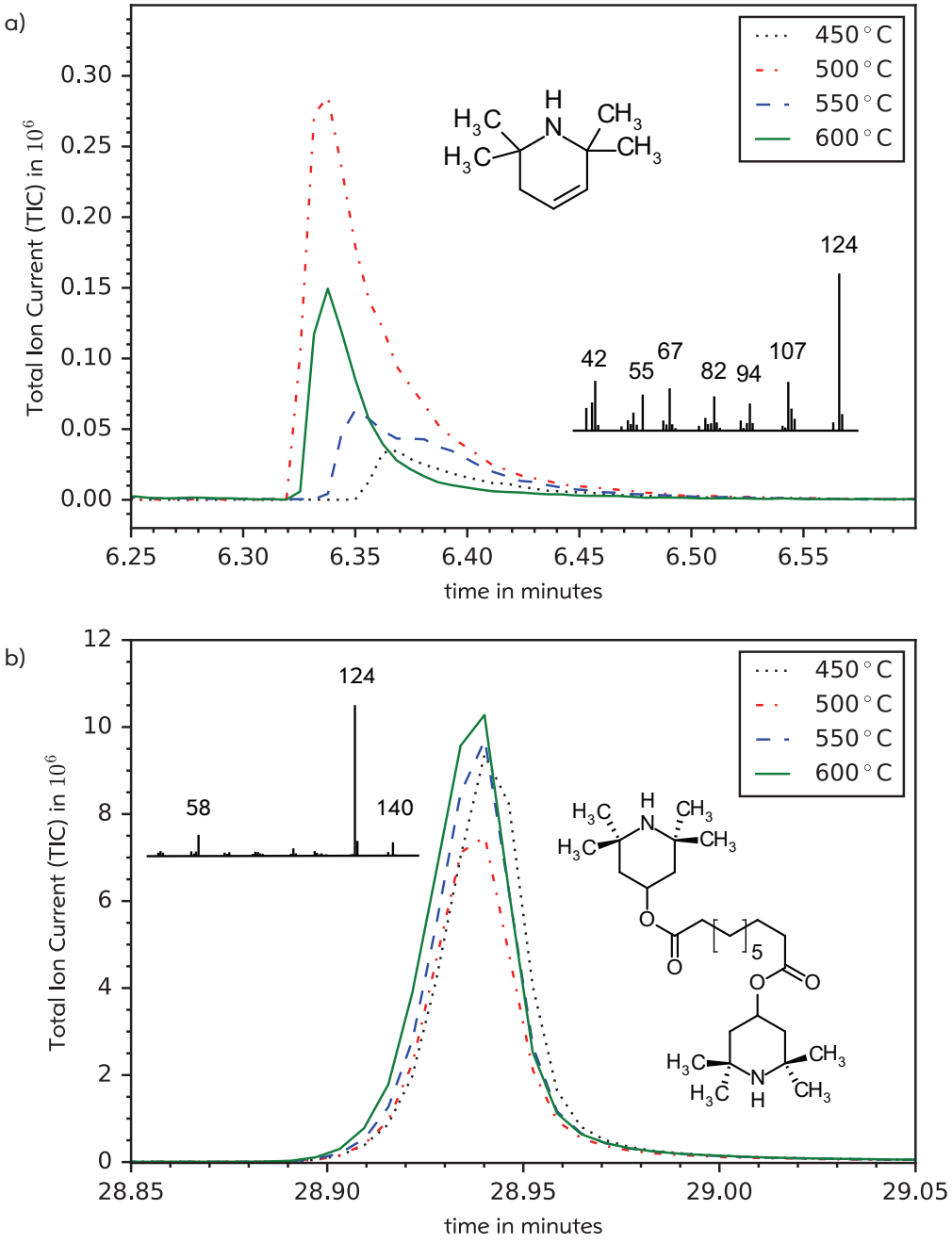

FIGURE 4.10: T-Pyro series of Tinuvin 770 @ 450 °C to 600 °C

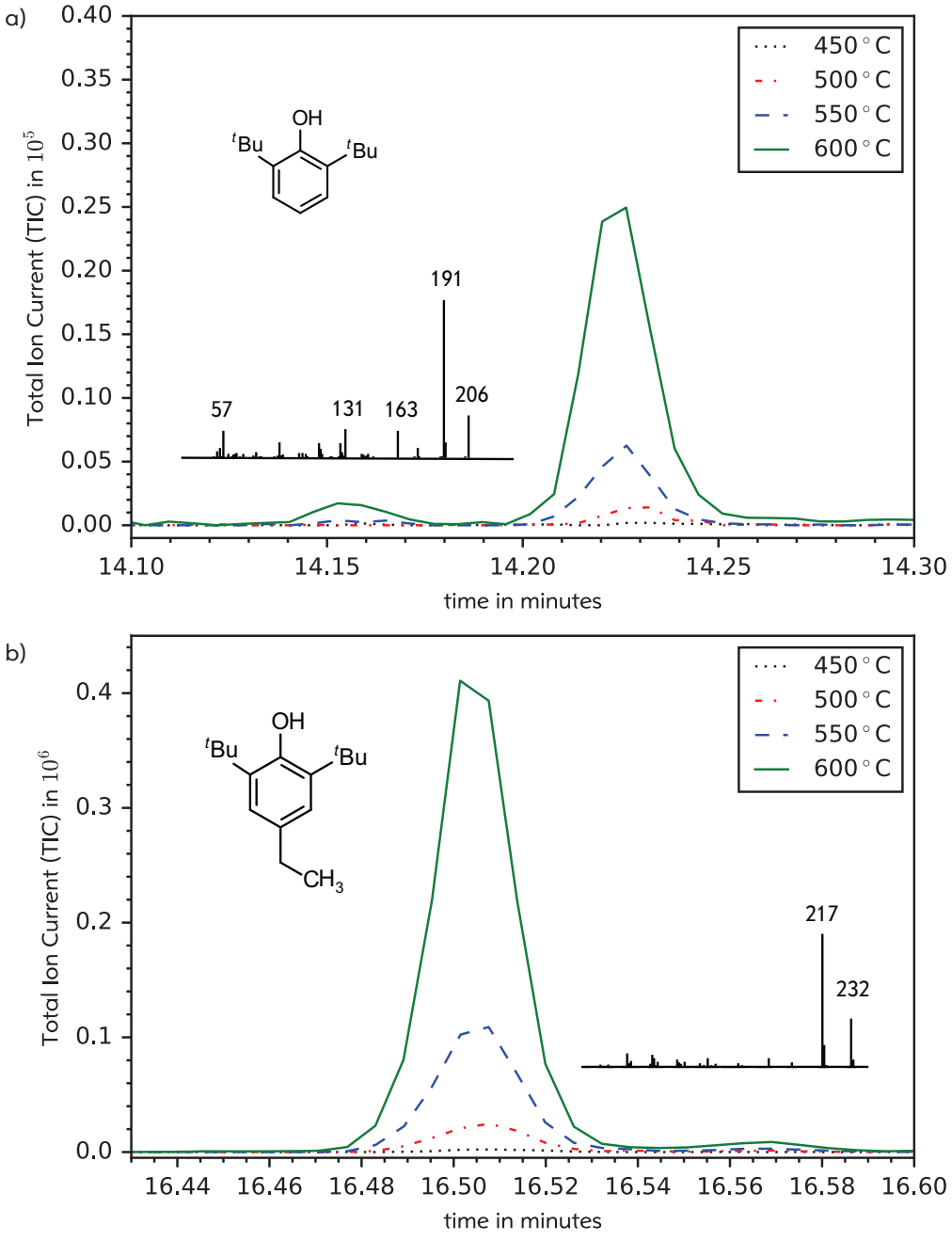

FIGURE 4.11: T-Pyro series of Irganox 1010 @ 450 °C to 600 °C

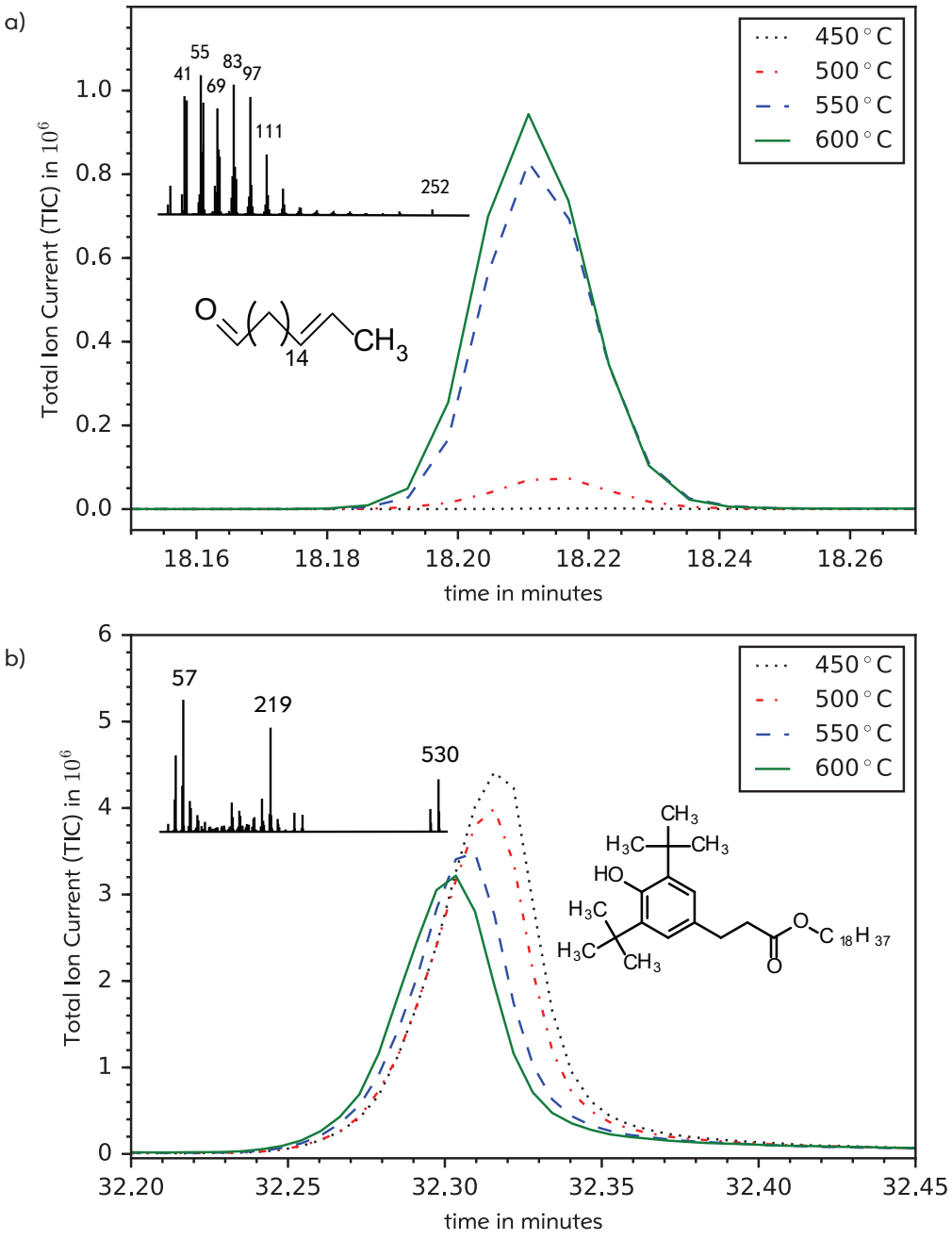

FIGURE 4.12: T-Pyro series of Irganox 1076 @ 450 °C to 600 °C

additives used in the standard reference samples was conducted. Figures 4.8 to 4.12 show the temperatures influence on the main peaks of interest.

Irganox 1098 (Figure 4.8) shows two thermally opposing peaks. At 16.5 minutes (4.8a) one finds a clearly defined peak which increases distinctly at higher temperatures, while at 60.5 minutes (4.8b) one finds a broad peak that diminishes at higher temperatures. Since the narrow, symmetrical peak at 16.5 minutes is better suited for quantification, this measurement is a strong argument for higher temperatures when analyzing a sample containing Irganox 1098. Additionally, avoiding very late eluting peaks has significant benefits for a measurements duration and thus it's cost. While the peaks could not be identified via library search, the proposed structures in Figure 4.8 are plausible both from a chemical as well as a mass-spectral point of view. Since (a) is a degradation product of (b), their reversed response to higher temperatures is to be expected.

Irgafos 168 (Figure 4.9) gives two peaks. At 15 minutes (4.9a) we see the main degradation product of Irgafos 168, 2,4-Di-tert-butyl-phenole. This peak increases with higher temperatures, as the undegraded molecule's peak (4.9b) decreases. Both peaks have been positively identified via library matching and are plausible both from a chemical as well as a mass-spectral point of view. Compared with Irganox 1098, the Irgafos 168 peaks are large and well above the limit of detection at all temperatures.

Two peaks can be identified for Tinuvin 770, lying at 6.35 minutes (4.10a) and 28.9 minutes (4.10b). The first has been identified manually as 2,2,6,6-tetramethyl-1,3-dihydropyridine, a degradation product of 4.10b, which has been identified via library match as Tinuvin 770. No consistent temperature dependency of the peak size can be observed for Tinuvin 770. At all temperatures, the main peak is large and easily quantifiable.

The two Irganox 1010 peaks used for this analysis lie at 14.2 minutes (4.11a) and 16.5 minutes (4.11b). Both peaks increase significantly with higher temperatures, especially between $550\,^{\circ}\mathrm{C}$ and $600\,^{\circ}\mathrm{C}$. The first has been identified via library match as 2,6-Di-tert-butyl-phenole. The second peak was manually identified as 4-Ethyl-2,6-di-tert-butyl-phenol.

The last additive, Irganox 1076, also displays an undegraded peak at 32 minutes (4.12b), which decreases slightly at higher temperatures. It degrades to (4.12b), as can be seen in the increase from no peak at $450\,^{\circ}\mathrm{C}$ to a significant peak at $550\,^{\circ}\mathrm{C}$ to $600\,^{\circ}\mathrm{C}$. Both peaks are readily identified by library match.

In conclusion, both Irganox 1010 and 1098 benefit considerably from higher temperatures and should be analyzed at $600\,^{\circ}\mathrm{C}$ if possible. Especially Irganox 1098 is destined for higher temperatures since it displays a late eluting and broad peak at lower temperatures. Irgafos 168, Tinuvin 770 and Irganox 1076 also show differing degradation ratios at low and high temperatures. However, all three additives display large and easily detectable peaks at all temperatures within the tested range.

4.1.3 Additive pyrogram peak library

Having determined $600\,°C$ as the best temperature to analyze the additives used in the PA-6 and PP standard samples, the next step was creating an additive library containing the retention time and mass spectra of the major peaks. To achieve this, all additives were individually analyzed at $600\,°C$. The major peaks of interest were than identified and cataloged. The results are shown in Figures 4.13 to 4.17 and in Table 4.2. Criteria for these peaks were sufficient intensity and peak purity. Identification was done either by achieving a good library match or manual MS-interpretation taking into consideration plausible degradation pathways.

Irganox 1098 (Figure 4.13) Three main peaks were chosen for Irganox 1098. No library matches were possible, therefore identification is uncertain. Peak 1 at $14.6\,\mathrm{min}$ appears to be a debutylated and dehydrogenated fragment of the additive's phenolic end group. Peak 2 at $16.3\,\mathrm{min}$ appears to be the end group 2,6-di-tert-butyl-4-ethenylphenol formed by elimination of the carboxamide group. Peak 3 at $19.4\,\mathrm{min}$ is the complete end group with one tert butyl group demethylated.

The identification of the second is supported by Jansson, Zawodny and Wampler in their 2007 publication [27], which focuses on Irganox 1010 instead of Irganox 1098. However, this fragment is identical for both Irganox 1010 and Irganox 1098 as well as Irganox 1076.

Irgafos 168 (Figure 4.14) Two peaks were chosen for Irgafos 168. The undegraded phosphite (peak 2 at $30.8\,\mathrm{min}$) and the intact phenolic pyrolysis fragment (peak 1 at $14.9\,\mathrm{min}$). Both could be successfully identified via library match. Peak 3, the oxidized additive, co-elutes with peak 4 of Irganox 1076 and can therefore not be used. However, as seen in the pyrogram, this peak only plays a very minor role in unaged polymer samples. It was included in the additive library for the use of monitoring aging processes in samples containing Irgafos 168 but no Irganox 1076 (section 4.2.4).

Jansson et al. come to the same conclusion concerning peak 1 [27], confirming the library match.

Tinuvin 770 (Figure 4.15) The most volatile (Table 4.1) additive used in this analysis mainly remains intact (Peak 3 at $28.8\,\mathrm{min}$, identified via library match). The two pyrolysis fragments formed are peak 1 at $6.3\,\mathrm{min}$, which was manually identified as a piperidine fragment and peak 2 at $23.4\,\mathrm{min}$, which was manually identified as Tinuvin 770 missing one piperidine end group. Both fragments are formed by thermally activated elimination reactions.

The identification of peak 1 is also confirmed in a 2001 publication by Marianne Blazsó on the thermal decomposition of polymeric hindered amine light stabilizers (compound A) [64] as well as the 2007 Jansson paper [27].

Irganox 1010 (Figure 4.16) Owing to their analogous structures, Irganox 1098 and Irganox 1010 show very similiar peaks. Peak 1 and 2 at $14.6\,\mathrm{min}$ and $16.3\,\mathrm{min}$ are identical. Peak 3 at $19.6\,\mathrm{min}$ differs since Irganox 1010 does not include a carboxamide group. Also, peak 3 could be positively identified via library match. For peak 1 & 2, while no library match could be achieved, the same conclusion by Jansson et al. [27] cited above apply.

Irganox 1076 (Figure 4.17) This additive shows large conformance with Irganox 1010 and 1098, all three being derivatives of the classic butylhydroxytoluene (BHT). Peaks 1 and 2 at $14.6\,\mathrm{min}$ and $16.3\,\mathrm{min}$ are consequently identical, also confirmed by Jansson et al. [27]. Peak 3 at $18.0\,\mathrm{min}$ is the alkyl chain end group in aldehyde form, created through thermally activated elimination. Peak 4 at $32.0\,\mathrm{min}$ is the intact Irganox 1076 molecule. Peaks 3 and 4 could be successfully identified via library match.

Conclusions for the method development Regarding the information gathered in the construction of this small additive library, one can see that Irgafos 168 and Tinuvin 770 should be easy to analyze within the same sample. They do not share any common fragments and no co-elution is to be expected from the other additives. For the Irganox additives a more complicated situation presents itself. They all have peaks 1 and 2 in common, making them useless for identification or quantification if more than one of them is present in a sample, such as is the case with the polypropylene standard sample. Irganox 1098 and 1010 both only have one unique peak (peak 3 at $19.4\,\mathrm{min}$ and $19.6\,\mathrm{min}$ respectively). Also, both show very weak signal intensity compared to the other three additives. Irganox 1076 has two strong, unique peaks at $18.0\,\mathrm{min}$ and $32.0\,\mathrm{min}$, making identification and quantification next to Irganox 1010 less problematic.

4.1.4 Reproducibility of pyrolysis

Each additive analysis for the library was performed eight times. A statistic analysis of these measurements can be found in Table 4.3. The data was obtained by integrating the main peaks and forming their sum. Then, the arithmetic mean, the standard deviation and the relative standard deviation were calculated for each additive. Additionally, the RSD for the individual peaks is displayed below the sum data.

The results show, that the relative standard deviation of the total peak area in quantitative reproducibility of Py-GC/MS experiments fluctuates between $10\,\%$ to $35\,\%$. The fluctuation of individual peaks ranges up to $70\,\%$. This clearly shows the necessity of using the total peak area and performing a sufficient number of experiments to get acceptably accurate and reliable results.

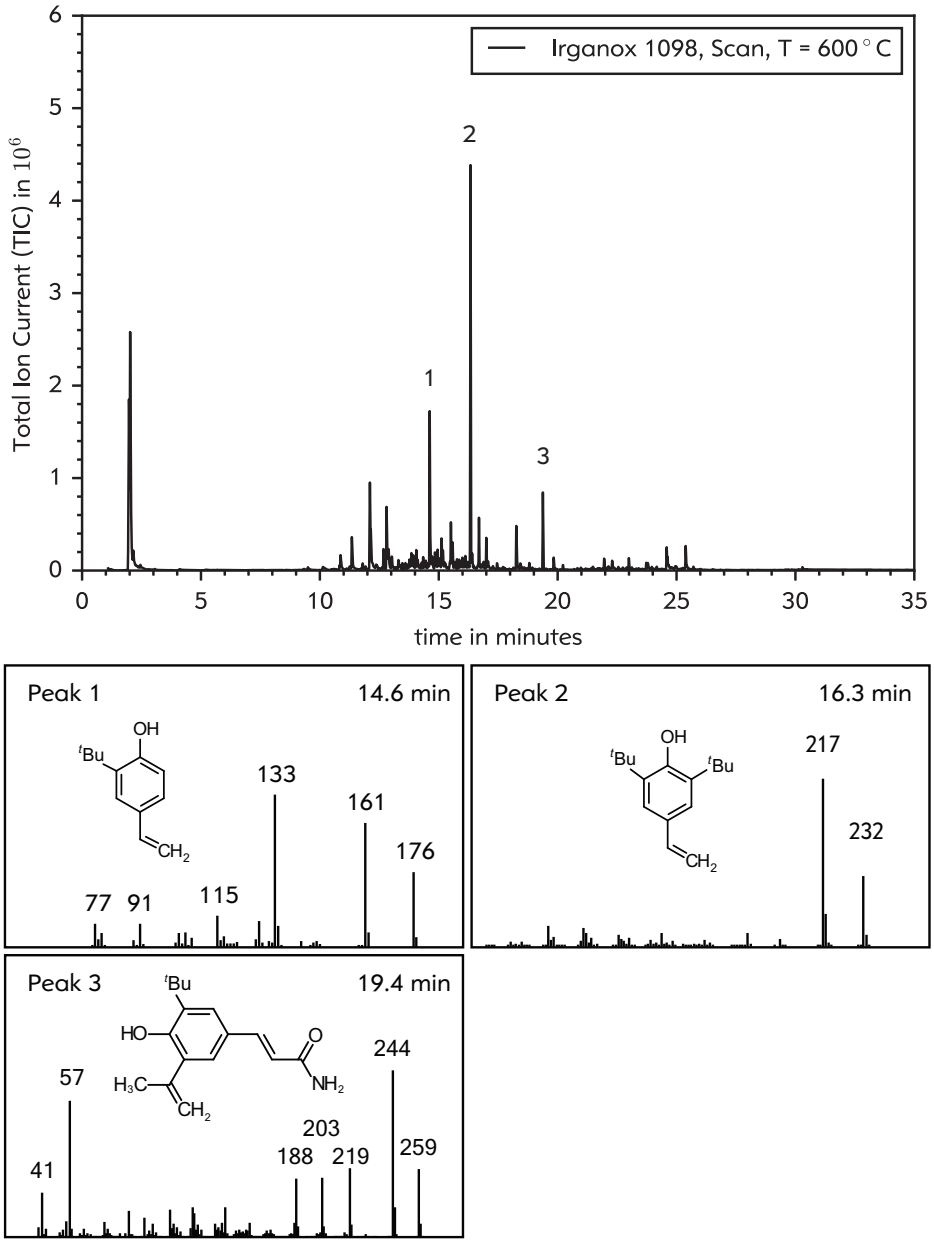

FIGURE 4.13: Additiv-analysis: Irganox 1098 at 600 °C

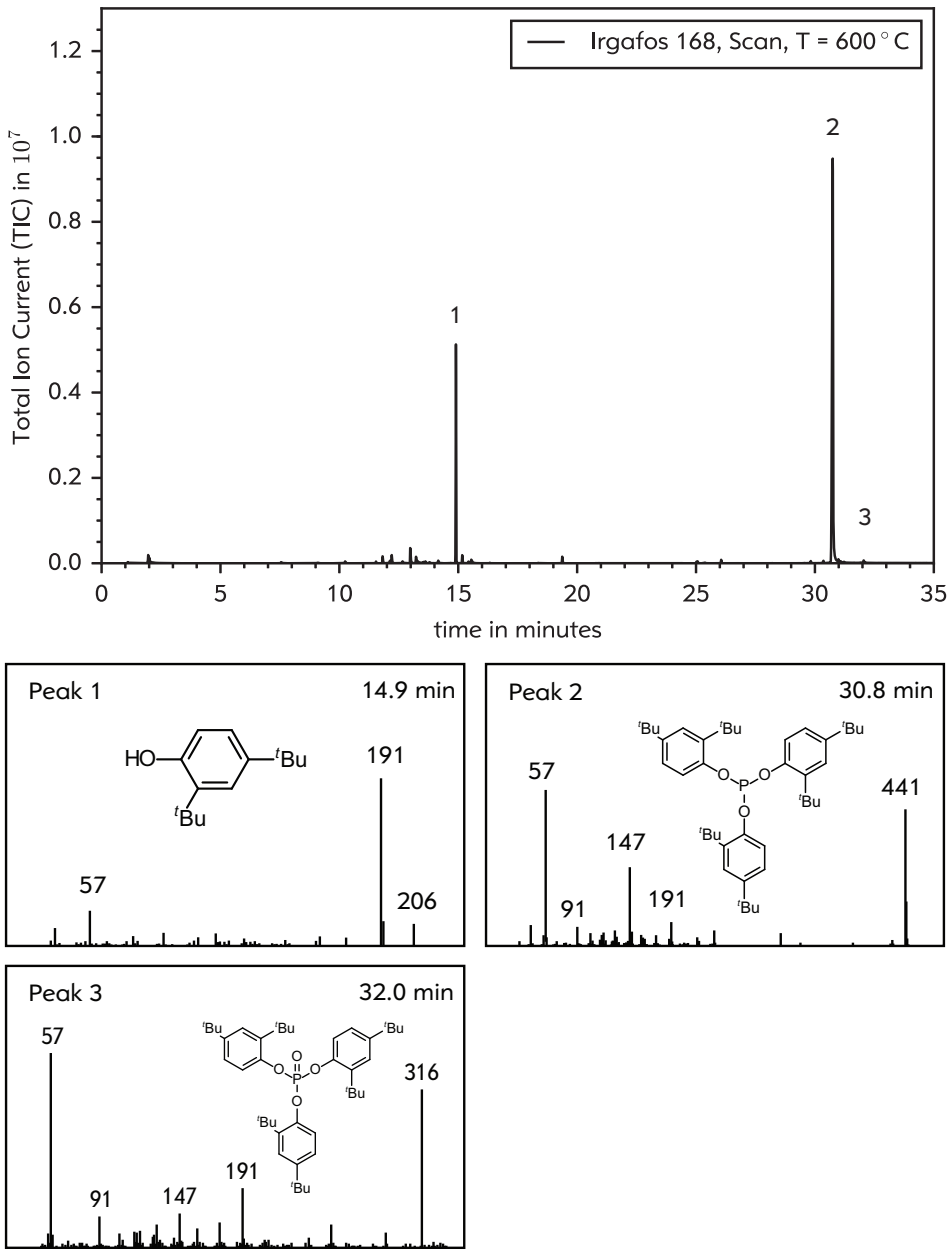

FIGURE 4.14: Additiv-analysis: Irgafos 168 at 600 °C

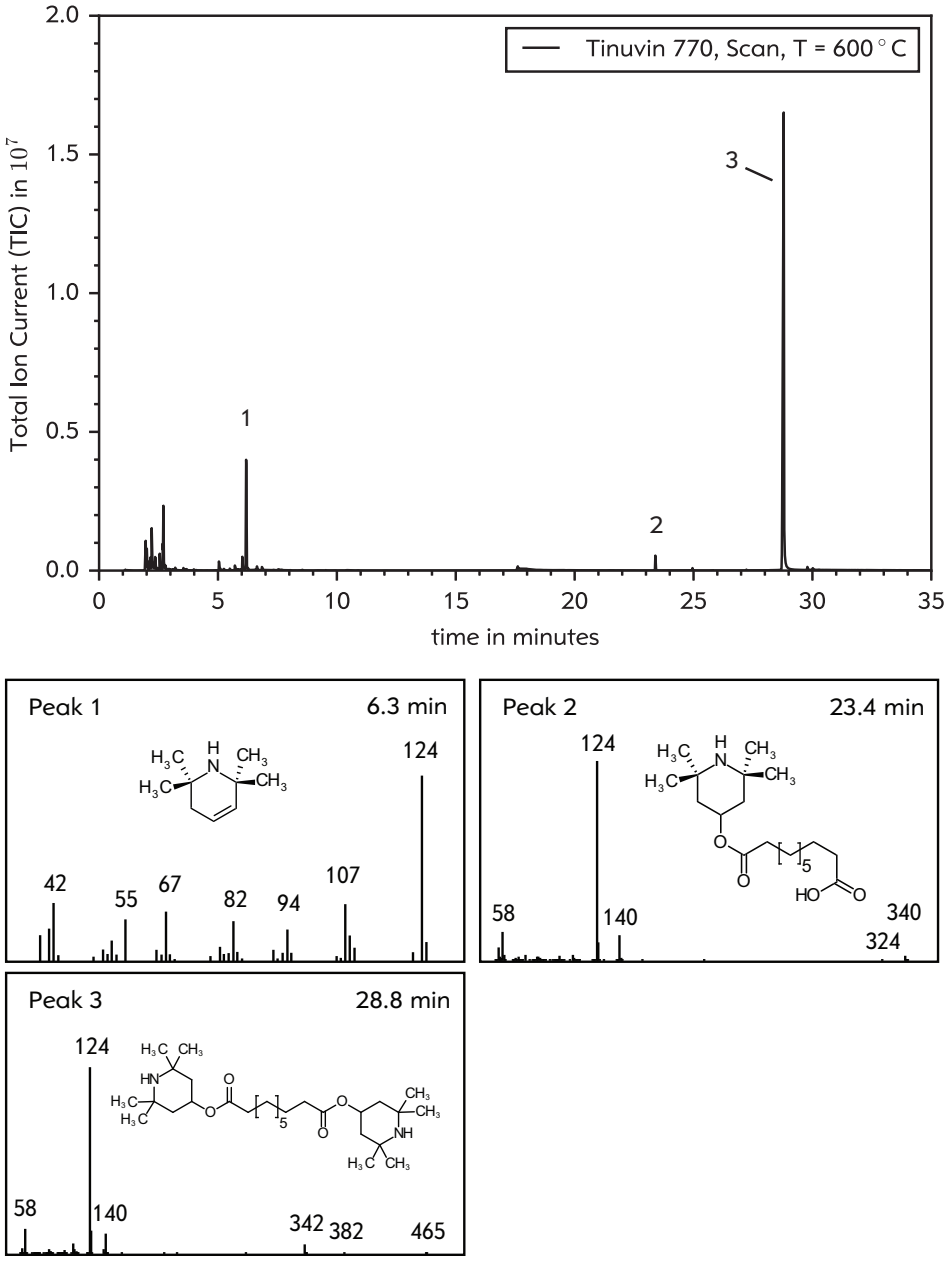

FIGURE 4.15: Additiv-analysis: Tinuvin 770 at 600 °C

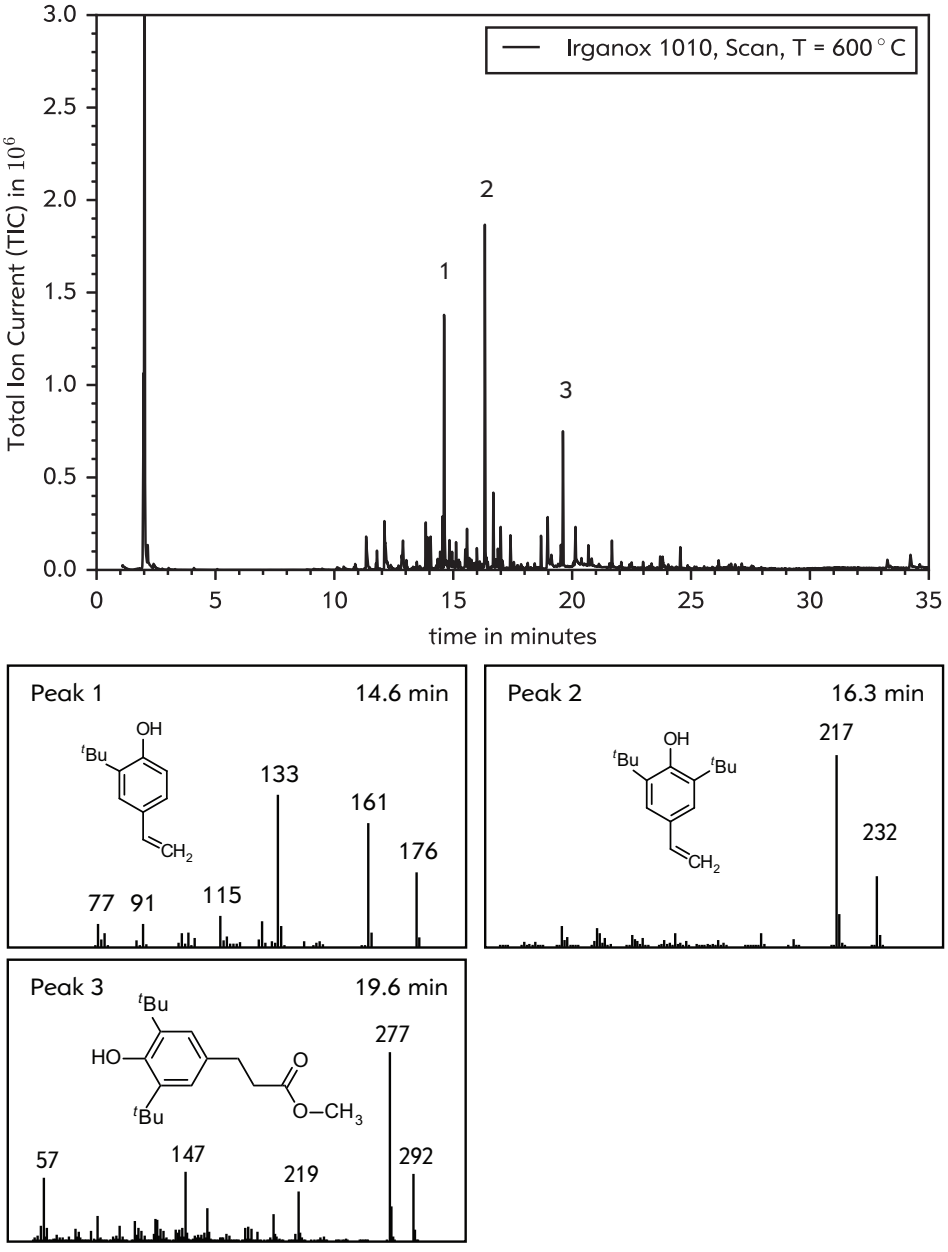

FIGURE 4.16: Additiv-analysis: Irganox 1010 at 600 °C

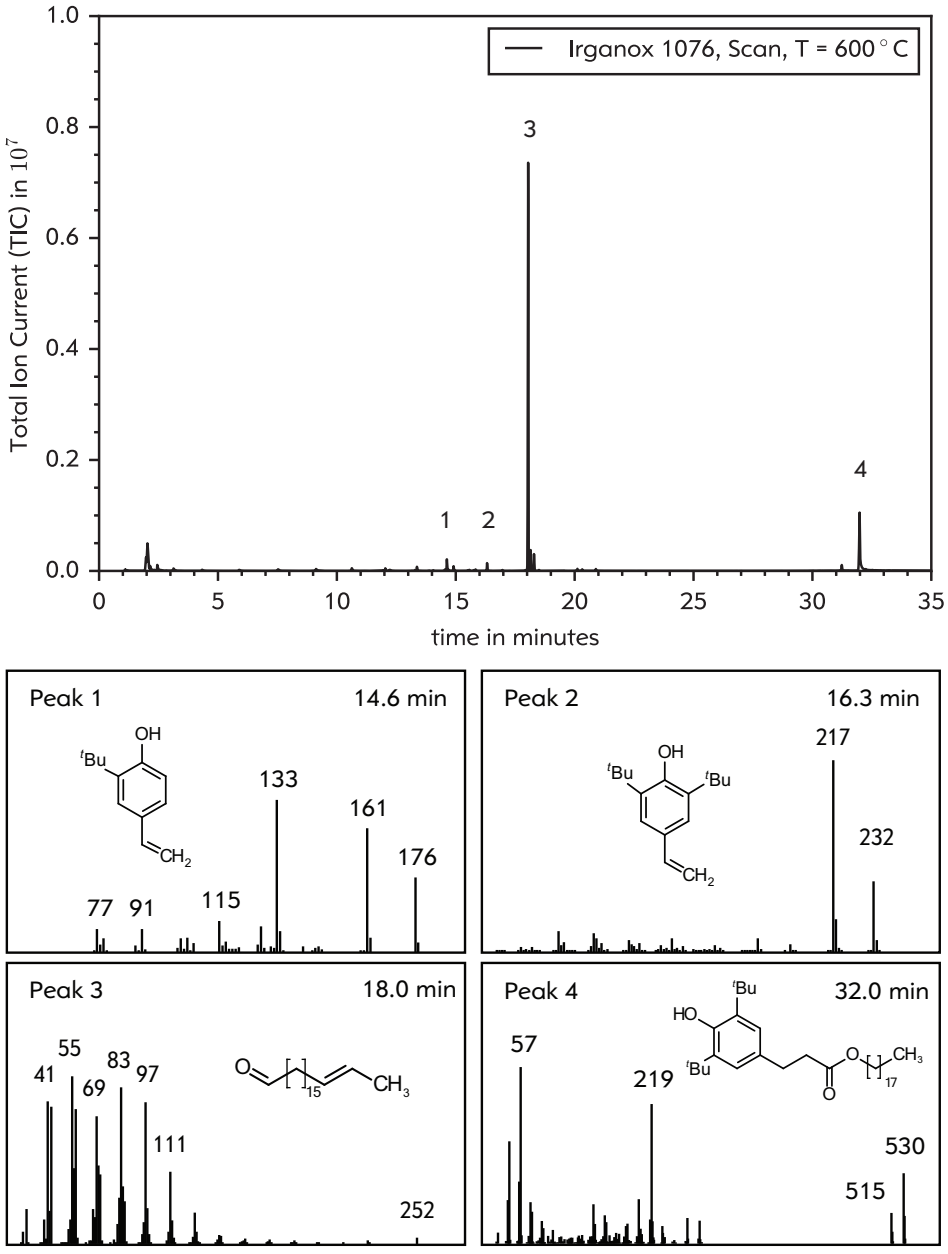

FIGURE 4.17: Additiv-analysis: Irganox 1076 at 600 °C

TABLE 4.2: Additive library for 600 °C

Additive	Retention time	*m/z*
Irganox 1098	14.6 min	176, 161, 133
	16.3 min	232, 217
	19.4 min	259, 244
Irgafos 168	14.9 min	206, 191
	30.8 min	441, 191, 147
Tinuvin 770	6.3 min	124, 107
	23.4 min	140, 124
	28.8 min	342, 140, 124
Irganox 1010	14.6 min	176, 161, 133
	16.3 min	232, 217
	19.6 min	292, 277
Irganox 1076	14.6 min	176, 161, 133
	16.3 min	232, 217
	18.0 min	252, 111, 97
	32.0 min	530.5, 515.5

TABLE 4.3: Reproducibility of peak areas in Py-GC/MS

	Ix 1098	**If 168**	**Tin 770**	**Ix 1010**	**Ix 1076**
Mean	1.05E+08	3.39E+08	5.37E+08	5.40E+07	3.06E+08
SD	2.78E+07	1.14E+08	1.89E+08	5.33E+06	9.48E+07
RSD	26.4%	33.6%	35.3%	9.9%	31.0%
RSD - P1	58.5%	14.7%	41.2%	18.7%	26.0%
RSD - P2	36.8%	40.3%	15.3%	23.7%	43.5%
RSD - P3	52.2%	-	35.8%	20.7%	19.5%
RSD - P4	-	-	-	-	69.2%

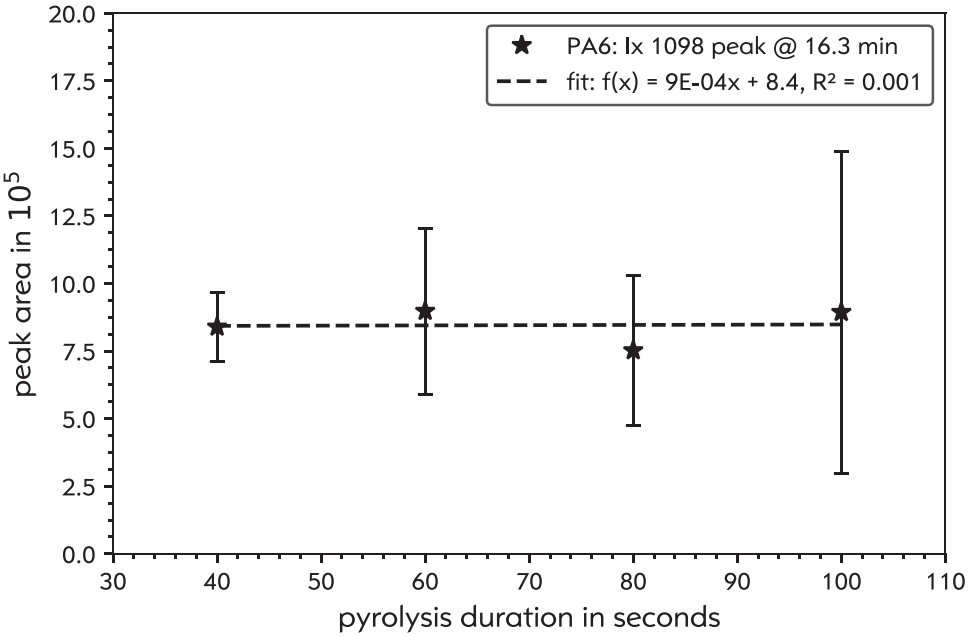

FIGURE 4.18: Optimization of pyrolysis duration at 600 °C - Ix 1098 (16.3 min)

4.1.5 Pyrolysis duration

To determine the ideal pyrolysis duration for additive desorption, a critical additive peak was chosen and monitored in a series of different pyrolysis duration from 40 s to 100 s using the 600 °C SIM method. For every t_{Pyro} five polyamide-6 samples were measured. The Irganox 1098 peak at 16.3 min was integrated and the resulting value weighted by the respective sample mass. Figure 4.18 shows a plot of the m-weighted peak area against the pyrolysis duration. The data was fitted using Python to analyze the influence of the pyrolysis duration on the peak area.

For the finalization of the method it was concluded, that a pyrolysis duration above 40 s has no significant impact on the resulting peak area. Only an increase in standard deviation was observed, which is not a desirable effect. It was therefore left at 40 s.

4.1.6 Quantification of PA6 and PP-N additives via HPLC (BASF)

TABLE 4.4: HPLC quantification results (BASF)

Sample	Additive	BASF result (HPLC)	Formulation
PA6	Irgafos 168	0.27%	0.40%
	Tinuvin 770	0.17%	0.20%
	Irganox 1098	0.41%	0.40%
PP-N	Irganox 1010	0.04%	0.05%
	Irgafos 168	0.19%	0.23%
	Tinuvin 770	0.23%	0.20%
	Irganox 1076	0.29%	0.30%

An analysis of both the polyamide-6 and the polypropylene standard samples was conducted by BASF in their Basel laboratory. The analysis was done by liquid extraction of the additives and subsequent quantification via HPLC. The results can be found in Table 4.4 and serve as a reference for the pyrolysis method development.

The formulation plan is also displayed in Table 4.4. As can be seen, the BASF results show good concordance with the formulation plan, with the exception of Irgafos 168 in the polyamide-6 sample. This deviation is likely due to degradation of the phosphite during processing caused by the high temperatures necessary for PA6 extrusion. While the maximum temperature during the compounding of the polypropylene sample was $205\,^{\circ}\mathrm{C}$, a temperature of $260\,^{\circ}\mathrm{C}$ was reached in the case of polyamide-6.

No detailed information on the method, procedure or analysis exceeding the above was disclosed by BASF for intellectual property reasons.

4.1.7 Quantification of PA6 and PP-N additives at 450°C

In section 4.1.2 it was shown, that while Irganox 1010 and 1098 require higher temperatures (i.e. $600\,^{\circ}\mathrm{C}$) to be analyzed. However, Irgafos 168, Tinuvin 770 and Irganox 1076 do not. Therefore, a quantification experiment was performed at $450\,^{\circ}\mathrm{C}$ aiming at these additives.

Calibration The calibration run is detailed in Table 4.5. As samples, $0.02\,\%$ standard solutions of the additives in dichloromethane (DCM) were used.

TABLE 4.5: Additive calibration at $450\,^{\circ}\mathrm{C}$

Measurements:	1 - 5	6 - 10	11 - 15
Irgafos 168	4 µL	6 µL	8 µL
Tinuvin 770	4 µL	6 µL	8 µL
Irganox 1076	4 µL	6 µL	8 µL

Figures 4.19 and 4.20 show the calibration pyrograms and analysis. Peak 1 is Tinuvin 770, peak 2 Irgafos 168 and peak 3 Irganox 1076. Two additives remain mostly

undecomposed. Only negligible amounts of fragmented Tinuvin 770 and Irgafos 168 can be found at $6.3\,\mathrm{min}$ and $15\,\mathrm{min}$. For Irganox 1076 there is no information on possible fragmentation, since the peak at $18.0\,\mathrm{min}$ had not yet been implemented in the SIM method at the time of this experiment. The amount of substance used, total peak area as well as the standard deviation and relative standard deviation of the total peak area are listed in Table 4.6. For this calibration, a low mean RSD of $16.3\,\%$ was achieved.

TABLE 4.6: Results of calibration at $450\,°\mathrm{C}$

Additive	V_{Cal} in µL	n_{Cal} in mol	TPA	SD_{TPA}	RSD_{TPA}
If 168	4	1.54E-09	1.70E+07	2.24E+06	13.2%
	6	2.32E-09	2.96E+07	4.05E+06	13.7%
	8	3.09E-09	3.80E+07	2.65E+06	7.0%
Tin 770	4	2.08E-09	2.12E+07	3.08E+06	14.5%
	6	3.12E-09	3.64E+07	1.51E+07	41.4%
	8	4.17E-09	6.49E+07	1.27E+07	19.6%
Ix 1076	4	1.89E-09	5.72E+06	4.30E+05	7.5%
	6	2.84E-09	1.07E+07	2.46E+06	23.0%
	8	3.79E-09	1.91E+07	1.35E+06	7.1%

TABLE 4.7: Quantification of PA6 and PP at $450\,°\mathrm{C}$

	If 168	**Tin 770**	**If 168**	**Tin 770**	**Ix 1076**
Mean	**0.47%**	**0.13%**	**0.35%**	**0.26%**	**0.45%**
SD	0.039%	0.007%	0.032%	0.057%	0.067%
RSD	8.34%	5.34%	8.90%	22.09%	15.00%
Formulation	-17.5%	35.0%	-52.2%	-30.0%	-50.0%
BASF	-74.1%	23.5%	-84.2%	-13.0%	-55.2%

Table 4.7 contains the quantification results. The PA6 contents are on the left side and the PP contents on the right side. A comparison of the results with the formulation (Tables 3.1 and 3.2) and the HPLC quantification performed by BASF (Table 4.4) is shown beneath the actual results.

Polyamide-6 The SIM pyrogram of the polyamide is shown in Figure 4.21. Pyrolyzed within the polymer matrix, both Irgafos 168 (2) and Tinuvin 770 (1) partly decompose. Their functional groups (phenole and piperidine) elute at $6.3\,\mathrm{min}$ (1a) and $15\,\mathrm{min}$ (2a). The peaks located between $22\,\mathrm{min}$ and $25\,\mathrm{min}$ are artifacts of the SIM method, which was not thoroughly refined when this experiment was performed. However, this has no impact on the results.

The value obtained for Irgafos 168 is $17.5\,\%$ higher than it should be according to the formulation. In comparison to the result provided by BASF, it is $74.1\,\%$ higher. A reason for this could be decomposition of the additive during compounding, which occurs at temperatures around $200\,°\mathrm{C}$ in a not completely oxygen-free environment.

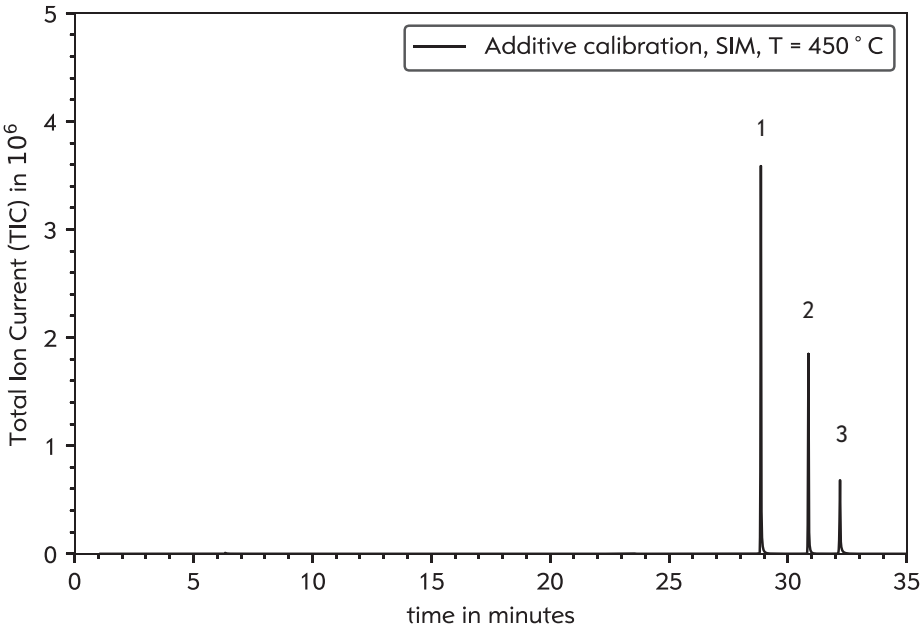

FIGURE 4.19: Calibration for If168, Tin770 and Ix1076 at $450\,°C$

BASF calibrated with and analyzed undecomposed Irgafos 168, therefore oxidized or fragmented fractions arisen from processing would not be included in the analysis. The pyrolysis method however includes the main fragmentation product (2,4-ditert-butyl-phenol). Taking this into account, the determined concentration of Irgafos 168 is still significantly too high.

The Tinuvin 770 concentration was determined as $0.13\,\%$, which is considerably lower than both the formulation ($35\,\%$) and the BASF result ($23.5\,\%$). One possible explanation is the good solubility of the polar molecule within the polymer matrix, which in case of polyamide-6 is also quite polar.

Polypropylene Figure 4.22 shows the polypropylene sample. Fragments of Tinuvin 770 (1a) and Irgafos 168 (2a) as well as the undecomposed additives (1-3) can be found. For Irganox 1076 only the complete molecule at $32.0\,\mathrm{min}$ is found. As explained, this is due to the method and does not reflect on the actual fragmentation pattern.

All additives were determined in greater quantity than is plausible according to the formulation plan. Irgafos 168 and Irganox 1076 lie $50\,\%$ above and Tinuvin 770 $30\,\%$. Again, for Irgafos 168 the BASF results lie far below the pyrolysis value ($84.2\,\%$). For Tinuvin 770 the difference amounts to only $13\,\%$ while Irganox 1076 lies $55\,\%$ below. In the case of Irgafos 168 the same argument given for the polyamide-6 sample is valid. Overall however, this does not explain why all values are too high.

The mean RSD of all additives in the quantification at $450\,°C$ amounts to approximately $12\,\%$.

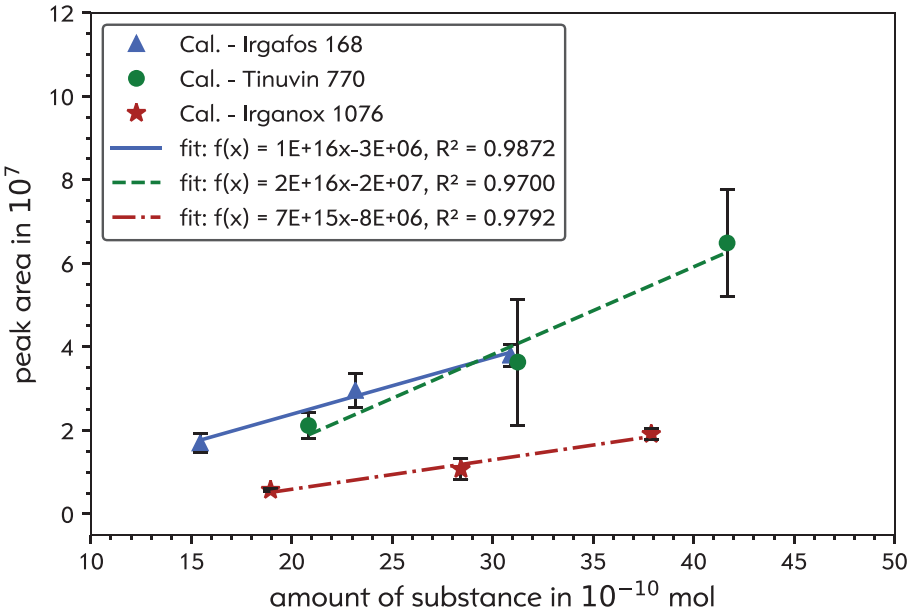

FIGURE 4.20: Calibration curves for If168, Tin770 and Ix1076 at 450 °C

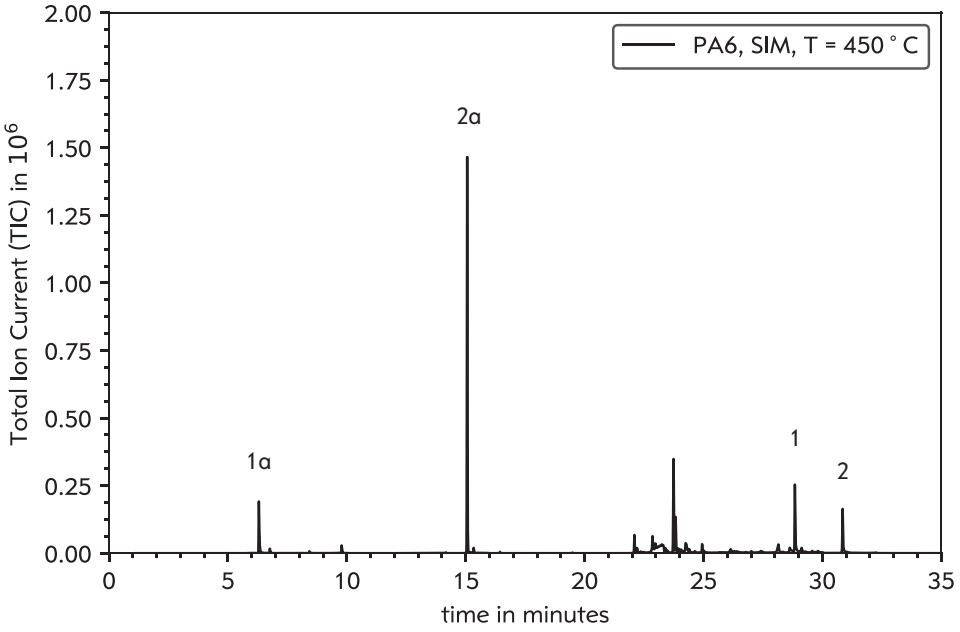

FIGURE 4.21: PA6 at 450 °C

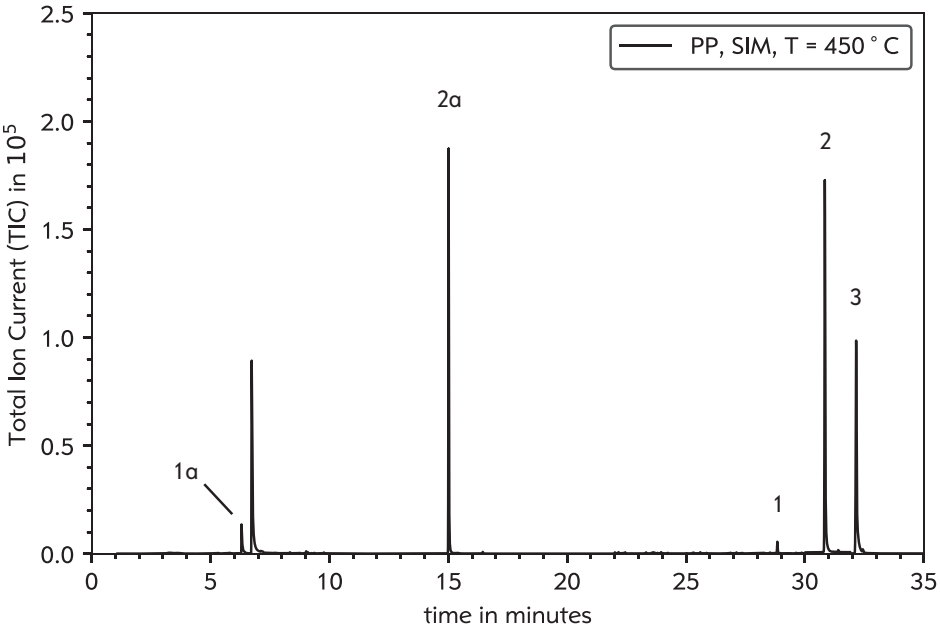

FIGURE 4.22: PP-N at $450\,°C$

4.1.8 Quantification of PA6 and PP-N additives at 600°C

To achieve the goal of analyzing all additives used in the standard samples, a $600\,°C$ method was developed (section 3.2). However, as we learned from the generation of the additive library, Irganox 1010, Irganox 1076 and Irganox 1098 share common peaks. This knowledge is very important and allows us to prevent false quantification. Several consequences ensue from this. First, since Irganox 1098 is only contained in the PA6 sample and Irganox 1010/1076 are contained in the PP sample, two calibration runs are performed. The polyamide-6 and polypropylene samples were prepared in analogy to the $450\,°C$ quantification.

Calibration The calibration runs are detailed in Table 4.8. As before, the $0.02\,\%$ standards were used. Irganox 1098, Irgafos 168 and Tinuvin 770 were measured together, since there are no coinciding peaks for these additives. Irganox 1010 and Irganox 1076 were measured together because they are both contained in the PP sample. This prohibits the use of their peaks at $14.6\,min$ and $16.3\,min$ in any case. Only the $19.6\,min$ peak of Irganox 1010 and the $18.0\,min$ and $32.0\,min$ peaks of Irganox 1076 are left for calibration at quantification. For Irganox 1076 this should not be a problem, since these two peaks make up approximately $99\,\%$ of the total peak area at $600\,°C$. For Irganox 1010 however, only about $18\,\%$ of the peak area usable for quantification remain when in the presence of Irganox 1076. Due to the significant variability of both relative and absolute peak areas found in pyrolysis experiments (section 4.1.4), a great uncertainty must be assumed for the Irganox 1010 result.

TABLE 4.8: Additive calibration at 600 °C

Measurements:	1 - 5	6 - 10	11 - 15	16 - 20	21 - 25	26 - 30
Irganox 1098	2 µL	4 µL	6 µL	-	-	-
Irgafos 168	2 µL	4 µL	6 µL	-	-	-
Tinuvin 770	2 µL	4 µL	6 µL	-	-	-
Irganox 1010	-	-	-	2 µL	4 µL	6 µL
Irganox 1076	-	-	-	2 µL	4 µL	6 µL

Figures 4.23 to 4.25 show the calibration pyrograms and analysis. For both calibration runs the peak at 14.6 min was below both the limit of detection and consequently the limit of quantitation. All other peaks listed in Table 4.2 were detectable and quantifiable. The amount of substance used, total peak area as well as the standard deviation and relative standard deviation of the total peak area are listed in Table 4.9. This calibration displays a noticeably high mean RSD of 44.2 %, which lies considerably higher than the 27.2 % determined in the additive library experiments and the 16.3 % achieved in the 450 °C calibration.

TABLE 4.9: Results of calibration at 600 °C

Additive	V_{Cal} in µL	n_{Cal} in mol	TPA	SD_{TPA}	RSD_{TPA}
Ix 1098	2	7.80E-10	1.08E+05	8.18E+04	75.9%
	4	1.56E-09	3.63E+05	2.43E+05	67.0%
	6	2.34E-09	8.30E+05	2.62E+05	31.6%
If 168	2	7.72E-10	4.20E+06	1.78E+06	42.4%
	4	1.54E-09	9.69E+06	4.48E+06	46.2%
	6	2.32E-09	1.94E+07	5.34E+06	27.6%
Tin 770	2	1.04E-09	5.32E+05	3.70E+05	69.5%
	4	2.08E-09	5.94E+06	3.91E+06	65.9%
	6	3.12E-09	1.93E+07	8.17E+06	42.4%
Ix 1010	2	9.47E-10	1.31E+04	1.82E+03	13.9%
	4	1.89E-09	2.02E+04	6.78E+03	33.5%
	6	2.84E-09	3.97E+04	1.15E+04	29.0%
Ix 1076	2	9.47E-10	9.24E+05	3.24E+05	35.1%
	4	1.89E-09	1.72E+06	7.47E+05	43.5%
	6	2.84E-09	3.07E+06	1.23E+06	40.1%

Polyamide-6 The SIM pyrogram of the PA6 quantification is shown in Figure 4.26. The major peak in the pyrogram is 2,4-di-tert-butyl-phenole the main degradation product of Irgafos 168 (3a) followed by the undegraded Tinuvin 770 (2) and the undegraded Irgafos 168 (3). The degradation products of Tinuvin 770 (2a, 2b) and the degradation products of Irganox 1098 (1a, 1b, 1c) have also been found.

The quantification results of PA6 featuring both the standard deviation and relative standard deviation are displayed in Table 4.10. Below the results a comparison with the formulation plan and the BASF reference quantification is shown.

Irganox 1098 was determined at $0.54\,\%$ with a RSD of $47\,\%$. This value lies $32\,\%$ to $35.5\,\%$ above both the formulation plan as well as the BASF result. Irgafos 168 was determined at $0.35\,\%$ with a RSD of $29.5\,\%$. This value lies $12\,\%$ below the formulation plan and $30.5\,\%$ above the BASF result. Tinuvin 770 was determined at $0.25\,\%$ with a RSD of $20\,\%$. This value lies $25\,\%$ above the formulation plan and $47\,\%$ above the BASF results. The mean RSD of the PA6 quantification lies at $32\,\%$ which lies higher than the value ensued from the additive library buildup. It is however, better than the mean RSD from the calibration measurements. The formulation plan and BASF values of Irganox 1098 and Irgafos 168 all lie within the range of two standard deviations or the 68^{th} percentile of the quantification results. For Tinuvin 770 the formulation plan lies slightly outside of this range, while the BASF results lie distinctly outside.

TABLE 4.10: Quantification of PA6 at $600\,°\text{C}$

	Ix 1098	**If 168**	**Tin 770**
Mean	**0.54%**	**0.35%**	**0.25%**
SD	0.25%	0.10%	0.051%
RSD	46.9%	29.5%	20.3%
Formulation	-35.5%	11.9%	-24.9%
BASF	-32.2%	-30.5%	-46.9%

Polypropylene Figure 4.27 shows the pyrogram of the polypropylene quantification. Again, the pyrogram is dominated by the main degradation product of Irgafos 168 (2a), followed by the cleaved alkyl tail of Irganox 1076 (3a). The peaks of the undegraded additives (168, 770 and 1076) are also present in a quantifiable extent. The Irganox 1076 peak (3) being the smallest one. The unique Irganox 1010 peak at $19.6\,\text{min}$ was vaguely perceptible as a bump in the background. However, it lies significantly below the limit of detection. The peaks at $14.6\,\text{min}$ and $16.3\,\text{min}$, while clearly discernable, could not be used for quantitation purposes, since they derive from both Irganox 1010 and 1076.

The quantification results of PP featuring both the standard deviation and relative standard deviation are displayed in Table 4.11. Below the results a comparison with the formulation plan and the BASF reference quantification is shown.

Irgafos 168 was determined at $0.27\,\%$ with a RSD of $16\,\%$. This shows good conformance with both the formulation plan and the BASF results, both of which lie within the standard deviation. Tinuvin 770 was determined at $0.23\,\%$ with a RSD of $16\,\%$. This shows good conformance with the formulation plan and excellent accordance with the BASF result, lying only $0.5\,\%$ above their value. Irganox 1076 was determined at $0.44\,\%$ with a RSD of $14\,\%$. This value lies approx. $50\,\%$ above both the formulation plan and the BASF result. The mean RSD of the PP quantification lies at $15\,\%$, which is considerably better than both the additive library buildup as well as the PA6 quantification.

TABLE 4.11: Quantification of PP at 600 °C

	Ix 1010	If 168	Tin 770	Ix 1076
Mean	**-**	**0.27%**	**0.23%**	**0.44%**
SD	-	0.042%	0.036%	0.063%
RSD	-	15.9%	15.6%	14.2%
Formulation	-	-15.6%	-14.4%	-48.0%
BASF	-	-39.9%	0.5%	-53.1%

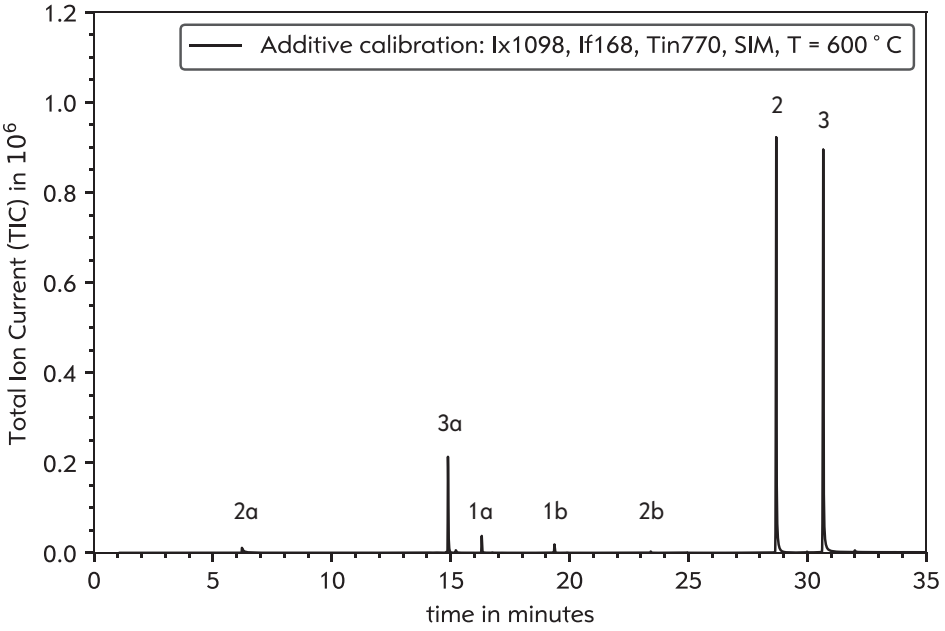

FIGURE 4.23: Calibration for If168, Tin770 and Ix1098 at 600 °C

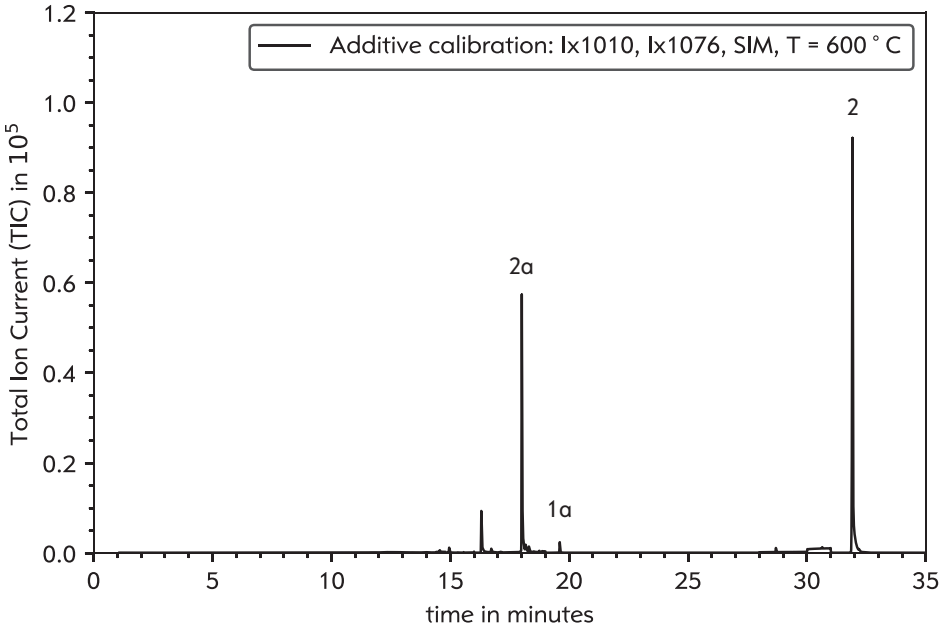

FIGURE 4.24: Calibration for Ix1010 and Ix1076 at 600 °C

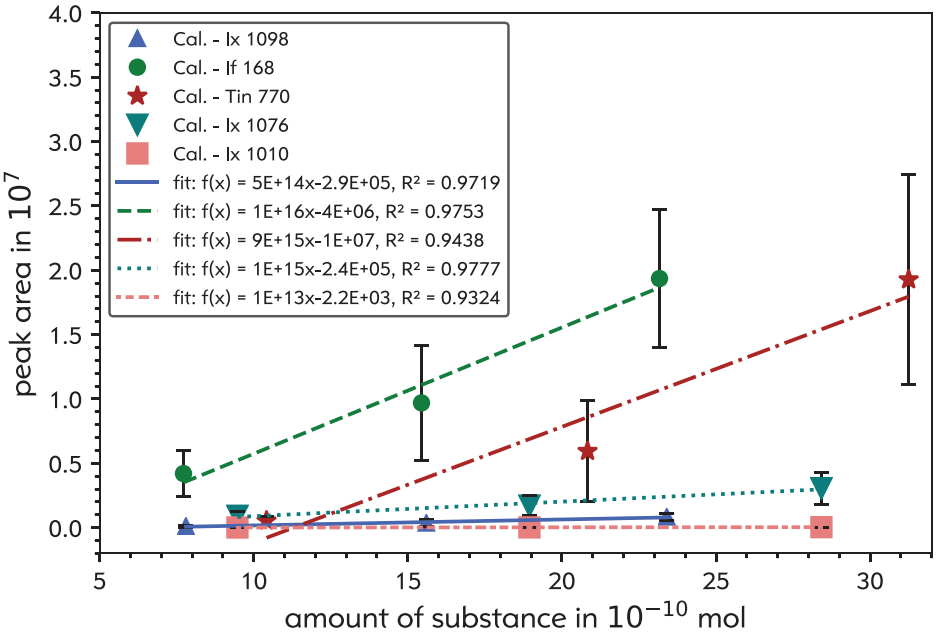

FIGURE 4.25: Calibration curves for If168, Tin770, Ix1076, Ix1098 and Ix1010 at 600 °C

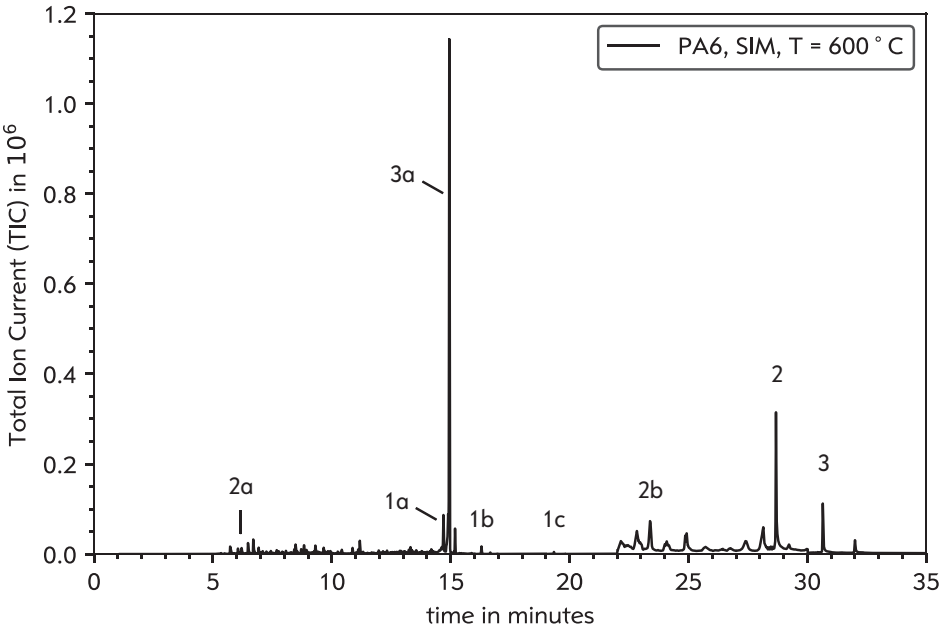

FIGURE 4.26: PA6 at 600 °C

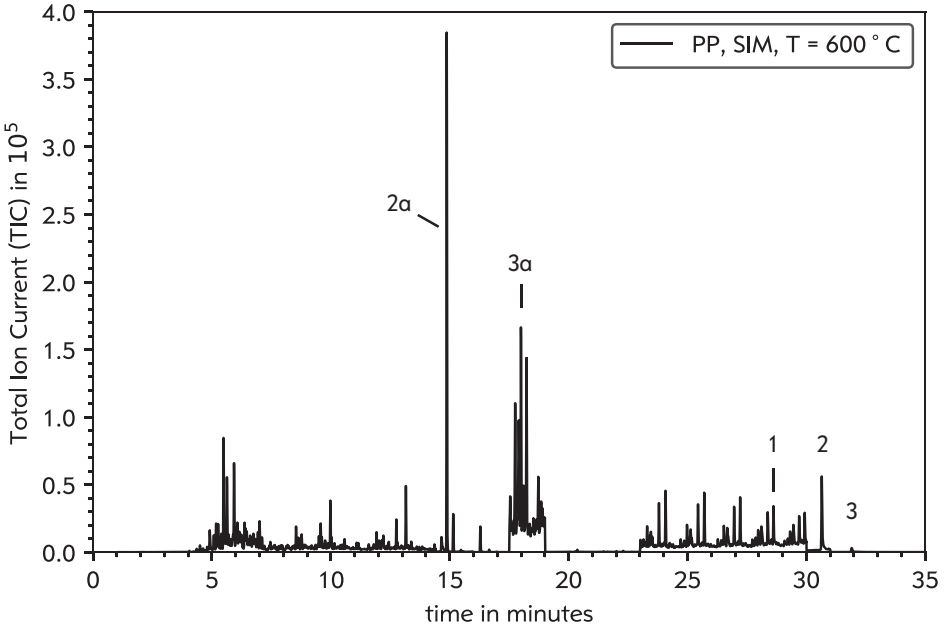

FIGURE 4.27: PP-N at 600 °C

4.1.9 Summary

In the course of the Py-GC/MS method development, the additives and polymers used for the standard samples were first examined by TGA to determine the main thermal degradation stages to give an orientation for the pyrolysis method (Table 4.1 and Figures 4.1 - 4.7). The additives Irgafos 168, Irganox 1076 and Tinuvin 770 decomposed between $360\,^{\circ}\mathrm{C}$ and $430\,^{\circ}\mathrm{C}$ depending on the technique of analysis. Irganox 1010, 1098 and polyamide-6 decomposed between $440\,^{\circ}\mathrm{C}$ and $460\,^{\circ}\mathrm{C}$ and polypropylene at approx. $490\,^{\circ}\mathrm{C}$. It was concluded, that Irgafos 168, Tinuvin 770 and Irganox 1076 could probably be analyzed at $450\,^{\circ}\mathrm{C}$, avoiding degradation of the polymer matrix and thus significantly simplifying detection and quantification without the need for single ion monitoring. For Irganox 1010 and 1098 however, higher temperatures would be necessary. To avoid overlaying of the additive peaks by the polymer matrix, it was decided to employ single ion monitoring for detection.

Taking $450\,^{\circ}\mathrm{C}$ as the starting point, a pyrolysis temperature series of the additives used in the samples was performed (Figures 4.8 - 4.12). In $50\,^{\circ}\mathrm{C}$ steps, the additives were examined from $450\,^{\circ}\mathrm{C}$ to $600\,^{\circ}\mathrm{C}$. The main focus being their fragmentation behavior and the resulting peak areas. For Irgafos 168, Tinuvin 770 and Irganox 1076, fragmentation increased at higher temperatures. however, the total peak area for each additive did not significantly change. For Irganox 1010 and 1098 this picture differs greatly. The quantifiable TPA of both additives profited distinctly from higher temperatures. The greatest increase in intensity lying within the step from $550\,^{\circ}\mathrm{C}$ to $600\,^{\circ}\mathrm{C}$ in the case of Irganox 1010 and slightly below that for Irganox 1098. The conclusion of this experiment was, that while $450\,^{\circ}\mathrm{C}$ would be sufficient for Irgafos 168, Tinuvin 770 and Irganox 1076, but $600\,^{\circ}\mathrm{C}$ would be necessary to analyze Irganox 1010 and 1098. Combined with the knowledge about the decomposition temperature of the polymers gained from the TGA experiments, it became clear, that the use of SIM techniques would be necessary to identify and quantify the additives within the polymer matrix.

The next step was the buildup of an additive library containing the retention times and mass spectra of all peaks suitable for quantification. Each additive was measured eight times to reduce the result's uncertainty to a minimum (Table 4.2 and Figures 4.13 to 4.17). Additionally, the statistical information gained from these measurements was used to characterize the methods reproducibility (Table 4.3). At least two peaks were identified for each additive. However, Irganox 1010, 1076 and 1098 have three peaks in common due to their similar structure (based on Butyl hydroxy toluene). This leaves one unique peak each for Irganox 1010 and 1098 ($19.6\,\mathrm{min}$ and $19.4\,\mathrm{min}$ respectively) as well as two unique peaks for Irganox 1076 ($18.0\,\mathrm{min}$ and $32.0\,\mathrm{min}$). In most cases, peak identification was confirmed either by library match or from literature.

Using the information gathered in the additive library, two SIM methods were developed. One at $450\,^{\circ}\mathrm{C}$ and one at $600\,^{\circ}\mathrm{C}$. Both were used for a quantification. To achieve this, a three-point calibration was produced for both experiments (Tables 4.5

and 4.8). The calibration results are displayed in Tables 4.7, 4.10 and 4.11 as well as in Figures 4.20 and 4.25. The quantification results of Irgafos 168, Tinuvin 770 and Irganox 1076 in PA6 and PP at $450\,^{\circ}\mathrm{C}$ yielded the results summarized in Table 4.7. Comparison with the formulation plan and the reference values obtained from BASF shows, that the determined concentrations of all additives with the exception of Tinuvin 770 in PA6 were too high. However, all values were in the correct order of magnitude. Irganox 1010 and 1098 were not determined at $450\,^{\circ}\mathrm{C}$.

The $600\,^{\circ}\mathrm{C}$ quantification yielded the results displayed in Tables 4.10 and 4.11. Apart from Irganox 1010, all additives were determined in good accordance with the formulation plan and the BASF results, with the maximum deviation lying at approx. $50\,\%$ from the BASF results in the case of Tinuvin 770 in PA6 and Irganox 1076 in PP. For PA6 all peaks expected from the additive library could be found and quantified. In the case of PP, the decomposition products of Tinuvin 770 and the unique Irganox 1010 peak could not be found. Irganox 1010 could therefore not be quantified. The mean RSD of the measurements significantly improved from the calibration ($44.2\,\%$) and the PA6 quantification ($32\,\%$) to the PP quantification ($15.2\,\%$).

4.1.10 Discussion

Reproducibility Both the quantification results and the additive library data show, that reproducibility is an issue with pyrolysis. A relative standard deviation for a series of experiments of $30\,\%$ is not unusual. The quantitative reproducibility is poor, especially when comparing them to quantitation workhorses such as liquid injection GC/FID or HPLC/UV. This is due to two factors. The main source of variation being the pyrolysis process, which not only involves a physical process like evaporation but also entails chemical processes e.g. pyrolysis reactions. The outcome of these reactions is mainly dependent on the amount of energy introduced into the sample. However, factors such as the exact location and distribution of the analyte within the sample vial, the grain size of solid samples or impurities also have a significant influence on the result. The second source of variation is the mass detector. While it provides unparalleled analytical power to the GC, it does not compare to the FID in terms of quantitation stability. The mass detector's influence is a possible explanation for the marked improvement of the mean RSD in the progress of the quantification at $600\,^{\circ}\mathrm{C}$. The experiment was performed after the christmas holiday shutdown. Apparently, despite three full days of equilibration before the start of the experiment, the detector's stability had not fully recovered yet, leading to a broad distribution in the first two thirds of the run.

Quantification When comparing the $450\,^{\circ}\mathrm{C}$ and $600\,^{\circ}\mathrm{C}$ quantification, the results vary. Apart from Tinuvin 770 in PA6 the concentrations found at $450\,^{\circ}\mathrm{C}$ were higher than those found at $600\,^{\circ}\mathrm{C}$. However, the difference lies within the range of uncertainty expected for pyrolysis quantifications.

The same is mostly true for the comparison of the pyrolysis results to the formulation plan and the BASF results. The largest deviations are Irganox 1076, which differs bei approx. $50\,\%$ and Irgafos 168 which differs by up to $85\,\%$.

In the case of Irganox 1076, a slightly higher uncertainty is to be expected, since only $50\,\%$ of the available peaks could be used in the quantification. As discussed above, the deviation of an additive's peaks among each other is considerable and heightens the measurement's uncertainty distinctly when not all possible peaks are taken into account.

In the case of Irgafos 168 it is likely, that the sample processing is partly responsible for the deviation. The compounding process of the samples takes place at $260\,°C$ for PA6 and $205\,°C$ for PP. Additionally, a completely oxygen free environment cannot be assumed despite of degassing measures due to oxygen adsorbed on and solved in the raw materials [52]. Irgafos 168 protects the polymer during processing but is partly decomposed in the process. This explains the deviation from the formulation plan. For polypropylene an effect discussed by Brander and Wold [16] must be taken into consideration. These samples contain $15\,\%$ talcum, which according to their 2014 publication causes an increase in antioxidant consume during processing.

The difference to the BASF results can possibly be explained by looking at how the HPLC quantification is performed. The additive is extracted from the polymer by solvent extraction and analyzed via HPLC. It is quantified by calibration with standard solutions. However, degradation products are not taken into consideration since the goal of the analysis was the concentration of Irgafos 168 and not e.g. 2,4-di-tert-butylphenol. In the pyrolysis quantification this is different. Since the pyrolysis step also causes decomposition, the degradation products are a part of the scope of analysis. This results in higher values than the HPLC analysis performed by BASF.

When comparing this new technique with the standard liquid extraction / HPLC quantification in general, there is an important factor to take into consideration: the size of the sample used for the analysis. With liquid extraction and HPLC it is possible to take a large sample (several grams) for the extraction. This significantly improves the representativeness of the sample. After the extraction one can accurately pipette an aliquot for the HPLC analysis, preserving the representativeness. When performing an quantification via Py-GC/MS, one is constricted to very small samples up to a maximum of about $500\,\mu g$. Using more will cause problems with clogged split vents and overloading of the column and mass detector. While the goal of every compounding process is a homogeneous distribution of all ingredients within the polymer matrix, one has to consider a certain heterogeneity on the μg scale.

So, from a purely results oriented point of view, HPLC quantification with a UV detector and prior liquid extraction is clearly superior in respect to validity and accuracy of the results so long as the extraction process has been optimized. However, there are also strong arguments for the pyrolysis method. No prior sample

treatment is necessary reducing the amount of necessary lab equipment. The mass detectors analytical power makes the assignment of degradation products to their parent-additives possible. And the limitation to very small samples, while reducing representativity, can also be a benefit. Especially in failure analysis, the amount of sample at hand is often quite small. Here, methods which only require minute amounts have an advantage.

4.2 OIT/DSC vs. oven-aging

A secondary project of this thesis was to examine the correlation of classic oven-aging experiments with DSC/OIT measurements in regard to lifetime expectancy predictions. As mentioned before, the state of the art method entails oven aging of standard specimens at $150\,°\mathrm{C}$ for at least $336\,\mathrm{h}$ (two weeks). During this time the specimens optical and mechanical properties must remain stable, otherwise the test is failed. In analogy to the DSC/OIT discussed in section 2.1.3, we can define the aging-duration in which the optical or mechanical properties remain stable as the *Oven/OIT*.

In order to compare these techniques, DSC/OIT measurements were performed on the unaged samples V1-3 described in Table 3.3. Then, these samples were subjected to oven-aging at $150\,°\mathrm{C}$ in air circulated ovens. The sample's mechanical properties were monitored by regular three-point flexural tests throughout the aging process. Finally, the order in which the samples reached their OIT under oven-aging and DSC/OIT conditions was compared. Additionally, DSC/OIT measurements and optical evaluations were also performed on the aged samples.

4.2.1 Mechanical testing

The three-point flexural test provides three values to characterize a samples condition. The flexural strain, flexural strength and flexural modulus.

Flexural strain The flexural strain i.e. the deflection at the point of maximum flexural stress ε_{fM}, is a characteristic indicator of embrittlement [65]. The value, which at the onset of polymer oxidation will match the flexural strain at break point ε_{fB}, will drastically decay at the end of the induction period.

In Figure 4.28, a clear order of oxidation resistance is obvious. The first sample to reach the end of it's OIT is V2, mainly stabilized with the phosphitic process stabilizer Irgafos 168. A sharp decline in flexural strain is observed after day 17, dropping from about $7\,\%$ to under $4\,\%$. The next sample to reach the end of it's OIT is V1, mainly stabilized with the phenolic long term thermal stabilizer Irganox 1010. The drop in ε_{fM} is observed after day 20, dropping from about $6\,\%$ to under $3\,\%$. The most stable sample by far was V3, containing the thio based Irganox PS 802. It outlasts V1 by more than a week, showing major decay after day 29 when it drops from $6\,\%$ to $1\,\%$.

All samples show signs of post crystallization in the first few days. This can be seen in the slight decrease in flexural strain by about $0.3\,\%$.

The standard deviation of ε_{fM} is low for all samples during the induction period, never exceeding a relative standard deviation of $5\,\%$. In the phase of decay, the SD grows distinctly, reaching RSD values of over $30\,\%$.

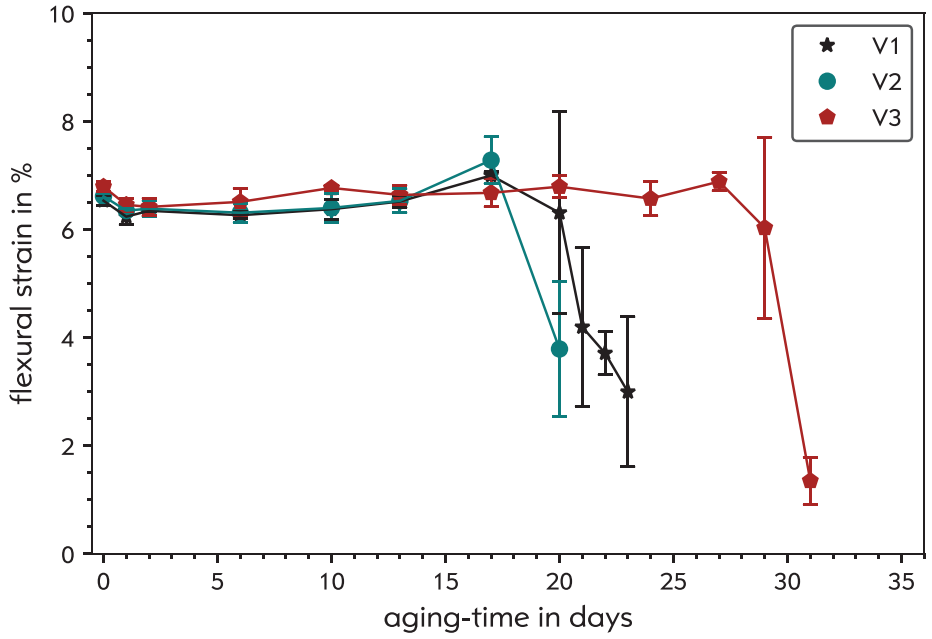

FIGURE 4.28: Flexural strain of V 1-3 during oven-aging

Flexural strength Figure 4.29 shows the course of the materials flexural strength throughout the aging process. It represents the maximum amount of stress tolerated by the samples. The curves are very similiar to the flexural strain plots in Figure 4.28. In the first two days a slight increase in flexural strength due to post crystallization is visible. All samples then stay at one level throughout their respective induction periods. After 17 days, V2 is the first sample to reach the end of it's OIT, clearly marked by a sharp decline in flexural strength. After 20 days, V1 also reaches the end of it's OIT, followed by V3 after 29 days. V3 displays a distinct dent in flexural strength on day 24, which completely recovers by day 27.

As already seen with the flexural strain, the standard deviations are very small during the induction period but increase markedly when the samples start deteriorating.

Flexural modulus Figure 4.30 shows the flexural modulus of the samples throughout aging. It is a measure of how much stress a sample can withstand while remaining in the range of elastic deformation. Again, the curves greatly resemble those for flexural strain and flexural strength.

In the first two days a significant increase in the flexural modulus of $350\,\mathrm{MPa}$ to $400\,\mathrm{MPa}$ due to post crystallization can be observed for all samples. During the induction period the values stay at a constant level and then rise slightly towards the end of the OIT, when the material begins to harden due to incipient chain scission. The decrease in molar mass leads to a higher degree of crystallinity [44].

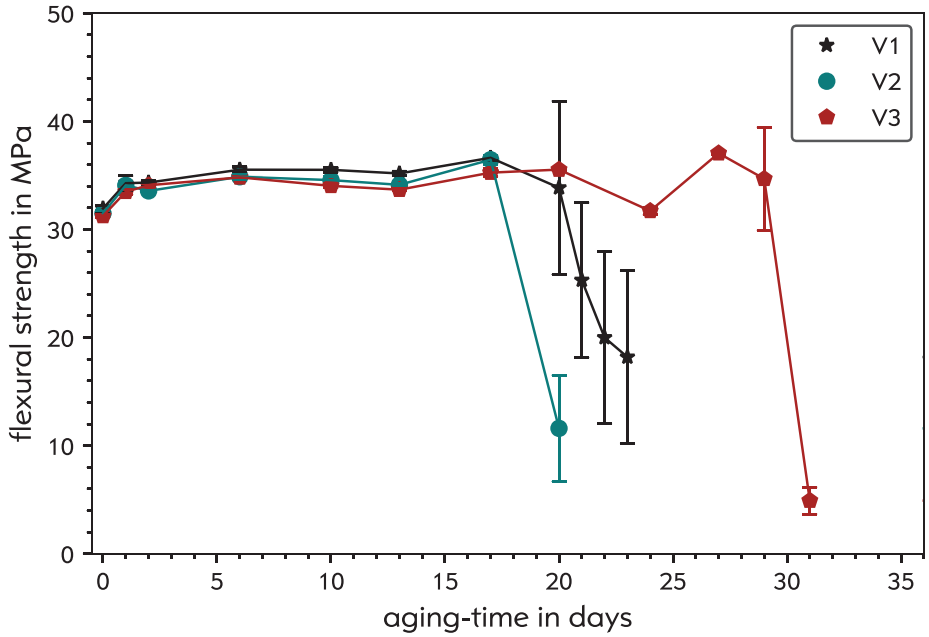

FIGURE 4.29: Flexural strength of V 1-3 during oven-aging

The order of failure is unchanged, as V2 fails after day 17, V1 after day 20 and V3 outlasting both until after day 29.

In conclusion of the mechanical tests throughout oven aging, one can say that the formulation V2 ($0.4\,\%$ If 168) offers the lowest resistance to oxidation at $150\,°C$, followed closely by V1 ($0.35\,\%$ Ix 1010). The best protection is afforded by V3 ($0.3\,\%$ Ix PS 802) outlasting V1 by 9 days and V2 by 12 days.

4.2.2 DSC/OIT testing

Parallel to mechanical testing, DSC/OIT measurements of the samples were performed on microtome sections before the begin of the oven aging and throughout, to monitor the change in OIT at $200\,°C$. Figure 4.31 shows the results of these measurements with the DSC/OIT values of the unaged samples displayed in the plot's legend. Figure 4.32 shows boxplots of the DSC/OIT measurements on the unaged samples.

At $200\,°C$ in the $100\,\%$ oxygen atmosphere of the DSC instrument, the samples show a different order of oxidation stability then observed during the $150\,°C$ oven tests. The first sample to reach the end of it's OIT after $108\,\mathrm{min}$ and decompose exothermally is the thio-stabilized V3. Soon thereafter, at $116\,\mathrm{min}$, the phenol stabilized V1 degrades. The most oxidation resistant sample by far under these conditions is V2 with it's high phosphitic process stabilizer content, reaching the end of it's OIT about twenty minutes after V1 at $135\,\mathrm{min}$.

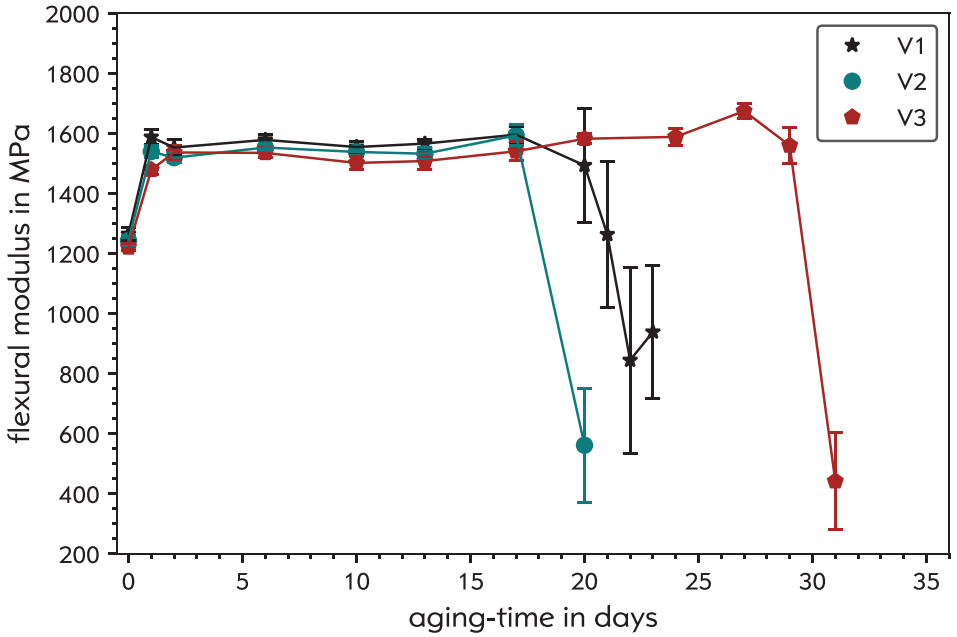

FIGURE 4.30: Flexural modulus of V 1-3 during oven-aging

The DSC/OIT values in the further course of the aging process follow the same order as the mechanical tests. V2 is the first sample to reach a DSC/OIT value of under $10\,\mathrm{min}$ on day 10. V1 reaches the sub $10\,\mathrm{min}$ level on day 13, while V3 endures until day 17. In all cases this is at least a week before the end of the Oven/OIT.

Unlike the mechanical characteristics, the DSC/OIT does not remain constant throughout the aging process but shows an exponential decay. The data in Figure 4.31 show very good concordance with the exponential fit curves, reaching R-squared values of 0.9959, 0.9488 and 0.9613 respectively.

The boxplots in Figure 4.32 show the precision of the DSC/OIT measurements similiar to the way errorbars do. An additional figure was chosen to ensure clarity for both the values uncertainty and their course throughout aging. It can be seen, that the differences for the DSC/OIT values are statistically significant.

4.2.3 Optical degradation

Photographic documentation of the sample's optical degradation was produced. As can be seen in Figure 4.33, the optical degradation follows the same order as the mechanical characteristics. All samples turn from the unaged grey to a beige color during the aging process. At the end, when all stabilizers have been consumed and the induction period has ended, oxidation of the polymer causes severe crack formation and intense coloring ranging from a dark yellow to brown tone.

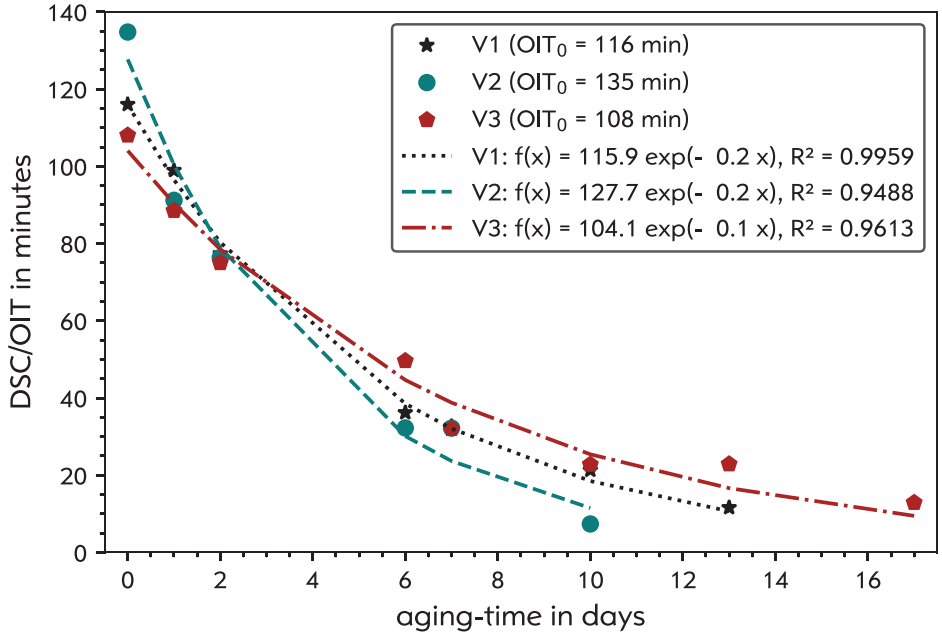

FIGURE 4.31: DSC/OIT values and fit of unaged and aged PP samples

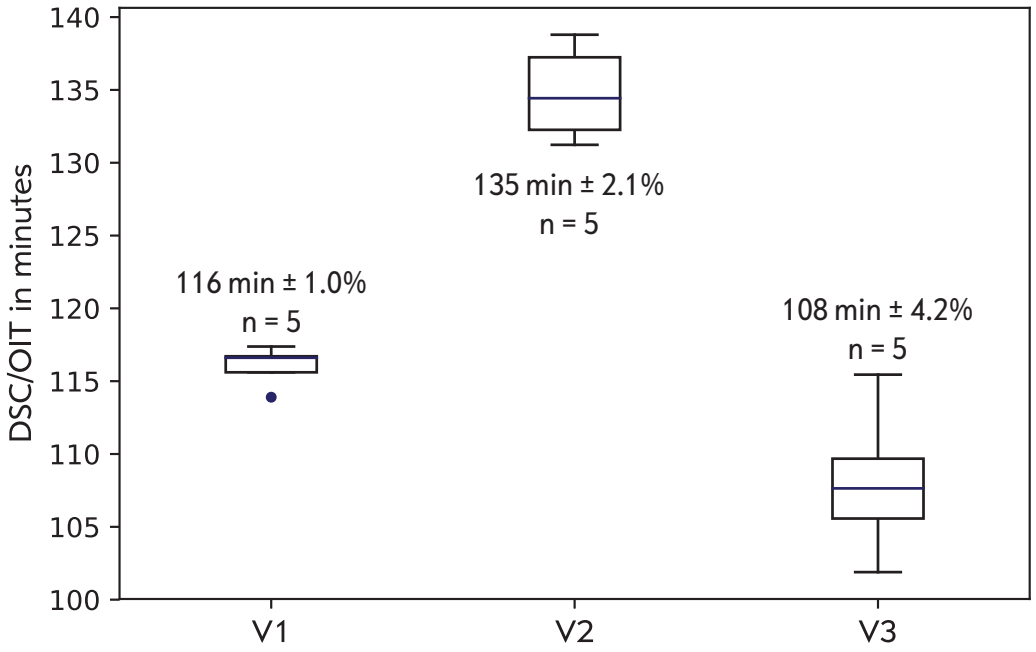

FIGURE 4.32: DSC/OIT boxplots of unaged PP samples

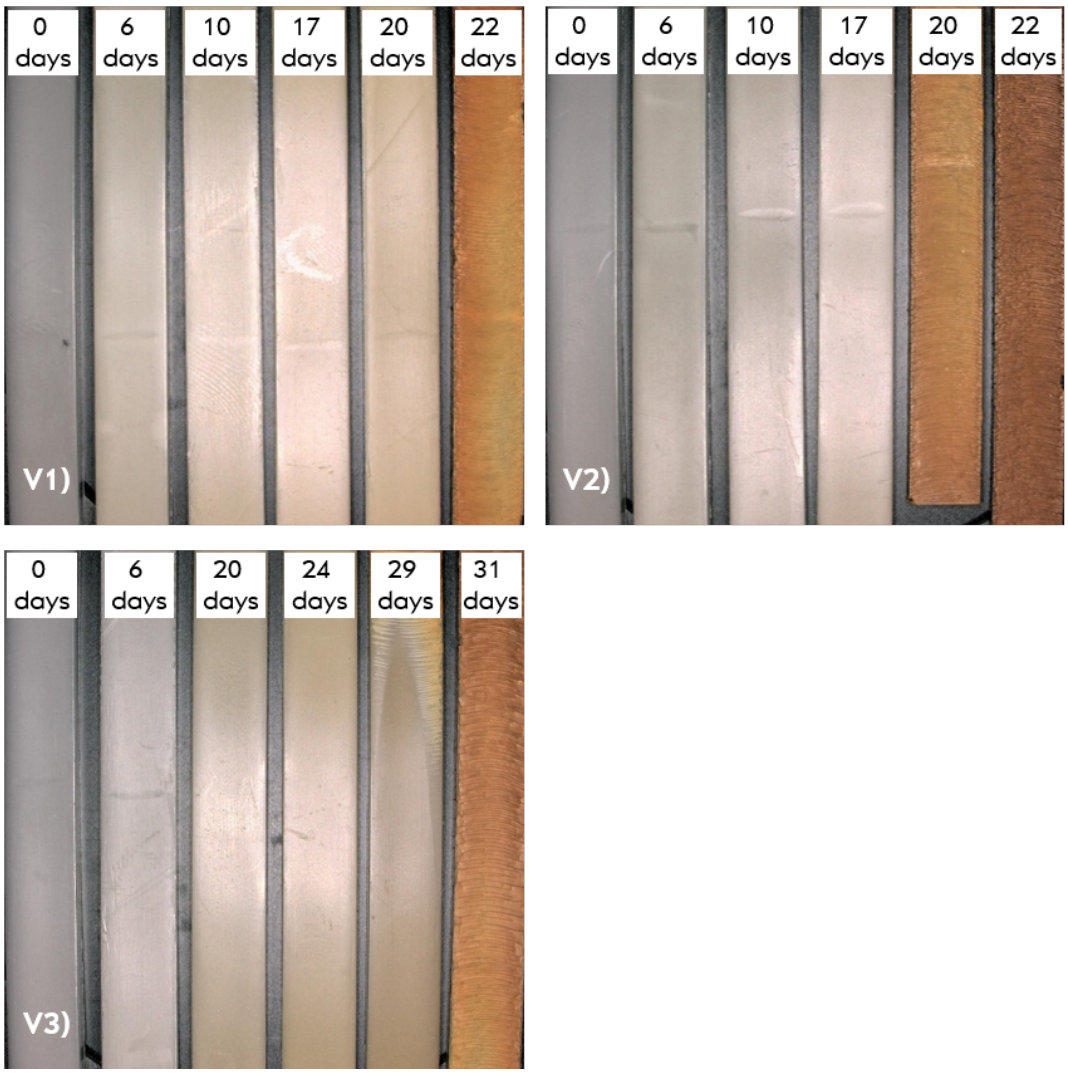

FIGURE 4.33: Optical degradation during aging of PP samples

4.2.4 Pyrolysis-GC/MS

In order to gain more information on the correlation between the sample's additive content, DSC/OIT and Oven/OIT, the change in additive content of V1 and V2 was monitored with the quantitative pyrolysis method developed in the course of this thesis. In addition to providing more data for the DSC/OIT vs. Oven/OIT, this was an opportunity to further test and validate the quantification method, since it would have to prove sufficiently precise and sensitive to observe small changes in the samples additive content.

The SIM method used for this quantification was slightly altered. Since there was no need to monitor Irganox 1076, it was possible to include the primary oxidation peak of Irgafos 168 at $32.0\,\mathrm{min}$ (Figure 4.14 - peak 3), which usually co-elutes with the undegraded Irganox 1076 peak (Figure 4.17 - peak 4).

As with the quantifications performed during the pyrolysis method development for the standard polyamide-6 and polypropylene samples at $450\,^{\circ}\mathrm{C}$ and $600\,^{\circ}\mathrm{C}$, 5 measurements were taken for every data point in both the calibration and the subsequent quantification, with at least one blank measured in between each run.

Calibration To get the best comparability for the measurement of V1 and V2, a mutual calibration was used. This was deemed viable, since the complete test sequence was run in the course of 1.5 weeks. The calibration parameters can be found in Table 4.12.

TABLE 4.12: Additive calibration for V1 and V2

Measurements	**1 - 5**	**6 - 10**	**11 - 15**
Irgafos 168	2 µL	4 µL	6 µL
Irganox 1010	2 µL	4 µL	6 µL

TABLE 4.13: Results of calibration for V1 and V2

Additive	$\mathbf{V_{Cal}}$ **in** µL	$\mathbf{n_{Cal}}$ **in** mol	**TPA**	$\mathbf{SD_{TPA}}$	$\mathbf{RSD_{TPA}}$
If 168	2	7.72E-10	6.01E+06	1.48E+06	24.5%
	4	1.54E-09	1.19E+07	7.97E+05	6.7%
	6	2.32E-09	2.12E+07	1.84E+06	8.7%
Ix 1010	2	4.25E-10	6.99E+04	2.42E+04	34.6%
	4	8.50E-10	2.19E+05	4.27E+04	19.5%
	6	1.27E-09	6.76E+05	1.45E+05	21.5%

Figure 4.34 shows all three concentrations measured for both Irgafos 168 and Irganox 1010 as well as the linear fit used to obtain the calibration functions. The results of the calibration measurements can be found in Table 4.13.

Additive depletion during the aging of V1 and V2 was monitored by choosing five points during the course of the aging process. This was done by looking at the mechanical tests performed. The first point in both cases was the unaged sample,

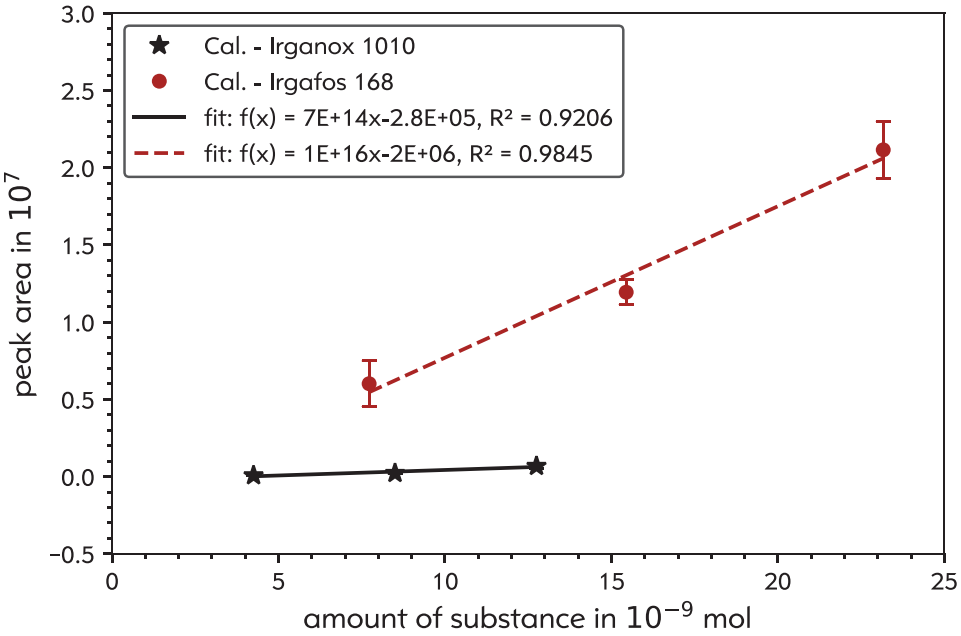

FIGURE 4.34: Calibration curves for Ix1010 and If168 at 600 °C

followed by two points during the induction period (days 6 and 10 for both V1 and V2). The last two points chosen were the end-point of the induction period (days 20 and 17 respectively) and the last sample taken from the oven (days 23 and 20 respectively).

TABLE 4.14: Quantification of V1 at 600 °C

V1	Days	0	6	10	20	23
Ix 1010	**Mean**	0.178%	0.171%	0.146%	0.129%	0.105%
	SD	0.016%	0.039%	0.033%	0.009%	0.014%
	RSD	9.1%	22.7%	22.6%	7.0%	13.5%
If 168	**Mean**	0.093%	0.087%	0.073%	0.106%	0.066%
	SD	0.016%	0.018%	0.018%	0.022%	0.010%
	RSD	16.7%	20.4%	24.5%	21.1%	14.8%

V1 Table 4.14 shows the quantification results for Irganox 1010 and Irgafos 168 in V1 throughout the aging process. Plot and fit of the data are shown in Figure 4.35. Both additives show a declining trend, which is stronger for Irganox 1010. It falls to 59 % of it's original concentration during the course of the aging process. Irgafos 168 falls to 71 % of it's original concentration. The Irgafos 168 value at day 20 (bracketed in Figure 4.35) was disregarded as an error in measurement. There is no way to explain why it's concentration should peak at day 20.

The values of both Irganox 1010 and Irgafos 168 show good to moderate concordance with a linear fit, reaching an R-squared value of 0.9402 and 0.8647 respectively.

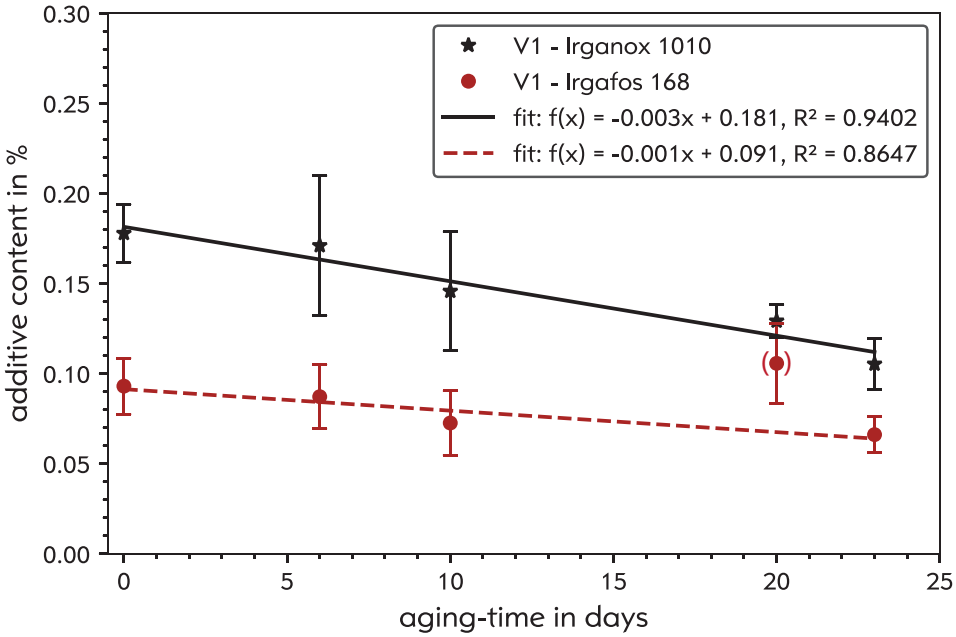

FIGURE 4.35: V1: Ix1010 and If168 content during aging process

Figures 4.36 to 4.39 show the additive peaks used for quantification. All peaks were weighted on the basis of their sample mass.

The Irganox 1010 peak in Figure 4.36 shows the expected decline in peak area over the course of time. Peak 1 of Irgafos 168 shows the same behavior with the exception of the day 20 anomaly mentioned above. Peak 2, the undegraded phosphite only has a pronounced appearance in the unaged sample. In the aged samples it disappears in the background. Peak 3, the phosphate peak, grows until day 10 and then remains constant if one disregards the result of day 20.

V2 The quantification results of Irganox 1010 and Irgafos 168 in V2 throughout the aging process are displayed in Table 4.15. A plot with linear fit of the data can be found in Figure 4.40. As with V1, both additives show a declining trend, falling to $58\,\%$ (Ix 1010) and $35\,\%$ (If 168) of their concentrations in the unaged sample by day 20. The decline in concentration shows good concordance with the linear fit for both additives, with an R-squared value of 0.9342 and 0.8715 respectively.

The additive peaks used for the V2 quantification are shown in Figures 4.41 to 4.44. As before, they have been weighted on the basis of their sample mass.

The Irganox 1010 peak at $16.3\,\mathrm{min}$ shows the same reduction as already observed for V1. The Irgafos 168 peak at $14.9\,\mathrm{min}$ now also shows this behavior, without a break in trend such as was observed for day 20 in V1. Peak 2 at $30.6\,\mathrm{min}$ quickly deteriorates into the background in the first few days of aging. Peak 3 at $32\,\mathrm{min}$ shows a steep rise between days 0 and 6 followed by a gradual decline towards day 20 as the phosphate degrades.

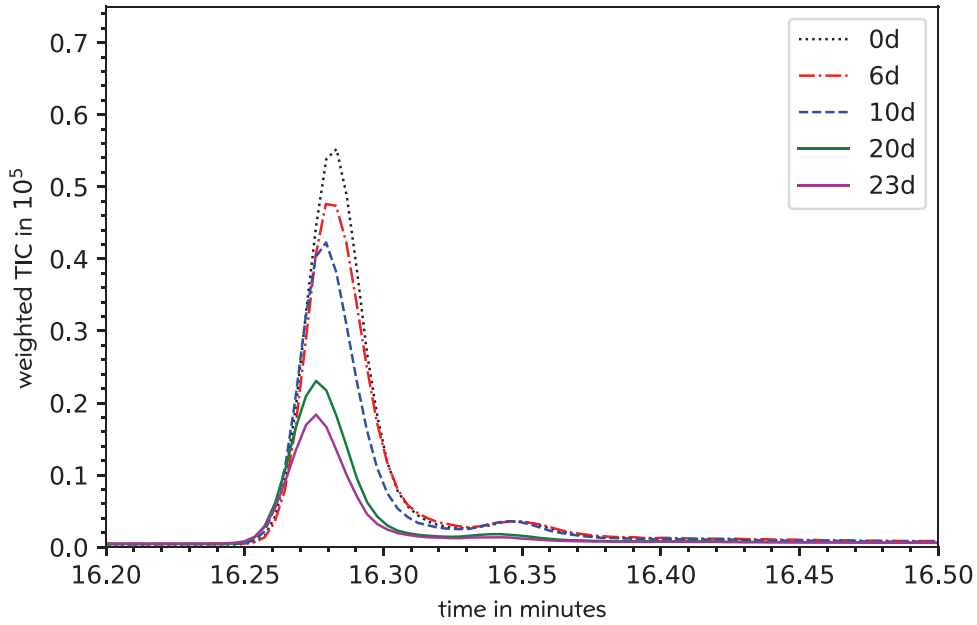

FIGURE 4.36: V1: Weighted Ix 1010 main peak at 16.3 min during aging process

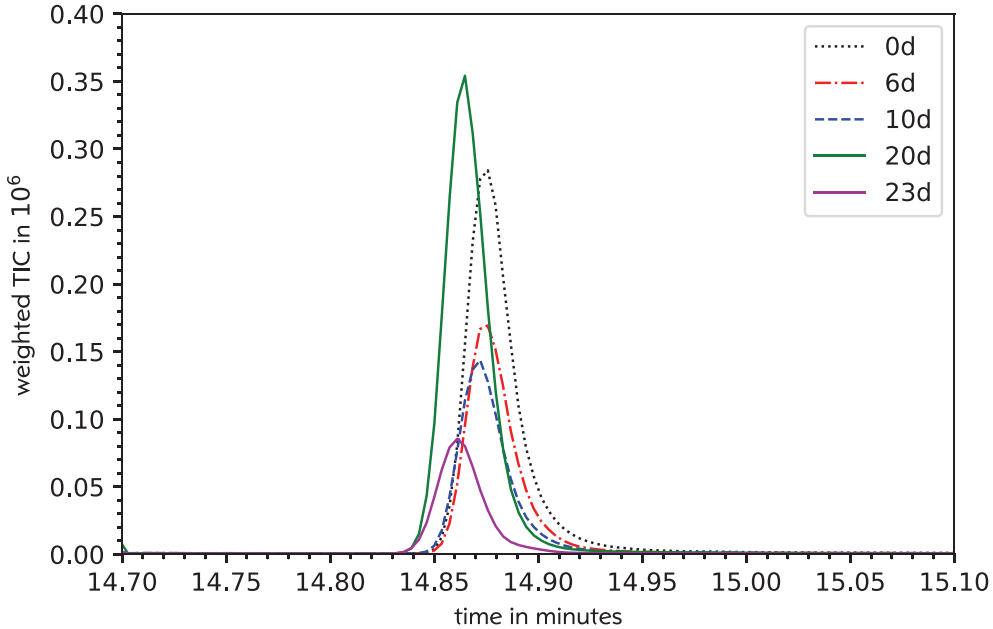

FIGURE 4.37: V1: Weighted If 168 peak at 14.9 min during aging process

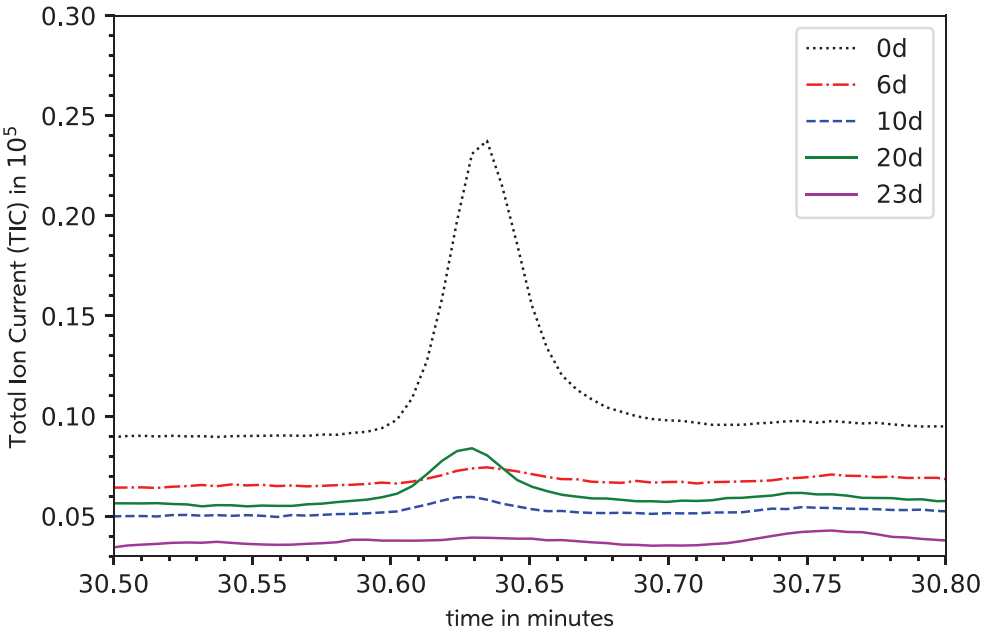

FIGURE 4.38: V1: Weighted If 168 peak at 30.6 min during aging process

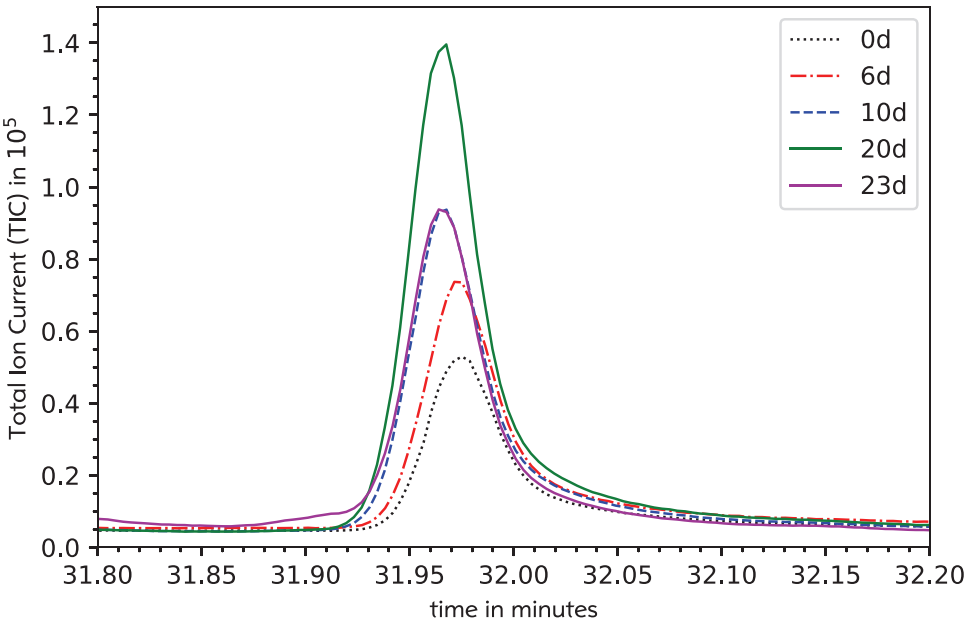

FIGURE 4.39: V1: Weighted If 168 oxidation peak at 32.0 min during aging process

TABLE 4.15: Quantification of V2 at 600 °C

V2	Days	0	6	10	17	20
Ix 1010	**Mean**	0.122%	0.106%	0.103%	0.090%	0.071%
	SD	0.003%	0.015%	0.015%	0.016%	0.008%
	RSD	2.8%	14.0%	14.7%	18.1%	11.3%
If 168	**Mean**	0.156%	0.098%	0.085%	0.077%	0.055%
	SD	0.017%	0.009%	0.011%	0.012%	0.006%
	RSD	11.2%	9.1%	12.6%	15.4%	10.6%

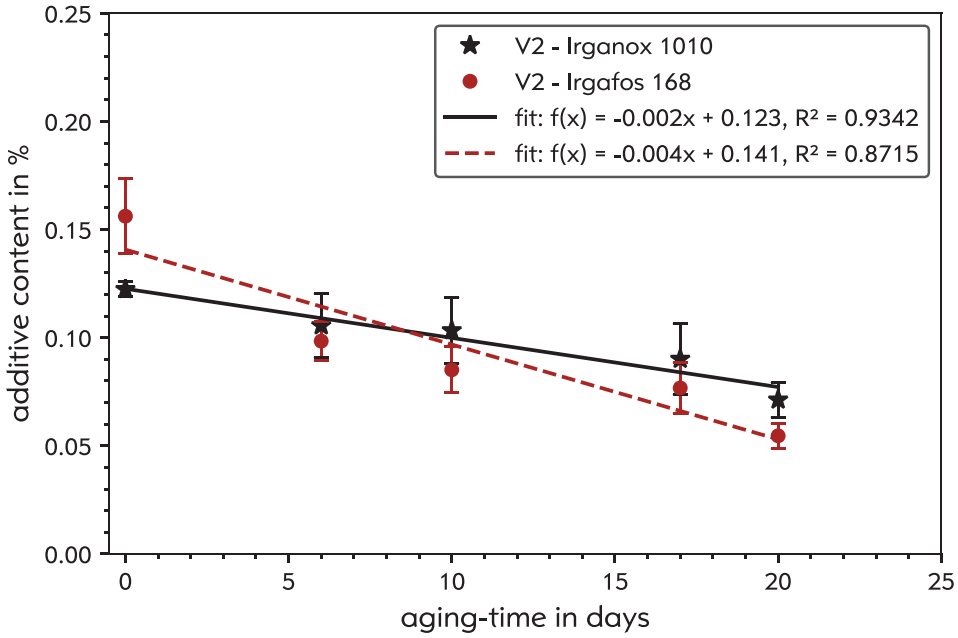

FIGURE 4.40: V2: Ix1010 and If168 content during aging process

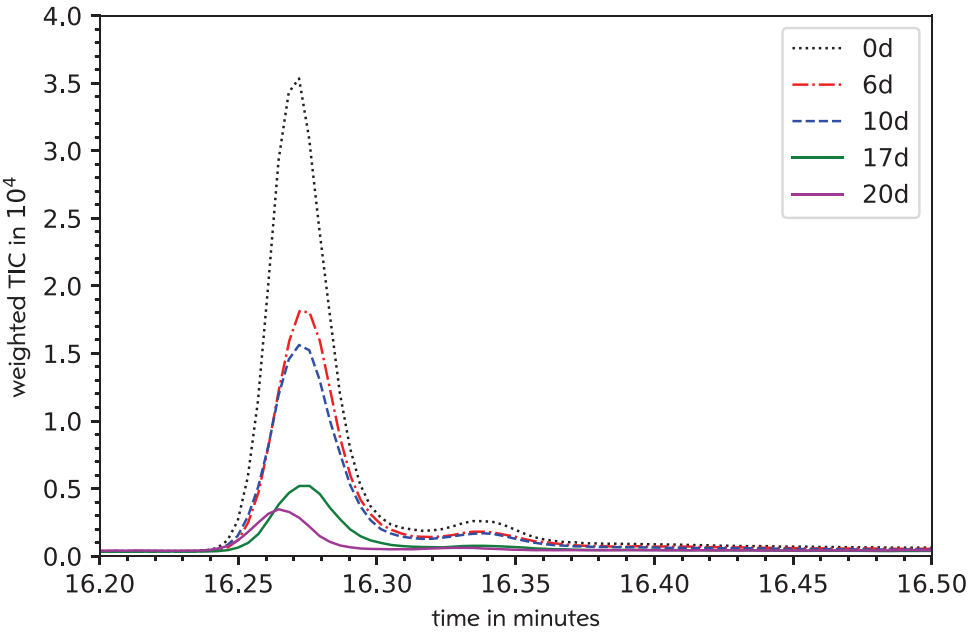

FIGURE 4.41: V2: Weighted Ix 1010 main peak at 16.3 min during aging process

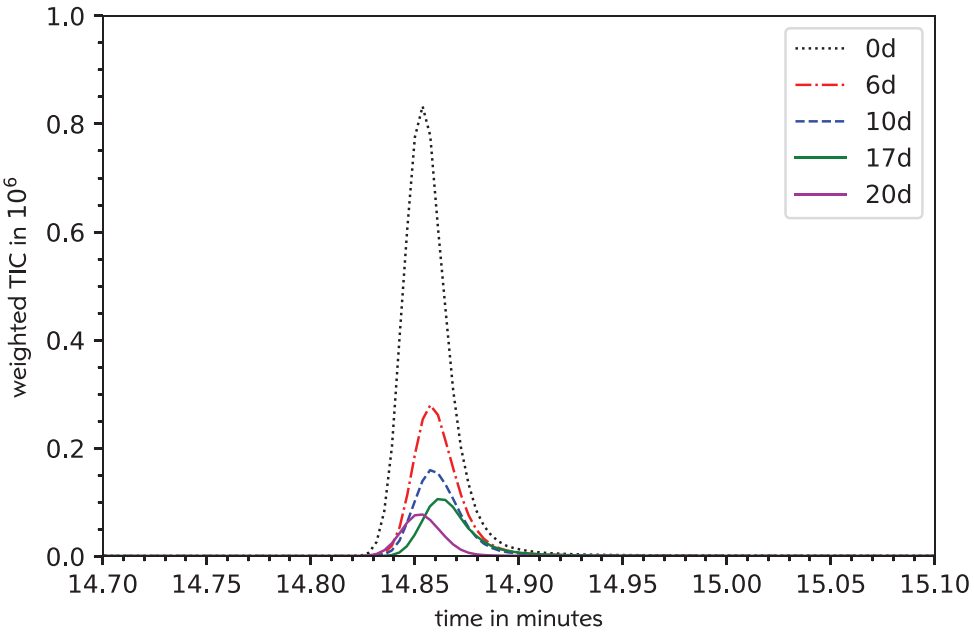

FIGURE 4.42: V2: Weighted If 168 peak at 14.9 min during aging process

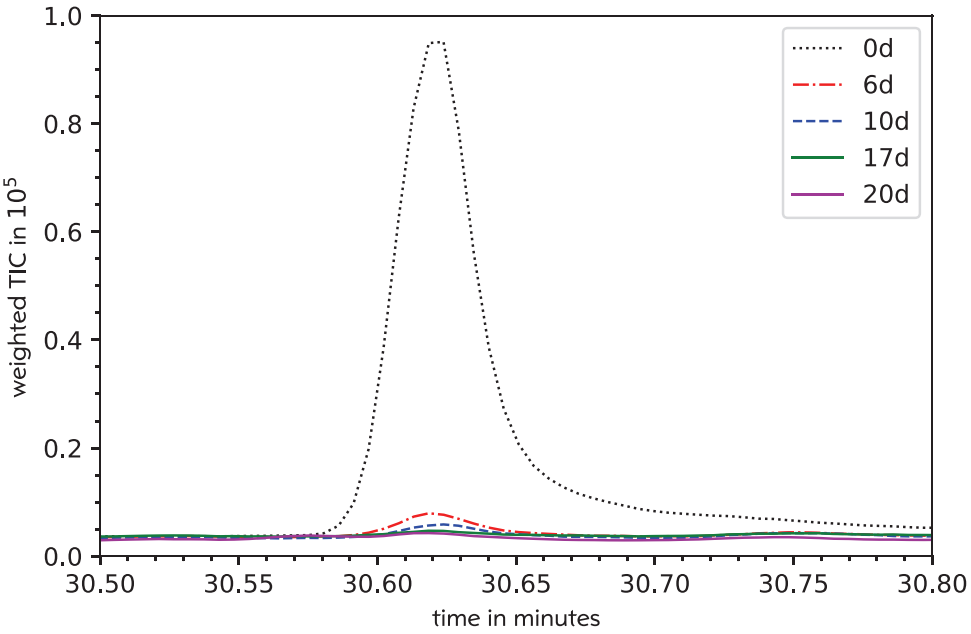

FIGURE 4.43: V2: Weighted If 168 peak at 30.6 min during aging process

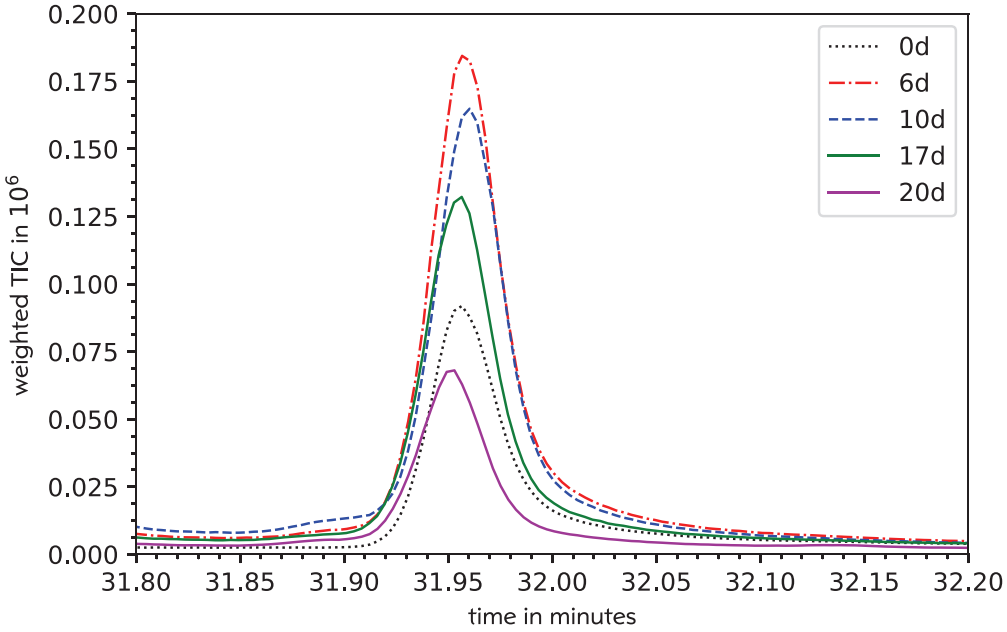

FIGURE 4.44: V2: Weighted If 168 oxidation peak at 32.0 min during aging process

4.2.5 Summary

In this section, the correlation between the oxidation induction times of variously stabilized Polypropylene samples determined at $150\,°C$ with the help of the three-point flexural test and at $200\,°C$ within a DSC instrument as well as the additive concentration determined by quantitative Pyrolysis-GC/MS was examined.

Oven/OIT It was observed, that in oven aging at $150\,°C$, additive packages containing a higher amount of long term thermal stabilizers such as Irganox 1010 (phenolic) or Irganox PS 802 (thiolic) achieve longer OITs than packages containing high amounts of process stabilizers such as the phosphitic Irgafos 168. The Irganox PS 802 package reached an Oven/OIT of 29 days, followed by a 20 day OIT from the Irganox 1010 package and a 17 day OIT by the Irgafos 168 package.

DSC/OIT The opposite was found when determining the OIT at $200\,°C$ in a DSC instrument. In this case, the phosphitic stabilizer package clearly outperformed the LTTS versions, reaching a OIT of $135\,\mathrm{min}$ as opposed to the $116\,\mathrm{min}$ and $108\,\mathrm{min}$ reached by the Irganox 1010 and Irganox PS 802 based packages respectively. In the further course of the aging process the DSC/OITs decayed exponentially as shown by fitting the data collected from the aged samples.

A direct comparison of the obtained Oven/OIT and DSC/OIT_0 values can be seen in Table 4.16.

TABLE 4.16: Comparison: Oven/OIT vs. DSC/OIT

Method	V1	V2	V3
Oven/OIT	20 days	17 days	29 days
DSC/OIT (unaged)	116 min.	135 min.	108 min.

While the DSC/OIT order of the unaged samples differed from the Oven/OIT order, the order in which the DSC/OITs of the aged samples dropped below $10\,\mathrm{min}$ corresponded with the results of the Oven/OIT test.

Py-GC/MS The additive concentrations for both Irganox 1010 and Irgafos 168 in V1 and V2 throughout the aging process were determined using the quantification method developed for this thesis. Both additives in both variations show a linear decrease in concentration. The concentrations decreased to $59\,\%$ and $71\,\%$ of their initial concentration for V1 and to $58\,\%$ and $35\,\%$ of their initial concentration for V2.

At the end of their respective Oven/OITs, Irganox 1010 had decreased to $68\,\%$ (V1) and $74\,\%$ (V2). Irgafos 168 had decreased to $49\,\%$ in V2. The value for V1 cannot be given due to an anomaly in the measurement.

Appearance The optical degradation of the samples (coloring and crack formation) adhered to the same order as the Oven/OIT. The onset of discoloration was observed

very early at 6 to 10 days, however the change remained faint until after the end of the induction period, when the color turned to a strong orange/brown tone and crack formation ensued.

4.2.6 Discussion

Oven/OIT vs. DSC/OIT The data gathered, analyzed and summarized in section 4.2 clearly shows, that lifetime expectancy predictions based solely on data gained through DSC/OIT experiments at high temperatures ($200\,°C$ or higher) can lead to misleading results. This is due to the effective temperature ranges of the additives in use. Additives from the category of long term thermal stabilizers such as the Irganox range, which consists mostly of hindered phenolic antioxidants, perform best at lower temperatures. As the name suggests, their role is protecting a polymer against oxidation throughout it's lifetime i.e. at common usage temperatures. On the other hand, process stabilizers such as the phosphitic Irgafos 168 were specifically designed to protect the polymers from oxidation during processing i.e. temperatures around and above their respective melting or softening temperatures. The consequence is, that a polymer with a stabilization package containing a high amount of process stabilizer paired with a low quantity of long term thermal stabilization can yield a high OIT in a DSC experiment conducted at e.g. ($220\,°C$, while the same sample performs poorly in an oven aging test at ($150\,°C$. At the same time, a sample such as V3, containing a fair amount of LTTS additives, performs significantly poorer in the DSC test compared with a sample such as V2, while it outlasts V2 by almost $100\,\%$ in the oven test.

While it is obvious that the DSC/OIT test is no appropriate substitute for oven aging in respect to lifetime expectancy predictions, it is entirely justified to use this method for batch control. When comparing to samples with the same relative additive composition, the DSC/OIT will correlate directly with their concentration. However, due to the exponential decay of the OIT with the additive concentration, the method will quickly fail at very low concentrations because a correct analysis of the data (section 2.1.3) is no longer possible. This is also the reason why the DSC/OIT measurements performed in this work were executed at $200\,°C$ leading to OITs clearly exceeding the $60\,\mathrm{min}$ maximum duration demanded by the standard [41]. At $210\,°C$ to $220\,°C$ it would have become impossible to determine the OIT past day 6.

Polymer hardening During two phases of the aging process a hardening of the polymer was observed in the mechanical tests.

The first occurred during the first few days in the oven. The most likely explanation for this is post crystallization. After production by injection molding, the specimens quickly cool from approximately $200\,°C$ to room temperature, freezing polymer chains in an amorphous state. For this reason nucleation agents are added

to the formulation when high crystallinity is desired. Upon heating to $150\,°C$ the mobility of the chains is increased, enabling them to rearrange to local linear domains and thus enhancing the specimens crystallinity. Hardening is a direct consequence of this higher degree of order within the sample.

The second hardening process occurred toward the end of the induction period upon the onset of polymer degradation. Oxidation induced chain scission leads to shorter polymer chains, which in turn allows for a higher mobility of the chains. In analogy to the post crystallization of the first few days, this higher mobility leads to the formation of more linear domains and results in a higher overall crystallinity and hardness. In the further course of the aging process this leads to embrittlement and cracking.

Increase of SD during degradation The mechanical tests revealed a marked increase in the standard deviation of ε_f, σ_f and E_f during the degradation phase. A possible reason is a temporal offset of specimen degradation, leading to a broader distribution of the measured values. Another reason could be the heterogeneous oxidation of the polymer due to the far greater solubility of oxygen in the amorphous regions [59]. This can lead to differing strength of the material at critical points within the specimen.

Appearance All samples display faint discoloration well before the end of the induction period and the onset of any significant oxidation. At this early stage, discoloration can mainly be attributed to to formation of quinone methides [66], an oxidation product of phenolic antioxidants. This theory is supported by the discoloration of V3, which is visibly less yellowed on day 6 than V1 and V2. V3 contains the same amount of the phenolic antioxidant Irganox 1010. However, it also contains significant amounts of the non-phenolic antioxidant Irganox PS 802, leading to less oxidation of the phenol and consequently less yellowing quinone methides.

Pyrolysis-GC/MS The quantification results of V1 and V2 both showed a decreasing tendency, which is what was expected. The fact, that this could be demonstrated with statistical reliability proves the principle validity of the method. The effort involved also highlights the main advantage of the method over the standard HPLC technique. Performing a thorough extraction and subsequent solvent reduction for ten samples would have required quite some time in most laboratories. This step could be completely omitted.

The Irgafos 168 peak at $32\,\mathrm{min}$ was the only peak in the analysis that grew larger before beginning to decay. The explanation can be found in Figures 4.43 and 4.44. Between day 0 and day 6 the peak at $30.6\,\mathrm{min}$ almost completely dissipates, while it's oxidized counterpart grows significantly. This is due to the fact, that Tris(2,4-di-tert-butylphenyl)phosphate (Ox. Irgafos 168 - $32\,\mathrm{min}$) is the principle oxidation product of Tris(2,4-di-tert-butylphenyl)phosphite (Irgafos 168 - $30.6\,\mathrm{min}$).

A possible explanation for the high values obtained for V1 - day 20 was discussed in section 4.1.10. Due to the very small sample size used for pyrolysis, the method is inherently sensitive to heterogeneity within the samples. Representativeness cannot be guarantied to the same extent as the HPLC equivalent in which several hundred milligrams are extracted and then aliquoted as opposed to a sample of only $200\,\mu g$ to $300\,\mu g$. This seems to be one of the major downsides of the method.

4.3 Color-dependency of the OIT

The previous project discussed the influence of different additive packages and temperatures on the oxidation stability of Polypropylene compounds. The focus of this project is the influence of a common colorant for automotive interior PP compounds, carbon black. Two samples with identical composition except for their percentage of carbon black were used. The natural variant contains no carbon black masterbatch, while the black variant contains $2\,\%$ of a $40\,\%$ black masterbatch.

As with the DSC/OIT vs. Oven/OIT project, standard specimens were aged in an air circulating oven and regularly subjected to a three-point flexural test. In parallel, DSC/OIT measurements were conducted before and during the aging process. The goal was to identify a difference in oxidation stability between both samples.

4.3.1 Mechanical testing

Flexural strain The overall mechanical behavior of the color samples is identical to the samples used in the previous project (V1-3). Throughout the induction period the flexural strain determined in the three-point flexural tests remains at a constant level of approx. $6\,\%$. This is slightly less than the $6.5\,\%$ to $7\,\%$ observed with the V1-3 samples.

In accordance with the expectations, the sample containing carbon black reaches the end of it's OIT first. After 17 days a sharp decline in flexural strain can be observed, dropping to approx. $1\,\%$ by day 21. The uncolored natural sample retains it's full flexibility until day 21, after which it too declines to about $1\,\%$ by day 23.

Flexural strength The flexural strength follows the same principle trend as the flexural strain. The black sample starts to degrade after day 17 while the natural sample lasts until day 21 before showing any signs of oxidation. However, the slope of the flexural strength's decline is not quite as steep as that of the flexural strain, which seems to be more sensitive to changes in the samples.

Both samples show a slight increase in flexural strength over the first few days due to post crystallization, reaching their induction period level of approx. $32\,\mathrm{MPa}$. Both samples decline to under $10\,\mathrm{MPa}$ by days 23 and 24.

Flexural modulus As before, the flexural modulus shows a strong feedback to both the post crystallization in the first few days, rising by approx. $250\,\mathrm{MPa}$ and to the onset of oxidation induced rigidity towards the end of the OIT. The difference between both samples is not as clearly defined as with the the flexural strain, which is partly due to a broad distribution of the values during oxidation. However, the general trend corresponds to the flexural strain and strength data, showing a greater oxidation resistance for the uncolored sample.

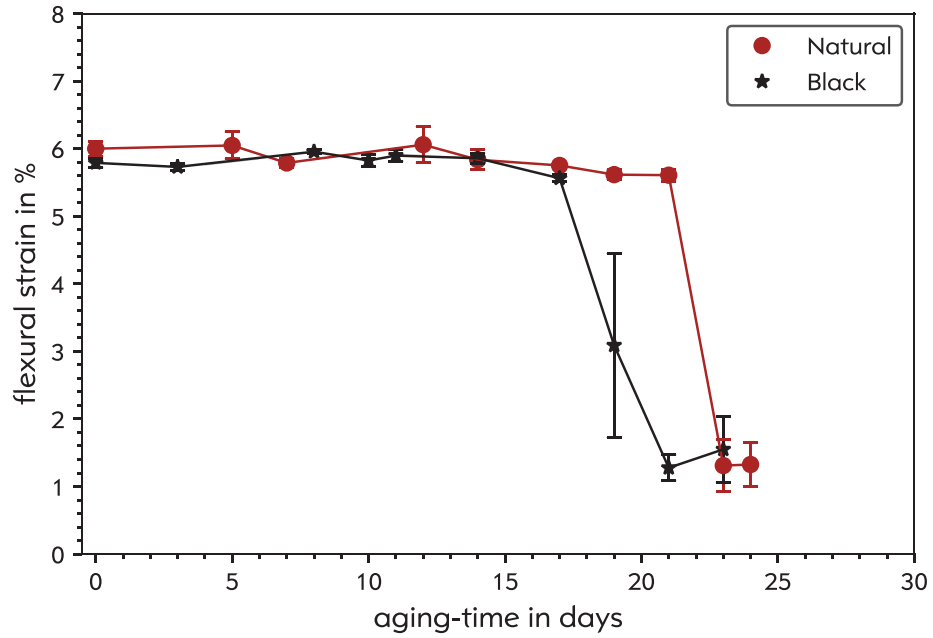

FIGURE 4.45: Flexural strain of colored PP during oven-aging

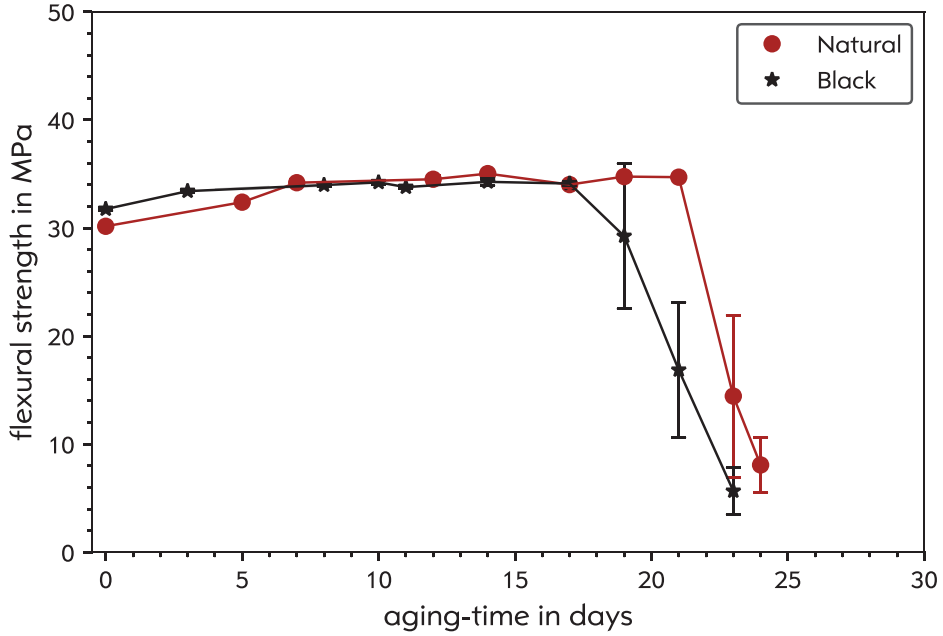

FIGURE 4.46: Flexural strength of colored PP during oven-aging

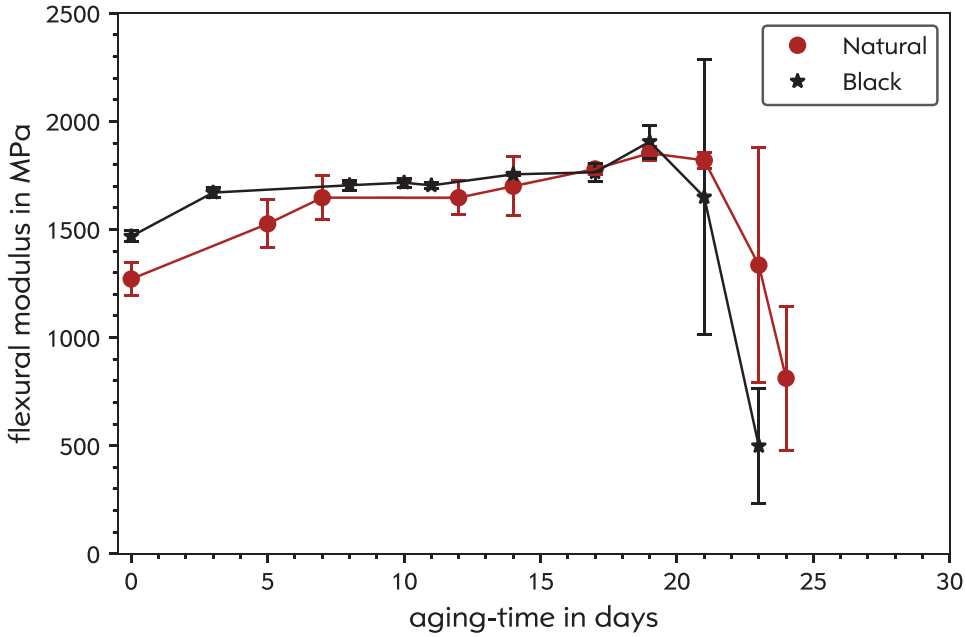

FIGURE 4.47: Flexural modulus of colored PP during oven-aging

In conclusion, mechanical testing during the oven aging process shows, that the naturally colored sample without any carbon black exhibits a distinctly higher resistance to oxidation in the form of an OIT which is four days or slightly over 20 % longer than the carbon black containing sample's OIT.

4.3.2 DSC/OIT testing

Figure 4.48 shows the results of the DSC/OIT measurements before and during the aging process of the colored PP samples. Unlike the samples with varying additive packages, the carbon black content shows no significant impact on the DSC/OIT. Both the values of the unaged samples as well as the development of the values during aging lie within the methods uncertainty. This also becomes clear by looking at the equations of the fit curves, which are very similiar.

As with the measurements on the samples V1-3, the DSC/OIT values display an exponential decay in the course of the aging process.

4.3.3 Optical degradation

The optical examination of the unaged and aged sample specimens can be seen in Figure 4.49. The result supports the conclusion drawn from the mechanical tests. At 24 days of aging, the uncolored, natural sample is still in a better optical condition (less cracks) than the colored, black sample after 21 days. In contrast to samples V1-3, the discoloration cannot be used as comparison, since the black samples remains black. Apparently, the carbon black covers any discoloration that might be visible.

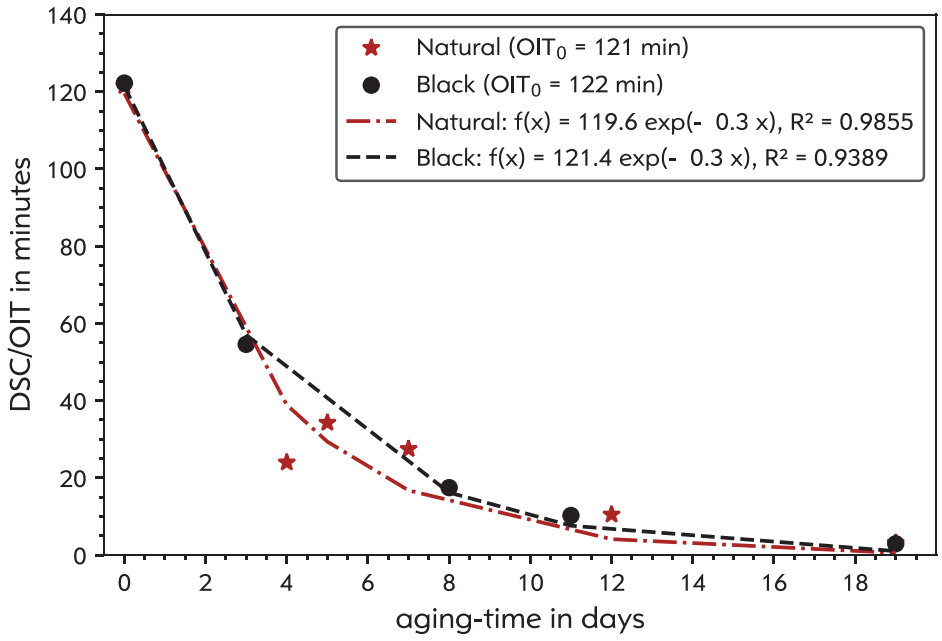

FIGURE 4.48: DSC/OIT values of unaged and aged colored PP samples

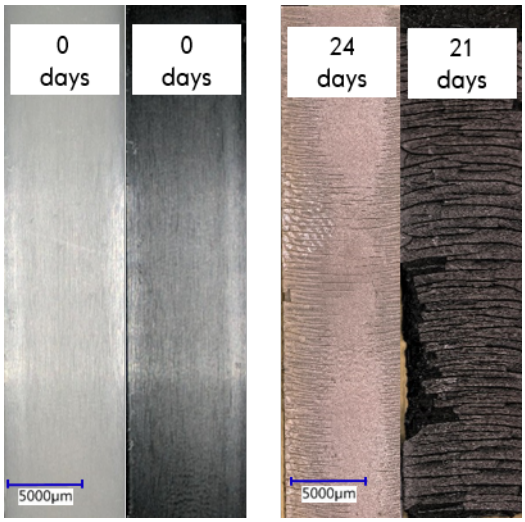

FIGURE 4.49: Optical degradation of aged colored PP samples

4.3.4 Summary

The aim of this project was to examine the influence of carbon black used as a colorant on the oxidation stability of Polypropylene samples. Two samples varying only in their carbon black content were compared in respect to their performance in oven aging and DSC/OIT.

Oven/OIT The mechanical tests (three-point flexural) performed throughout the aging process showed conclusively, that carbon black has a negative influence on the oxidation stability of Polypropylene compounds. The black sample reached the end of it's OIT after 17 days at $150\,°\mathrm{C}$. The uncolored sample containing no carbon black outlasted the black sample by more than $20\,\%$, reaching the end of it's OIT after day 21.

Both samples displayed signs of post crystallization in the 3 to 7 days and a steep decline in mechanical properties after the end of their induction period. During this decline, the standard deviation of ε_f, σ_f and E_f increased significantly, as was previously observed with samples V1-3 in the Oven/OIT vs. DSC/OIT project.

DSC/OIT No discernable difference between the samples could be observed in the DSC/OIT measurements. Their respective OIT_0 values lay only about $0.5\,\mathrm{min}$ apart, which lies within the methods margin of error.

Appearance The optical degradation of the samples follows the same trend as the mechanical properties. However, any possible discoloration of the black sample is masked by the carbon black content.

4.3.5 Discussion

The previous section's discussion already discussed many of the topics which arise when performing oven aging experiments with mechanical and caloric tests, such as the polymer hardening at the beginning of the aging process and toward the end of the induction period, or the increase in standard deviation of the recorded mechanical properties. To avoid redundancy, this discussion will focus only on the influence of carbon black on the oxidation stability of the polymer.

The carbon black used is a relatively pure form, produced from high temperature petroleum cracking fractions in the so called *furnace process*. It has an untreated surface with a low content of Oxygen and Sulfur and near neutral pH.

While the levels of Oxygen bound to the carbon black's surface might be low, this is a material with an extremely large surface. Only the external surface alone amounts to about $90\,\mathrm{m^2\,g^{-1}}$. In addition the total surface area includes micropores with pore diameters of less than $2\,\mathrm{nm}$ [61]. In spite of degassing measures during the manufacturing of the master batch, one has to assume that a non negligible amount of Oxygen is contained within. In combination with Oxygen-containing combustion

products remaining on the carbon's surface from production, this might act as an oxidizing accelerant during the oven aging process.

One of the main delays in the oxidation of solid samples is the speed with which Oxygen can diffuse into the material. It is evident, that the introduction of Oxygen into the material via carbon black during processing might accelerate the process.

However, the overall effect should not be exaggerated. The natural and the black Polypropylene samples represent both extremes of the color spectrum, containing no carbon black at all and $2\,\%$ of a $40\,\%$ black MB, rendering the sample black. While a difference in oxidation stability between both compounds could be clearly demonstrated, the uncolored sample only surpassed the black samples Oven/OIT by $24\,\%$. This difference can easily be balanced by slight adjustments to the stabilization package. Additionally, the stabilization for these samples was not designed with the goal of high lifetime expectancy, but to be a good compromise of application oriented engineering with practicality in respect to the experiments duration.

One should bear in mind however, that the choice of carbon black for plastics coloration must be considered carefully. Other forms of carbon black, such as those used for water based paints, can be surface treated to exhibit high amounts of oxygen-containing groups on the surface and an acidic pH of 2 to 3. Here, the influence on oxidation stability could be significantly higher.

Chapter 5

Summary, conclusion and Outlook

As was described in Section 1.2, this thesis entails three major projects. The first project, which constitutes the starting point, is the development of a quantitative method for the analysis of polymer additives using Py-GC/MS. A thorough thermal characterization of the polymers and additives used to manufacture reference samples was followed by mass-spectral analysis and concluded in the development of the method. Using a three-point calibration, the method was tested on polyamide-6 and polypropylene standard samples and verified on an oven-aging series of two additional polypropylene samples from another project. The results could not match the HPLC approach in terms of reproducibility but were accurate within the limits of the techniques inherent uncertainty. The method is therefore a viable alternative to HPLC, when a prior extraction step is undesirable.

The second project aimed at comparing oven-aging according to DIN EN ISO 4577 and 178 [43, 63] with the fast DSC/OIT method corresponding to DIN EN ISO 11357 [41]. The oxidation induction time was accordingly determined at $150\,^{\circ}\mathrm{C}$ with subsequent mechanical testing (three-point flexural test) and at $200\,^{\circ}\mathrm{C}$ in the DSC instrument using samples of varying stabilizer formulation. As expected, the order of stability differed with the change in temperature, confirming the conclusion, that DSC/OIT is no adequate alternative to oven-aging.

The final project's objective was investigating the influence of carbon black on the oxidation stability of polypropylene samples. A sample with no carbon black content and a sample containing $2\,\%$ of a carbon black masterbatch were compared using the same techniques as in the second project. The results showed a significant difference in oxidation resistance, with the uncolored sample outperforming the colored sample by over $20\,\%$. The most likely explanation being oxygen adsorbed to the large surface area of the carbon black and introduced to the polymer during processing.

5.1 Pyrolysis-GC/MS method development

Summary The development of the quantification method was begun by performing a thermal characterization of the additives and polymer samples via thermo gravimetric analysis in an inert nitrogen atmosphere (Table 4.1). This yielded lower

decomposition temperatures of $366\,°C$ to $410\,°C$ for Tinuvin 770, Irganox 1076 and Irgafos 168. Higher temperatures of $441\,°C$ to $462\,°C$ were determined for Irganox 1098, Irganox 1010 and polyamide-6, while polypropylene had the highest decomposition temperature at $485\,°C$. In addition, a pyrolysis temperature series of the additives was carried out in $50\,°C$ steps from $450\,°C$ to $600\,°C$ via the Py-GC/MS.

The results of these preliminary test lead to the conclusion, that it was feasible to analyze Irgafos 168, Tinuvin 770 and Irganox 1076 at $450\,°C$ and therefore avoiding major decomposition of the polymer matrix and it's accompanying downsides. Irganox 1098 and Irganox 1010 however, would have to be analyzed at $600\,°C$ to achieve reasonable intensity. It was also decided to use single ion monitoring to circumvent problems of co-elution and blanketing by the polymer matrices.

With the now established temperature program, scan series of the individual additives at $600\,°C$ were performed in order to build up a library of retention times and m/z values for the SIM methods (Table 4.2), which were developed on the basis of these measurements. Additionally, the reproducibility was examined (Table 4.3). Eight runs each per additive yielded relative standard deviations for their respective total peak areas of $10\,\%$ to $35\,\%$. This range was mostly confirmed in all following Py-GC/MS quantification experiments.

The method obtained was then used for several quantification experiments on the standard polyamide-6 and uncolored polypropylene samples. A first experiment was done at $450\,°C$ aiming only at Irgafos 168, Tinuvin 770 and Irganox 1076. The mean peak areas from five measurements each were quantified via a three-point calibration fabricated with the individual additives, also with five measurements each. The results (Tables 4.5 and 4.7) go in the right direction, diverging between $13\,\%$ to $84\,\%$ from the formulation plan and the reference values provided by BASF via their HPLC method. Except for Tinuvin 770 in PA6, all additives were over quantified. The strongest deviation was found between the Irgafos 168 value obtained via pyrolysis and HPLC, both in the PA6 and the PP sample. A possible reason for this deviation is degradation of Irgafos 168 by cleavage of 2,4-di-tert-butylphenol during processing. Since similiar degradation would take place during pyrolysis, it is not possible to differentiate between degradation products from processing and from pyrolysis in this case, leading to over-quantification.

The experiment was repeated at $600\,°C$, this time aimed also at Irganox 1098 and Irganox 1010. Due to partly identical degradation products from Irganox 1010, 1076 and 1098, only one small unique peak was available for quantification of Irganox 1010. Two large peaks were available for Irganox 1076. Irganox 1098 did not pose a problem, since it was the only additive of this sort used in the PA6 sample. The results of the quantification are displayed in Tables 4.10 and 4.11. For both PA6 and PP the results are better than those at $450\,°C$, displaying to deviations as large as observed for Irgafos 168 at $450\,°C$. The largest deviations are found for Irganox 1076, lying $48\,\%$ to $53\,\%$ higher than the formulation plan or the BASF results. However, this probably does not come from the additive itself, since it had already been

quantified with $0\,\%$ deviation in a previous experiment. The discrepancy in this run comes from the general variability of the resulting total peak areas. The quantification of Irganox 1010 was not possible alongside Irganox 1076. Due to the fact, that only a single unique peak was available and die additive was only present in very low quantities ($0.05\,\%$, the quantification failed because this unique peak was below both the limit of detection and consequently the limit of quantification.

In the course of the DSC vs. oven-aging project, this method was used to monitor the additive content of the samples V1 (Ix 1010 dominated) and V2 (If 168 dominated). Apart from revealing a linear decline over time, these tests proved the efficacy of the method, enabling effective monitoring of the concentration decline in the range of $0.178\,\%$ to $0.055\,\%$ with RSD values mainly below $20\,\%$. Here, Irganox 1010 could be successfully analyzed both due to the absence of other interfering additives and it's higher concentration.

The main issue for the presented method is the significant variability of the results. Several reasons were discussed. The first is uncertainty stemming from the pyrolysis process itself. Being not only a physical but also a series of chemical reactions, the result can vary depending on the sample size and exact location within the vial, precision and rate of heating in the pyrolysis unit and statistical uncertainties. A second reason is variability originating in the mass detector. While mass spectrometers are fantastic tools for identification, they fall behind other detectors such as the flame ionization detector or the UV detector in terms of reproducible peak areas. Lastly, the size of the samples in pyrolysis experiments, which commonly does not exceed $300\,\mu g$ makes it difficult to have representative samples. Homogeneity of standard polymer samples might not be given on this scale, which in turn would lead to varying results. However, since the measurements on additives pipetted from aliquoted stock solutions also show a high variability, this does not seem to be a principle concern.

Conclusion In general, the development of a quantitative Py-GC/MS method for additive analysis in polymers without prior extraction steps has been successful. There are some limitations to the method that must be mentioned. The failure to identify or quantify base stabilizers in low concentrations alongside stabilizers with similiar or overlapping degradation products is a serious downside. Of course, the base stabilization of a polymer is usually only designed to stabilize the product between polymerization and compounding and will generally not be of much interest. Still, this problem cannot be omitted. Here, methods with prior extraction steps will most often be superior, since the non decomposed additives can be isolated and quantified sequentially, wholly avoiding the problem.

While the variability of the results seems quite significant, it is easily within competitive range of alternative methods for polymer additive quantification such as the MALDI-ToF method published by Schwarzinger et al. [14]. Although HPLC analysis comes with a significantly lower uncertainty, offering RSD values in the low

percentage range, extraction is an issue. Not only in regard to experiment time, but also efficacy of extraction. As Vandenburg et al. have shown and discussed [9, 10], extraction via dissolution/precipitation can cause issues with re-precipitation of the additive. Soxhlet extraction avoids this, but requires large amounts of time at elevated temperatures and therefore has issues with volatile additives. Finally, methods such as accelerated solvent extraction work very well, but are initially cost intensive and require additional method optimization to obtain good results.

In conclusion, the Py-GC/MS method has it's legitimate place in the range of available methods, providing both advantages and drawbacks. Which method is the best for a particular situation cannot be resolved collectively but has to be individually decided. The main application field will be the analysis of samples in which prior extraction of the additives is undesirable. Reasons for this can range from the absence of the appropriate instruments to complications with volatile additives subjected to the threat of discrimination by the extraction method. Also, polymeric additives such as the light stabilizer Chimassorb 2020 pose a problem for the established HPLC approach.

Outlook To provide an outlook, I will elaborate both on possibilities of further optimizing this method as well as expanding it's scope.

There are several factors which can be explored. First, when examining volatile additives such as Irgafos 168, Tinuvin 770 or Irganox 1076, waiving the possibility of SIM-MS in favor of flame ionization detection (FID) can be viable. Especially in cases of routine quality control measurements this could reduce the methods uncertainty and range of application. Both the quantitational reproducibility as well as the linear dynamic range of the FID are superior to a quadrupole mass spectrometer.

Another possibility is further enhancing the SIM parameters. Especially for critical compounds such as Irganox 1010, the ratio of dwell time and cycles per second could be optimized [67] to maximize sensitivity. While this can deteriorate the result of peak integration due to less data points, a higher signal intensity enabling quantification can be worth the cost.

Concerning the expansion of the method to more additives, the approach described in this thesis is applicable. This entails the pyrolysis temperature series, followed by library measurements and subsequent expansion of the SIM method. In the case of problems with co-elution, reactive pyrolyzation entailing derivatization with e.g. hexamethyldisilazane (HMDS) and trimethylsilyl chloride (TMSCl) can be a viable approach, since it leads to both different retention times and potentially better peak forms and separation in the case of polar analytes in a standard $5\,\%$ phenyl PDMS GC column.

5.2 DSC vs. oven-aging

Summary In order to clarify whether the measurement of OIT values with a DSC instrument poses a valid alternative to oven-aging and mechanical testing in regard to oxidation stability tests and lifetime prediction, several samples with varying stabilization packages (V1-3, Table 3.3) were aged and examined via DSC. The DSC/OIT measurements at $200\,°C$ clearly favored the sample V2 ($135\,\mathrm{min}$) with it's high content in phosphitic process stabilizer, followed by V1 ($116\,\mathrm{min}$ - high in phenolic Ix 1010 - long term thermal stabilizer) and V3 ($108\,\mathrm{min}$ - thiolic Ix PS 802 - long term thermal stabilizer).

The oven aging experiments at $150\,°C$ with mechanical tests in form of the three-point flexural test revealed a different order of failure. Here, the sample V3 (29 days) with it's thiolic LTTS content (Ix PS 802) clearly outperformed the others, followed by V1 (20 days - Ix 1010) and V2 (17 days - If 168) degrading first. So, at the lower temperature of the oven test, the order of failure was exactly reversed from the DSC/OIT result. A summary of the results is displayed in Table 4.16.

This result confirms the expectations and the categorization of the additives into long term thermal stabilizers for in-use temperatures and process stabilizers for processing temperatures. Similiar findings were published by Müller et al. [31] when they monitored antioxidant levels in polypropylene via HPLC during long term aging at $80\,°C$ to $90\,°C$ while performing DSC/OIT tests. An overview of the effective temperature range of the additives can be found in the publication.

However, DSC/OIT values correspond well with the actual antioxidant concentrations, as figures 4.31, 4.35 and 4.40 show. The OIT values decay exponentially with both aging time and antioxidant concentration.

Conclusion It is very desirable to have a fast, instrumental test of potential lifetime expectancy such as the DSC/OIT. However, these results clearly show, that using DSC/OIT measurements at the appropriate temperatures as an accelerated aging technique to predict polymer lifetime has some rather severe limitations depending on the composition of the additive package. The stabilization potential of antioxidants is temperature dependent. This means, that reliable results can only be obtained, when the accelerated aging test is performed as close to the target use temperature as possible. Clearly, a good compromise has to be found between realistic conditions and time constraints often encountered in engineering and product development environments.

While DSC/OIT clearly is not a suitable substitute for oven aging, it is well equipped to monitor aging processes or for use in batch / quality control due to the correlation between additive concentration and DSC/OIT.

Outlook A possible outlook for this project is the expansion to other types of antioxidants such as monomeric and polymeric HALS, since they too are used for thermal stabilization in addition to their light stabilizer qualities.

Also, a test at lower and intermediate temperatures would be an interesting endeavor. A possible outcome would be a thermal map of defined stabilizer packages in combination with particular polymers. This would be a way to find the maximum temperature suited to give a useful result with a minimum time investment for a specific compoundation product. Due to the great initial effort, this would only be feasible for the quality control of compounds produced in large quantities over a long period of time. Also, for the sake of comparability, it would still be advantageous to test according to the standard.

5.3 Color-dependancy of the OIT

Summary The final topic of interest was the influence the colorant *carbon black* on the oxidation stability of the polypropylene. Carbon black is the most common colorant in automotive applications, especially interior plastics, apart from those used in paints for bodywork. Test specimen were produced from two formulations which were identical save for their carbon black content. The uncolored version had no carbon black added, while the black version had $2\,\%$ of a $40\,\%$ carbon black masterbatch. The carbon black is low in chemically bound surface oxygen and sulfur as well as neutral regarding to pH. As with the DSC vs. oven-aging project, the test specimen were oven aged at $150\,^{\circ}\mathrm{C}$ and test by three-point flexural test. The resulting Oven/OITs were 17 days for the black sample and 21 days for the uncolored sample. A difference of slightly over $20\,\%$.

DSC/OIT experiments were also performed before and during aging. However, no significant difference could be observed. This is another observation supporting the conclusion reached in respect to the suitability of DSC/OIT experiments for lifetime prediction.

A possible explanation is the introduction of oxygen adsorbed to the carbon black surface into the polypropylene during processing. Even small amounts of oxygen within the polymer would cause a faster depletion of antioxidants and subsequent oxidation of the matrix. This explanation seems plausible not least because of the considerable surface area of this carbon black of $90\,\mathrm{m^2\,g^{-1}}$ (STSA).

Conclusion It can be concluded, that the carbon black used in this work has an undeniable negative effect on the oxidation stability of polypropylene. This could be further exaggerated when types of carbon black are used which have been modified to have a higher amount of chemically bound oxygen in the form of phenols, aldehydes etc. on it's surface. These types also often exhibit acidic pH values of 2 to 3.

However, it must be taken into account, that in real life scenarios, carbon black has a stabilizing effect in respect to UV radiation. Also, the difference in oxidation stability observed can easily be balanced by slightly adjusting the stabilization package. Therefore, when developing new formulations, the influence of carbon black has to be viewed on the whole and it's negative impact on oxidation resistance should not be overrated.

Outlook The obvious further development of this project to gain more insight on the influence of carbon black, would be to test more concentrations as well as different forms of carbon black. Variations with higher oxygen levels and lower pH are conceivable and would lead to a more profound understanding.

To confirm the hypothesis stated in the discussion, concerning adsorbed oxygen, it would also be of interest to produce samples with a specially prepared black masterbatch. The preparation could entail baking the carbon black pigment in a vacuum chamber to desorb unwanted oxygen and immediately compounding the obtained pigment into it's polypropylene matrix.

Also, a holistic study of carbon black's influence on the overall performance of a compound would be of interest. This should also entail UV irradiation and possibly natural weathering tests.

5.4 Closing remarks

It was shown, that Pyrolysis-GC/MS is a powerful method, not only for identifying unknown polymers and other non volatile organic matrices, but also for quantitative trace analysis. Paired with single ion monitoring and accepting some limitations in respect to absolute reproducibility, several antioxidants could successfully be quantified within their polymer matrix without prior extraction. Further optimization could also solve the Irganox 1010/1076 issue by making the method sensitive enough for weak unique peaks.

For the application of DSC/OIT to lifetime expectancy predictions, the high temperatures used were shown to be a major limitation. The effectivity of the additives vary significantly between $150\,^{\circ}\mathrm{C}$ and $200\,^{\circ}\mathrm{C}$, confirming the oven-aging technique as the state of the art test. However, the OIT values measured by DSC still represent a powerful tool in polymer analytics, product development and quality control.

Finally, the potentially negative influence of carbon black on oxidation stability was shown. This is useful information for formulation development, especially when unnecessarily high stabilizer contents are undesirable.

Bibliography

(1) Statistisches Bundesamt Wirtschaftsbereiche - Industrie, Verabeitendes Gewerbe: Automobilindustrie: 407 Milliarden Euro Umsatz im Jahr 2016., 2017.

(2) Grundstein, A.; Meentemeyer, V.; Dowd, J. *International journal of biometeorology* **2009**, *53*, 255–261.

(3) Carrero, J.; Oliva, V.; Navascués, B.; Borrull, F.; Galià, M. *Polymer Testing* **2015**, *46*, 21–25.

(4) Beißmann, S.; Stiftinger, M.; Grabmayer, K.; Wallner, G.; Nitsche, D.; Buchberger, W. *Polymer Degradation and Stability* **2013**, *98*, 1655–1661.

(5) Reingruber, E.; Himmelsbach, M.; Sauer, C.; Buchberger, W. *Polymer Degradation and Stability* **2010**, *95*, 740–745.

(6) Himmelsbach, M.; Buchberger, W.; Reingruber, E. *Polymer Degradation and Stability* **2009**, *94*, 1213–1219.

(7) Marcato, B.; Vianello, M. *Journal of Chromatography A* **2000**, *869*, 285–300.

(8) Neelson, R. C. *Journal of Liquid Chromatography* **1993**, *16*, 1625–1638.

(9) Vandenburg, H. J.; Clifford, A. A.; Bartle, K. D.; Carroll, J.; Newton, I.; Garden, L. M.; Dean, J. R.; Costley, C. T. *The Analyst* **1997**, *122*, 101R–116R.

(10) Vandenburg, H. J.; Clifford, A. A.; Bartle, K. D.; Carlson, R. E.; Carroll, J.; Newton, I. D. *The Analyst* **1999**, *124*, 1707–1710.

(11) Paine, M. R. L.; Barker, P. J.; Blanksby, S. J. *Analytica chimica acta* **2014**, *808*, 70–82.

(12) Klampfl, C. W. *TrAC Trends in Analytical Chemistry* **2013**, *50*, 53–64.

(13) Barrère, C.; Maire, F.; Afonso, C.; Giusti, P. *Analytical chemistry* **2012**, *84*, 9349–9354.

(14) Schwarzinger, C.; Gabriel, S.; Beißmann, S.; Buchberger, W. *Journal of the American Society for Mass Spectrometry* **2012**, *23*, 1120–1125.

(15) Trimpin, S.; Wijerathne, K.; McEwen, C. N. *Analytica chimica acta* **2009**, *654*, 20–25.

(16) Brander, E.; Wold, C. *Journal of Chromatography A* **2014**, *1362*, 309–312.

(17) Kaal, E. R.; Alkema, G.; Kurano, M.; Geissler, M.; Janssen, H.-G. *Journal of Chromatography A* **2007**, *1143*, 182–189.

(18) Wampler, T. P.; Levy, E. J. *Journal of Analytical and Applied Pyrolysis* **1985**, *8*, 65–71.

(19) Wampler, T. P.; Levy, E. J. *Journal of Analytical and Applied Pyrolysis* **1985**, *8*, 153–161.

(20) Wampler, T. P.; Levy, E. J. *Journal of Analytical and Applied Pyrolysis* **1987**, *12*, 75–82.

(21) Wang, F. C.-Y. *Journal of Chromatography A* **2000**, *883*, 199–210.

(22) Wang, F. C.-Y.; Buzanowski, W. C. *Journal of Chromatography A* **2000**, *891*, 313–324.

(23) Wang, F. C.-Y. *Journal of Chromatography A* **2000**, *891*, 325–336.

(24) Wang, F. C.-Y. *Journal of Chromatography A* **2000**, *886*, 225–235.

(25) Herrera, M.; Matuschek, G.; Kettrup, A. *Journal of Analytical and Applied Pyrolysis* **2003**, *70*, 35–42.

(26) Coulier, L.; Kaal, E. R.; Tienstra, M.; Hankemeier, T. *Journal of Chromatography A* **2005**, *1062*, 227–238.

(27) Jansson, K. D.; Zawodny, C. P.; Wampler, T. P. *PYROLYSIS 2006: Papers presented at the 17th International Symposium on Analytical and Applied Pyrolysis, Budapest, Hungary, 22-26 May 2006* **2007**, *79*, 353–361.

(28) Markus Reil; Gabriele Kaiser; Karina Reiser *Kunststoffe International* **2015**, 27–30.

(29) Celina, M. C. *Polymer Degradation and Stability* **2013**, *98*, 2419–2429.

(30) Celina, M.; Gillen, K. T.; Assink, R. A. *Polymer Degradation and Stability* **2005**, *90*, 395–404.

(31) Müller, W. W.; Jakob, I.; Li, C.; Tatzky-Gerth, R. *Chinese Journal of Polymer Science* **2009**, *27*, 435.

(32) Schmid, M.; Affolter, S. *Polymer Testing* **2003**, *22*, 419–428.

(33) Rosa, D.; Sarti, J.; Mei, L.; Filho, M.; Silveira, S. *Polymer Testing* **2000**, *19*, 523–531.

(34) Hübschmann, H.-J., *Handbook of GC/MS: Fundamentals and applications*, 2., completely rev. and updat. ed.; Wiley-VCH: Weinheim, 2009.

(35) Rial-Otero, R.; Galesio, M.; Capelo, J.-L.; Simal-Gándara, J. *Chromatographia* **2009**, *70*, 339–348.

(36) Wampler, T. P. *Journal of Chromatography A* **1999**, *842*, 207–220.

(37) *Applied pyrolysis handbook*, 2nd ed.; Wampler, T. P., Ed.; Taylor & Francis distributor: Boca Raton, Fla, London, 2007.

(38) Teschl, G., *Ordinary differential equations and dynamical systems*; Graduate studies in mathematics, Vol. 140; American Math. Soc: Providence, RI, 2012.

(39) Snyder, L. R.; Kirkland, J. J.; Dolan, J. W., *Introduction to modern liquid chromatography*, 3rd ed.; Wiley: Hoboken, N.J, 2010.

(40) E. S. Watson; M. J. O'Neill Differential microcalorimeter., 1966.

(41) DIN Normenausschuss Kunststoffe, Dynamische Differenz Thermoanalyse (DSC) - Teil 6: Bestimmung der Oxidations Induktionszeit und Oxidations Induktionstemperatur; Deutsche Fassung EN ISO 11357-6:2013., Berlin, April 2013.

(42) DIN Normenausschuss Kunststoffe Thermogravimetrie (TG) von Polymeren - Teil 1: Allgemeine Grundsätze (ISO 11358-1:2014); Deutsche Fassung EN ISO 11358-1:2014., Berlin, October 2014.

(43) DIN Normenausschuss Kunststoffe, Bestimmung der Biegeeigenschaften (ISO 178:2010 + Amd.1:2013); Deutsche Fassung EN ISO 178:2010 + A1:2013., Berlin, September 2013.

(44) Domininghaus, H., *Die Kunststoffe und ihre Eigenschaften*, 5., völlig neu bearb. und erw. Aufl.; Springer: Berlin, 1998.

(45) Alewelt, W.; Bottenbruch, L.; Becker, G. W., *Polyamide*, Neuausg; Kunststoff-Handbuch Technische Thermoplaste, Vol. 4. Hanser: München, 1998.

(46) Hermans, P. H.; Heikens, D.; van Velden, P. F. *Journal of Polymer Science* **1958**, *30*, 81–104.

(47) Kuehner, M. Polypropylen PP - Marktstudie: Analyse, Trends; Ceresana., 2017.

(48) Kaminsky, W. *Journal of the Chemical Society, Dalton Transactions* **1998**, 1413–1418.

(49) Oswald, H. J.; Turi, E. *Polymer Engineering and Science* **1965**, *5*, 152–158.

(50) Gillen, K. T.; Bernstein, R.; Clough, R. L.; Celina, M. *Polymer Degradation and Stability* **2006**, *91*, 2146–2156.

(51) Pospisil, J.; Klemchuk, P. P., *Oxidation inhibition in organic materials*; CRC Press: 1989.

(52) Epacher, E. *Polymer* **2000**, *41*, 8401–8408.

(53) Gijsman, P.; Kroon, M.; van Oorschot, M. *Polymer Degradation and Stability* **1996**, *51*, 3–13.

(54) Shlyapnikov, Y.; Bogaevskaya, T. A.; Kiryushkin, S. G.; Monakhova, T. V. *European Polymer Journal* **1979**, *15*, 737–742.

(55) Haber, F.; Weiss, J. *Die Naturwissenschaften* **1932**, *20*, 948–950.

(56) Philippart, J. L.; Gardette, J. L. *Polymer Degradation and Stability* **2001**, *73*, 185–187.

(57) Russell, G. A. *Journal of the American Chemical Society* **1957**, *79*, 3871–3877.

(58) Kohler, D. R.; Kröhnke, C. *Polymer Degradation and Stability* **1998**, *62*, 385–393.

(59) Maier, R.-D.; Schiller, M., *Handbuch Kunststoff Additive*, 4., vollständig neu bearbeitete Auflage, 2016.

(60) Murphy, J., *Additives for plastics handbook*, 2. ed.; Elsevier Advanced Technology: Oxford, 2001.

(61) D24 Committee Test Method for Carbon Black: Total and External Surface Area by Nitrogen Adsorption., West Conshohocken, PA, 2010.

(62) DIN Normenausschuss Kunststoffe, Bestimmung der Zugeigenschaften - Teil 2: Prüfbedingungen für Form- und Extrusionsmassen; Deutsche Fassung EN ISO 527-2:2012., Berlin, February 2012.

(63) DIN Normenausschuss Kunststoffe, Polypropylen und Propylen Copolymere. Bestimmung der thermischen Oxidationsstabilität in Luft (Ofen Verfahren); Deutsche Fassung EN ISO 4577:1999., 10772 Berlin, September 1999.

(64) Blazsó, M. *Journal of Analytical and Applied Pyrolysis* **2001**, *58-59*, 29–47.

(65) Ehrenstein, G. W.; Pongratz, S., *Beständigkeit von Kunststoffen*; Edition Kunststoffe; Hanser: München, 2007.

(66) Pospisil, J.; Habicher, W.-D.; Pilar, J.; Nespurek, S.; Kuthan, J.; Piringer, G.-O.; Zweifel, H. *Polymer Degradation and Stability* **2002**, *77*, 531–538.

(67) Prest, H.; Peterson, D. *Agilent Library Database* **2001**.

Appendix A

Curriculum Vitae

This CV has been removed for online publication. Please refer to the printed version or contact the author for more information.